

**WASM: Minerals, Energy and Chemical Engineering**

**Evaluation of CO<sub>2</sub> Injection in Shale Gas Reservoirs through  
Numerical Reservoir Simulation and Supervised Machine Learning**

**Moataz Khamees Abdelfattah Mansi**

**0000-0002-5768-1949**

**This thesis is presented for the Degree of**

**Master of Philosophy**

**of**

**Curtin University**

**March 2023**

# Declaration

To the best of my knowledge and belief this thesis contains no material previously published by any other person except where due acknowledgement has been made. This thesis contains no material which has been accepted for any other degree or diploma in any university.

Signature: .....

Date: 24<sup>th</sup> March 2023

# Copyright

I warrant that I have obtained, where necessary, permission from the copyright owners to use any third-party copyright material reproduced in the thesis (e.g., questionnaires, artwork, unpublished letters), or to use any of my own published work (e.g., journal articles) in which the copyright is held by another party (e.g., publisher, co-author).

Signature: .....

Date: 24<sup>th</sup> March 2023

# Dedication

*I am dedicating this thesis to my dear parents who have been a constant source of inspiration and encouragement.*

*To my beloved wife and my daughters for their greatest support and patience*

*To my sister and brothers who shared their words of advice, support, and encouragement.*

# Acknowledgement

(And say “My Lord, increase me in knowledge”) The Qur’an 20:114. First, I thank Allah who has given me the power, patience, and success during the journey of my research.

I would like to express my sincere appreciation to my main supervisor Dr. Quan Xie for the guidance and support he has provided during my research work. His continuous encouragement has incredibly helped in moving my project forward and advanced my capabilities to achieving my research objective successfully. Additionally, I really appreciate his support which has extended further to my professional career and resulted in high achievements in my professional life. It has been a pleasure and honour to work under his professional supervision.

Also, I would like to extend my deepest gratitude to my co-supervisor Christopher Lagat for his assistance and contribution throughout this project. His knowledge and motivation along with his professional experience have deeply inspired me. His supervision and his insightful feedback have been really influential in developing my research skills.

I wish to express my thanks to my wonderful colleagues in Curtin University. I really appreciate their technical contribution to my publications and the sincere advice and encouragement they have been providing.

Finally, I would like to especially express my deepest appreciation to my parents, my sister, my brothers, my wife, and my daughters for their ultimate love, caring, and sacrifices throughout my research journey. Indeed, this would not have been possible without their prayers and support.

## Executive Summary

The increased concentrations of Greenhouse Gases (GHG) in particular carbon dioxide (CO<sub>2</sub>) in the atmosphere, and their impact on climate change is the most crucial issue of the world today. To address that global concern, there is a pressing need to intensify actions required to reduce CO<sub>2</sub> emissions and decarbonise the energy sector. It is perceived that CO<sub>2</sub> capture and storage (CCS) in subsurface formations such as oil and gas reservoirs is an effective means to meet net-zero emission targets.

In the last decades, remarkable and rapid breakthroughs have been made in shale gas exploitation as a result of the current advancements in multi-stage hydraulic fracturing and horizontal wells. Despite that, shale reservoirs have relatively low recovery factor (RF) where only up to 30% of the original gas in place (OGIP) could be produced economically. To maximise shale RF, releasing shale adsorbed gas has been considered to be a promising method. The great affinity of CO<sub>2</sub> over Methane (CH<sub>4</sub>) to be adsorbed on the surface of shale organic material has produced a conspicuous potential to unlock the adsorbed CH<sub>4</sub>. Thus, CO<sub>2</sub> enhanced gas recovery (CO<sub>2</sub>-EGR) in shales is taking on an active role in CO<sub>2</sub> subsurface storage and enhanced shale productivity.

Although the expected outstanding outcomes, CO<sub>2</sub>-EGR has not been commercialised nor applied in a field-scale yet. In literature, CO<sub>2</sub>-EGR has been extensively demonstrated through accomplished experimental investigations and numerical reservoir studies. Despite that, there has been a general lack in research concerning the factors influencing the efficiency. As a result, there is no clear screen tool has been yet presented to identify shale properties that yield the maximum amounts of enhanced CH<sub>4</sub> and sequestered CO<sub>2</sub>. From another perspective, numerical simulation of shale performance during CO<sub>2</sub> injection has evolved recently to consider more petrophysical mechanisms such as diffusion and multi-porosity and permeability models. However, the industry is still in need not only for a practical modelling framework, but also for more accurate modelling approaches. Therefore, constraining the uncertainties associated with the factors influencing CO<sub>2</sub>-CH<sub>4</sub> displacement, and presenting a more effective and reliable prediction approach of the process are highly recommended.

To address the above-mentioned aspects, this thesis first aims to enhance the current understating of adsorbed gas behaviour, and to constrain the uncertainties around adsorbed gas contribution to shale production in respect to reservoir depth and total organic content (TOC).

Secondly, this work seeks to present a comprehensive analysis on shale properties and engineering parameters that have the most influential effect on CO<sub>2</sub>-CH<sub>4</sub> displacement. The results of this analysis provide the industry with a screening tool to delineate a practical framework of CO<sub>2</sub>-EGR and its application on a field-scale. Additionally, due to the complexity of shale gas behaviour upon CO<sub>2</sub> injection and the intrinsic challenges in predicting CO<sub>2</sub>-EGR, the third part of this work is to develop a more effective and accurate predictive model. Basically, our model aims to employ the advancements of the artificial intelligence (AI) applications to accurately predict the efficiency of CO<sub>2</sub>-EGR. This new proposed approach of prediction enables the industry to preliminary evaluate the efficiency of CO<sub>2</sub>-EGR in an accurate and cost-effective way.

To achieve these objectives, a hybrid approach of numerical reservoir simulation, statistical analysis, and machine learning (ML) was adopted for this work. For the first objective, a reservoir simulation sensitivity study was carried out to collectively examine the impact of reservoir depth (pressure) and TOC on desorption behaviour. The model was generated and validated using the realistic data for Barnett shale reservoir. Moreover, our model incorporated a multi-porosity and multi-permeability model, hydraulic fractures, diffusion model, and local grid refinements for more precise capture of free and adsorbed gas behavior. To achieve the second and third objectives, the available datasets regarding shale properties and engineering parameters, and the amounts of enhanced production and stored CO<sub>2</sub> in shale gas were collected from the public domain. These data were then further analysed using a correlation analysis approach to identify the direction and magnitude of the correlation between the examined shale properties and engineering design parameters and the efficiency of CO<sub>2</sub>-EGR. Hence the results obtained from our correlation analysis provided more demonstration necessary to manage and predict the efficiency of CO<sub>2</sub>-EGR, these results were integrated to machine ML methods to develop a supervised ML-based predictive model. To predict CO<sub>2</sub>-CH<sub>4</sub> displacement in high precision, supervised ML method was employed to train and validate both Linear Regression and Artificial Neural Networks (ANNs) models. Afterwards, the predicted performance of training and validation was evaluated using the coefficient of determination ( $R^2$ ) to assess the accuracy in predicting the enhanced CH<sub>4</sub> due to CO<sub>2</sub> injection.

The obtained results from the simulation sensitivity study demonstrate that TOC is a major influencing parameter on adsorbed gas production in particular for shallow shale reservoirs. On the other hand, reservoir depth is found to have a negative effect of adsorbed gas contribution to shale production as adsorbed gas production decreases with increasing reservoir depth.

Together, our results indicate that adsorbed gas plays a key role in high TOC and shallow shale reservoirs. These findings further suggest that injecting CO<sub>2</sub> into deep shale reservoirs does not seem to be a viable option in particular with low TOC. This hypothesis is further supported by our statistical analysis results which reveal that shallow shale reservoirs with high fractures permeability, TOC, and CO<sub>2</sub>-CH<sub>4</sub> preferential adsorption capacity are favourable targets for CO<sub>2</sub>-EGR. Furthermore, our results indicate that a successful hydraulic-fractures network with effective values of fractures permeability and conductivity is essential for a higher CO<sub>2</sub>-EGR efficiency. Moving on to developing the ML predictive model, we based our criteria for features selection upon the above-mentioned results of correlation to adopt the best predictors for CO<sub>2</sub>-EGR efficiency. In this work, supervised machine learning techniques are used to develop, train, validate, and compare the prediction performance of linear regression and ANNs model. The result of comparison shows that ANNs of 100 gives the best predictive performance with R<sup>2</sup> of 0.78 compared to the linear regression model with R<sup>2</sup> of 0.68. Although preliminary, our developed Machine Learning (ML) model is expected to provide the industry with a practical, reliable, and cost-effective tool which can accurately predict the incremental enhanced CH<sub>4</sub> by CO<sub>2</sub> injection in shale gas reservoirs.

This work presents a significant contribution to the energy transition to the net-zero target of CO<sub>2</sub> emissions by demonstrating important insights into the application of CO<sub>2</sub>-EGR. Moreover, our results offer some important insights into the selection criteria on the physical properties and engineering parameters to yield maximum efficiency of CO<sub>2</sub>-EGR process. This work also presents for the first time a ML-based model which can accurately predict the incremental enhanced CH<sub>4</sub> by CO<sub>2</sub> injection in shale gas reservoirs.



# Table of Content

## Table of Contents

<b>WASM: Minerals, Energy and Chemical Engineering</b> .....	i
<b>Declaration</b> .....	i
<b>Copyright</b> .....	ii
<b>Dedication</b> .....	iii
<b>Acknowledgement</b> .....	iv
<b>Executive Summary</b> .....	v
<b>Table of Content</b> .....	viii
<b>List of Figures</b> .....	xi
<b>List of Tables</b> .....	xiii
<b>List of Publications</b> .....	xiv
Nomenclature.....	xv
Chapter 1. Introduction .....	1
1.1 Background .....	1
1.1 Shale Gas Production.....	1
1.3 Motivations of CO <sub>2</sub> Injection in Shale Gas Reservoirs.....	3
1.3.1. CO <sub>2</sub> Sequestration .....	3
1.3.2. Enhanced Shale Gas Recovery by CO <sub>2</sub> Injection.....	5
1.4 Research Objectives.....	7
1.5 Thesis Organisation .....	8
Chapter 2. Literature Review .....	10
2.1 Introduction.....	10
2.2 Adsorption-Desorption Behaviour .....	11
2.3 Factors Controlling the Efficiency of CO <sub>2</sub> -EGR.....	12
2.4 CO <sub>2</sub> -EGR Efficiency Prediction.....	13
2.5 Knowledge Gaps .....	15
2.5.1. The Effect of Reservoir Pressure and TOC on The Contribution of Adsorbed Gas Production. ....	15
2.5.2. Factors Controlling the Efficiency of CO <sub>2</sub> -EGR.....	16
2.5.3. Prediction of CO <sub>2</sub> -EGR Efficiency .....	16
Chapter 3. Research Framework and Methodologies .....	18
3.1 Research Framework.....	18

3.2	Research Methodologies .....	19
Chapter 4. Effect of Reservoir Pressure and Total Organic Content on Adsorbed Gas Production in Shale Reservoirs: A Numerical Modelling Study .....		
4.1	Abstract .....	21
4.2	Introduction.....	22
4.3	Theory .....	23
4.3.1.	Shale Gas Production .....	23
4.3.2.	Multi-Porosity and Multi-Permeability Model .....	25
4.3.3.	Gas Adsorption Isotherm .....	26
4.3.4.	Gas Transport Mechanism .....	27
4.4	Methodology of Reservoir Modelling.....	27
4.4.1.	Model Development.....	27
4.4.2.	Calibration of the Shale Mechanistic Model.....	30
4.5	Results and Discussion.....	33
<b>4.5.1.</b>	Effect of Reservoir Pressure on Adsorbed Gas Production .....	33
<b>4.5.2.</b>	Effect of TOC on Adsorbed Gas Production .....	35
4.6	Conclusions and Implications .....	36
Chapter 5. Statistical Analysis of Controlling Factors on Enhanced Gas Recovery by CO <sub>2</sub> Injection in Shale Gas Reservoirs .....		
5.1	Abstract .....	38
5.2	Introduction.....	39
5.3	Motivation of CO <sub>2</sub> Injection in Shale Gas Reservoirs .....	40
<b>5.3.2.</b>	CO <sub>2</sub> Sequestration .....	41
<b>5.3.2.</b>	Enhanced Gas Recovery .....	43
5.4	Correlation Coefficient for Factors Analysis .....	46
<b>5.4.1.</b>	Exploratory Data Analysis .....	46
<b>5.4.2.</b>	Spearman Correlation Coefficient .....	50
5.5	Results and Discussion.....	51
5.5.2.	The Effect of Shale Petrophysical Parameters on CO <sub>2</sub> -EGR .....	51
5.5.1.1.	The Effect of Permeability .....	52
5.5.1.2.	The Effect of TOC .....	53
5.5.1.3.	The Effect of Adsorption Capacities.....	54
5.5.1.4.	The Effect of Reservoir Depth (Pressure).....	54
5.5.1.5.	The Effect of Porosity .....	54
5.5.1.6.	The effect of Reservoir Temperature .....	55
5.5.1.7.	The Effect of Reservoir Thickness.....	55

5.5.2.	The Effect of Engineering Parameters on CO <sub>2</sub> -EGR .....	56
5.5.2.1.	The Effect of Injection Scenario .....	57
5.5.2.2.	The Effect of Fracture Conductivity and Permeability .....	57
5.5.2.3.	The Effect of Injection Pressure.....	57
5.5.2.4.	The Effect of Well Spacing.....	58
5.5.2.5.	The Effect of Fracture Half-Length .....	58
5.6	Conclusions and Implications .....	59
Chapter 6. Application of Supervised Machine Learning to Predict the Enhanced Gas Recovery by CO <sub>2</sub> Injection in Shale Gas Reservoirs .....		
6.1	Abstract .....	61
6.2	Introduction.....	62
6.3	Methodology .....	64
6.3.1.	Machine Learning Methods .....	64
6.3.2.	Exploratory Data Analysis .....	69
6.3.3.	Feature Selection.....	74
6.3.3.	Model Training and Validation.....	78
6.4	Model Selection .....	78
6.4.1.	Linear Regression Model.....	79
6.4.2.	Artificial Neural Networks (ANNs).....	80
6.5	Conclusion .....	83
Chapter 7. Conclusions and Recommendations.....		
7.1	Conclusions.....	85
7.2	Effect of Reservoir Pressure and Total Organic Content on Adsorbed Gas Production in Shale Reservoirs: A Numerical Modelling Study .....	86
7.3	The Controlling Factors on Enhanced Gas Recovery by CO <sub>2</sub> Injection in Shale Gas Reservoirs .....	87
7.4	Application of Supervised Machine Learning to Predict the Enhanced Gas Recovery by CO <sub>2</sub> Injection in Shale Gas Reservoirs.....	88
7.5	Recommendations for Future Work.....	89
References.....		90
<b>Appendix</b> .....		100
A.	Attribution Statement.....	<b>Error! Bookmark not defined.</b>
B.	Copyright Agreement.....	100

## List of Figures

Figure 1. 1 Global energy-related CO <sub>2</sub> emissions (1990-2021) [41].....	4
Figure 3. 1 A summary of the research framework and methodology approach taken for each objective.....	19
Figure 4. 1 The production profile of free and adsorbed gas for Barnett shale reservoir calculated by our predictive simulation model. ....	24
Figure 4. 2 Methane adsorption isotherms analysis at a range of pressure values calculated for New Albany Shale and Ohio Shale [23].....	25
Figure 4. 3 2D view of the Barnett shale reservoir model.....	30
Figure 4. 4 Typical gas content measured by core analysis for Barnett shale reservoirs at depth of 7640 feet and 4% of TOC reproduced from [117] .....	31
Figure 4. 5 The simulated fractions of adsorbed and free gas volumes are compared to fractions measured by core analysis for Barnett shale reservoirs at depth of 7640 feet and 4% of TOC .....	32
Figure 4. 6 The recovery factors estimated by our calibrated model at 8% of TOC.....	32
Figure 4. 7 Fractions of produced adsorbed gas to the total cumulative production at different reservoir depths at a range of 4 - 8% of TOC.....	34
Figure 4. 8 The simulated pressure decline profile for 4% TOC and 4000 psi initial pressure. ....	34
Figure 4. 9 The cumulative production from adsorbed gas volumes with range of 4 - 8% TOC.....	36
Figure 5. 1 -a: 2-D image of shale gas sample showing the organic material in a dark gray dispersed in light gray inorganic materials. b: 3-D shale segmentation showing in light color the interconnected organic pockets [9]. [Copyright 2011, Society of Petroleum Engineers].40	
Figure 5. 2 Typical shale gas pores system and storage mechanism [110][Copyright 2013, Society of Petroleum Engineers] .....	41
Figure 5. 3 Global CO <sub>2</sub> emission from fossil fuels [1] .....	42

Figure 5. 4 Spearman correlation for shale properties .....	52
Figure 5. 5 Spearman correlation for injection engineering parameters.....	56
Figure 6. 1 Shale gas production from shale and other resources in selected counties in 2015 and 2040 [153] .....	62
Figure 6. 2 The standard workflow of supervised ML .....	66
Figure 6. 3 A simple workflow for unsupervised learning to solve clustering problems.....	68
Figure 6. 4 Represents a basic workflow reinforcement learning .....	68
Figure 6. 5 Boxplots show the range of the main shale properties, incremental RF, and sequestered CO <sub>2</sub> in our dataset .....	71
Figure 6. 6 Spearman correlation between shale properties and incremental CH <sub>4</sub> .....	76
Figure 6. 7 Spearman correlation between the selected features and incremental CH <sub>4</sub> .....	77
Figure 6. 8 Prediction of enhanced gas recovery- training set for linear regression model ....	79
Figure 6. 9 Prediction of enhanced gas recovery- validation set for linear regression model.	79
Figure 6. 10 ANNS connected layers and outputs [185] .....	80
Figure 6. 11 Prediction of Enhanced Gas Recovery- Training Set for Neural Network Regression Model .....	81
Figure 6. 12 Prediction of Enhanced Gas Recovery- Validation set for Neural Network Regression Model .....	81

# List of Tables

Table 1. 1 A summary of gas transport mechanisms during the process of CO <sub>2</sub> -EGR .....	5
Table 4. 1 The fracture data for used for Barnett model.....	28
Table 4. 2 The reservoir properties of Barnett shale reservoir. ....	28
Table 4. 3 Langmuir constants of CH <sub>4</sub> for Barnett shale gas reservoir [17, 114].....	29
Table 5. 1 Simulation studies and shale types used for dataset. ....	46
Table 5. 2 The range of petrophysical parameters used in dataset .....	48
Table 5. 3 The range of engineering parameters used in dataset .....	49
Table 6. 1 The wide range of shale properties and engineering design parameters in our dataset .....	69
Table 6. 2 The breakdown of shale types and number of cases for each study used in our dataset .....	72
Table 6. 3 The methodology used for handling the missing values in our dataset .....	74
Table 6. 4 Overall performance comparison of linear regression and ANNs models .....	81
Table 6. 5 Hyper-parameters for the selected ANNs regression model .....	82

# List of Publications

Published papers forming parts of the thesis as standalone chapters:

## Chapter 4

Mansi, M., Almobarak, M., Lagat, C. *et al.* Effect of reservoir pressure and total organic content on adsorbed gas production in shale reservoirs: a numerical modelling study. *Arab J Geosci* **15**, 134 (2022). <https://doi.org/10.1007/s12517-021-09416-x>

## Chapter 5

Mansi, M., Almobarak, M., Lagat, C. and Xie, Q., 2023. Statistical Analysis of Controlling Factors on Enhanced Gas Recovery by CO<sub>2</sub> Injection in Shale Gas Reservoirs. *Energy & Fuels* (2023). <https://doi.org/10.1021/acs.energyfuels.2c03216>.

## Chapter 6

Mansi, M., Almobarak, M., Ekundayo, J., Lagat, C. and Xie, Q., 2023. Application of Supervised Machine Learning to Predict the Enhanced Gas Recovery by CO<sub>2</sub> Injection in Shale Gas Reservoirs. *Petroleum* (2023). <https://doi.org/10.1016/j.petlm.2023.02.003>

# Nomenclature

bcm	million cubic meters
tcf	trillion cubic feet
TOC	total organic content
CH <sub>4</sub>	Methane
CO <sub>2</sub>	Carbon Dioxide
CO <sub>2</sub> -EGR	enhanced gas recovery by CO <sub>2</sub> injection
ESGR	enhanced shale gas recovery
CBM	coal bed methane
OGIP	original gas in place
GHG	greenhouse gases
CCS	carbon capture and storage
RF	recovery factor
AI	artificial intelligence
ML	machine learning
LSSVM	support vector machine
MAR	missing at random
MNAR	missing not at random
ANOVA	analysis of variance
ANNs	artificial neural networks



*This page intentionally left blank*

# Chapter 1. Introduction

## 1.1 Background

Natural gas has become a significant contributor to the energy market and currently plays an important role in the energy transition to the clean energy. The global energy demand for natural gas has been continuously growing over the past two decades. Since 2020, the global economy has dramatically changed due to the impact of Covid-19 pandemic together with geopolitical instability. Nevertheless, the energy demand increased in 2021 by 4%, and it is projected to continue growing further by 1.3% per year up to 2030.

Moreover, the global increase in natural gas demand by 2030 is projected to reach up to 15% according to IEA [1]. In response to this accelerated trend, the reserves from conventional gas reservoirs are declining and are seen to be unable to effectively meet the emerging markets consumption. Consequently, due to the huge discovered reserves and clean burning, shale gas reservoirs have become increasingly important as a major alternative resource of natural gas supply before new energy backs up in future [2].

The development of shale gas resources has recently made a series of breakthroughs worldwide. With the fast-growing technologies of hydraulic fracturing and multi-stage horizontal drilling, many countries have widely commercialised production from shale gas resources [3]. Based on support of the current stated policies of net-zero emissions, natural gas production from shale reservoirs is expected to be 1013 (bcm) in 2030 and to increase further by 2050 to 1136 (bcm)[1]. China has the largest recoverable shale gas reserves in the world which accounted for 115 (tcf) in 2015 [4]. Gas production from shale and tight formations is expected to account for two-thirds of the total gas production in the United States (U.S.) in 2040 [5]. Along with large-scale shale development in U.S. and China, Canada, China, and Argentina are currently the top leading counties in commercialisation of shale gas production [6].

## 1.1 Shale Gas Production

Shale sediments have a complex geological and petrophysical system characterized by extremely low porosity and permeability and high total organic content (TOC) [7]. Shale formation is considered an unconventional resource as it is both a reservoir and source rock [8]. A typical shale pores system consists of two distinct types, fractures, and matrix pores.

Recently, typical 2-D and 3-D high resolution imaging have shown that large and interconnected organic matter pockets are dispersed within the shale matrix [9]. Shales store gas as free gas in fractures and matrix pores, with adsorbed gas on the surface on the organic materials, and dissolved gas in reservoir fluids [9, 10]. Consequently, thermally matured shales with high TOC are promising prolific reservoirs for gas production since they hold a considerable amount of adsorbed gas [11]. The adsorbed gas is the key component from shale gas recovery as it accounts for up to 85% of the total gas content [12]. Despite that, due to the extremely low-permeability nature, shale gas reservoirs typically show a very low recovery factor (up to 30%) compared with the conventional reservoirs [13]. In typical primary production of shales, gas production dramatically declines after a high initial rate. This early stage production is short-term and is mainly dominated by free gas flow within natural and induced fractures. As gas production decreases and reservoir pressure declines with time, the adsorbed gas presents as free gas in the shale matrix as a result of desorption phenomenon, hence contributing to total gas production. Unlike the early stage, this later stage is a long-term production which is dominated by the adsorbed and free gas [14]. Hence, the later stage of shale gas production is the significant contributor toward total shale gas production. In other words, the pintail of shale gas production curve over time has attracted a great attention associated with desorption behaviour. This process has a huge potential to increase shale productivity and achieve more shale gas at commercial rates.

Previous studies on shale gas production have paid a particular attention to adsorption and desorption behaviour. A few studies identified governing factors on gas desorption during shale gas production. Some of them focused only on the impact of hydraulic fracture parameters on both free and adsorbed gas [15, 16]. Additionally, several studies have attempted to examine the influencing reservoir parameters on shale gas production [14, 17]. However, the multi-porosity and diffusion models have not been considered in their studies. Although further investigations have been conducted to consider the multi-porosity and permeability model [18, 19], the impacts of TOC and reservoir pressure and depth have been widely investigated. Based on the publications, it appears that the parameters which govern the contribution of adsorbed gas on shale gas production remains unclear, which presents a substantial impediment on management and performance predictions of shale gas reservoirs. Whilst several sensitivities studies have been carried out in the literature to evaluate the desorption behaviour, to the best of our knowledge, no research has been carried out to investigate the impact of reservoir depth on the production of adsorbed gas considering TOC with a combination of the multi-

permeability and diffusion models. Therefore, the roles of reservoir depth (i.e., pressure) coupled with TOC have been taken into account as a part of this thesis, examining the contribution of adsorbed gas to quantify shale gas production.

### 1.3 Motivations of CO<sub>2</sub> Injection in Shale Gas Reservoirs

As mentioned above, the adsorbed gas plays a key role in shale gas production by maintaining the long-term production plateau. The pressure difference between the free and adsorbed gas is the key controller of the desorption phenomenon [20]. Given the low pressure drop due to the ultra-low matrix permeability nature of shales, adsorbed gas is very unlikely to desorb from the surface of organic matter. [7]. Furthermore, the transport of adsorbed gas is even more complex and takes longer time than free gas[21]. Consequently, the contribution of adsorbed gas can account for up to only 26% of the total gas production depending on initial reservoir pressure (depth), pressure draw down, and TOC [22]. Thus, presenting effective techniques to unlock the adsorbed CH<sub>4</sub> has been an increasingly important area in enhancing shale gas recovery.

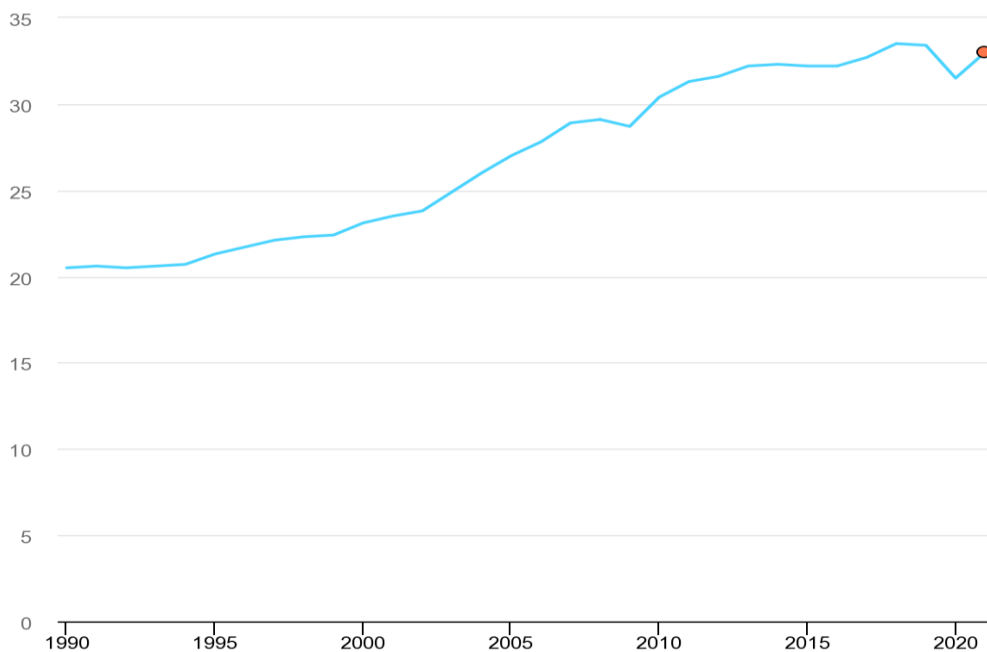
One of the promising techniques is the injection of Carbon Dioxide (CO<sub>2</sub>) into shale gas reservoirs to enhance CH<sub>4</sub> recovery which can be referred to (CO<sub>2</sub>-EGR). The potential of enhanced shale gas recovery (ESGR) was first presented experimentally by Nuttal in 2005 [23]. In his study, he concluded that shale gas reservoirs can behave very similarly to coal bed methane, CBM, where CO<sub>2</sub> molecules preferentially adsorb to the surface of shale organic materials over CH<sub>4</sub> at a ratio of 5:1. As a result of this remarkable finding, shale gas reservoirs have become potential targets not only for enhanced gas recovery, but also for long-term geological CO<sub>2</sub> sequestration to mitigate the adverse effect of anthropogenic CO<sub>2</sub> emissions which are strongly related to the global concern of climate change [24, 25]. Further studies have proven that the injected CO<sub>2</sub> into shale matrix could be permanently sequestered with a potential of additional CH<sub>4</sub> recovery up to 59% [7, 10, 26-34].

#### 1.3.1. CO<sub>2</sub> Sequestration

CO<sub>2</sub> emission generates a global public concern as being the direct cause of global climate change [35]. Since the industrial revolution, the emissions of Greenhouse Gases (GHG) in particular CO<sub>2</sub> have been increasing as a result of the extensive consumption of fossil fuels to meet the global energy demand as shown in Figure 1.1 [36]. For this reason, global agreements

have been made and net-zero emissions policies have been stated to intensify actions needed to mitigate the emissions of CO<sub>2</sub> [37]. To solve this problem, several approaches have been proposed. CO<sub>2</sub> geological sequestration is one of the most practical approaches that has been proposed for CO<sub>2</sub> long-term storage [38, 39].

The geological sequestration is a permanent storage solution in which CO<sub>2</sub> is injected into deep geologic formations such as Depleted oil and gas reservoirs, CBM, and deep saline formations have the potential to store CO<sub>2</sub> permanently [39, 40].



[41]

Figure 1. 1 Global energy-related CO<sub>2</sub> emissions (1990-2021) [41]

Despite the reduction gained in 2019 and 2020 due to COVID-19 outbreak, according to IEA [1], CO<sub>2</sub> emissions increased in 2021 and are projected to further increase due the expected increased energy demand as a result of global economic recovery after the COVID-19 pandemic. Obviously, this highlights the need for accelerating implementations of carbon capture and storage (CCS) projects. As previously mentioned, the great affinity of CO<sub>2</sub> to be adsorbed on the surface on shale organic materials more than CH<sub>4</sub>, presents an encouraging prospect for CO<sub>2</sub> injection due its dual benefit for CO<sub>2</sub> sequestration and improved shale gas recovery[42].

In the process of injecting CO<sub>2</sub> into shale reservoirs, identifying driving factors of the subsurface geochemical and geophysical process is the critical role to minimize the potential of CO<sub>2</sub> breakthrough and to minimise the costs [43]. The published work on evaluating the efficiency of CO<sub>2</sub>-EGR has been mostly restricted to limited sensitivity studies. These studies tended to examine the effect of influencing parameters on EGR and/or CO<sub>2</sub> sequestration in a separate approach of investigation. The key challenging issue is that some parameters have a profound dual-effect on the effectiveness of the process. For example, enhanced CH<sub>4</sub> production decreases with increasing the well spacing, while the amount of stored CO<sub>2</sub> increases as a limited amount of CO<sub>2</sub> is less likely to migrate to the zone of CH<sub>4</sub> producers due to the ultra-low matrix permeability of shale matrix. Similarly, although injection CO<sub>2</sub> at a high injection rate increases the total enhanced CH<sub>4</sub>, to some extent, it increases the mechanical mixing of CO<sub>2</sub>-CH<sub>4</sub> which results in an early CO<sub>2</sub> breakthrough [24]. Therefore, a correlation analysis must be carried out to investigate the controlling factors of CO<sub>2</sub> sequestration more broadly taking into consideration their effect on the enhanced CH<sub>4</sub>. By employing correlation analysis approach, the direction and the strength of the relationship between the examined parameters and both CO<sub>2</sub> sequestration and EGR need to be identified.

### 1.3.2. Enhanced Shale Gas Recovery by CO<sub>2</sub> Injection

In the process of CO<sub>2</sub>-EGR, the main mechanism of EGR and CO<sub>2</sub> storage is CH<sub>4</sub> desorption which is mainly driven by CO<sub>2</sub> competitive adsorption. Whilst shale reservoirs present a complexity in mechanisms by which free and adsorbed gas are stored and transmitted, more key challenges arise with CO<sub>2</sub> injection into shale matrix. Upon injection, a competitive adsorption phenomenon takes place where CO<sub>2</sub> molecules start to release the adsorbed CH<sub>4</sub> from the organic surface. Consequently, the desorbed CH<sub>4</sub> transports towards fractures and producers [33]. In addition to competitive adsorption, the injected stream of CO<sub>2</sub> initiates a counter-diffusive process in shale matrix between CH<sub>4</sub> and CO<sub>2</sub> molecules. With considering the multi-porosity system of organic, inorganic, and fractures pores, gas flow process can be represented as shown in Table.1.1 [44].

*Table 1. 1 A summary of gas transport mechanisms during the process of CO<sub>2</sub>-EGR*

<i>Pores system</i>	<i>Transport mechanism</i>	<i>Transported gas</i>
Fractures	Convective and dispersive	Injected CO <sub>2</sub> , free, and desorbed gas
Inorganic pores	Convective-diffusive	Free gas

Organic Pores	Surface diffusion	Free and desorbed gas
---------------	-------------------	-----------------------

Even though, EGR- CO<sub>2</sub> injection has not been commercialised yet, a considerable amount of laboratory tests and simulation studies have been carried out on the feasibility of the technique and to examine the driving factors of the process efficiency. CO<sub>2</sub>-EGR is a complex geophysical process as the efficiency of the process displacement is governed by shale properties (such as TOC, matrix permeability, and adsorption capacities) and engineering design parameters (such as injection pressure and well spacing) [45] [46]. Given the above-mentioned complexity in predicting gas transport, the previous research extensively investigated these factors to constrain the intrinsic uncertainties of the modelling of CO<sub>2</sub>-EGR process[26, 27, 47-52].

An in-depth review of scientific literature on CO<sub>2</sub>-EGR (discussed in detail in Chapter.2), shows that there are still uncertainties presenting a substantial impediment in determining the main factors that control CO<sub>2</sub> sequestration and enhanced CH<sub>4</sub> recovery in shale reservoirs. In addition, no quantitative framework and accurate CO<sub>2</sub>-EGR modelling, and design process has been developed.

The knowledge gap mentioned above may be attributed to the following reasons:

1. The complexity of storage and transport mechanisms coupled with the heterogeneity nature of shale formations are presenting challenges when modelling and predicting CO<sub>2</sub>-EGR in lithology, TOC, pore size, texture, and petrophysical properties [53].
2. Most researchers to date have tended to conduct sensitivity analysis to investigate the effect of a few parameters individually rather than treating the controlling parameters collectively in much detail.
3. The lack of field-scale test observations.

Therefore, there is a need to bridge this gap and thus provide a comprehensive understanding on the correlation between shale properties as well as engineering parameters and the efficiency of CO<sub>2</sub>-EGR. The outcome of this analysis helps the industry with conceptual understanding whilst designing and implementing CO<sub>2</sub>-EGR in shale gas reservoirs.

Numerical reservoir simulation techniques are widely accepted as indispensable tools for realistic prediction and evaluation of reservoir performance [22]. Reservoir simulation techniques have been providing the industry a preliminary stage of CO<sub>2</sub>-EGR efficiency

evaluation on a field-scale. In literature, a considerable volume of numerical simulation studies has presented the applicability of CO<sub>2</sub>-EGR on a wide range of investigations. For example, examined the applicability of the process to several shale types such as Barnett shales [7, 31, 54] and Devonian shales [10, 32]. Furthermore, few studies have been made to evaluate the performance of huff-and-puff injection [7, 10, 28, 32, 55] while great attention was paid to flooding injection scenario such as studies done by [30, 33, 56, 57]. From previous numerical modelling, some of previous studies have employed multi-porosity and permeability model [28, 32]. In recent simulation work, the multi-component effect of gas transport and adsorption has been taken into consideration [44, 54]. Nevertheless, challenges arise when simulating CO<sub>2</sub> /CH<sub>4</sub> displacement within the complex pores system of shales and quantifying the efficiency enhanced CH<sub>4</sub> recovery and CO<sub>2</sub> sequestered.

It is widely accepted that numerical modelling of shale reservoirs has presented unique challenges not only due to the heterogeneity nature of shale petrophysical properties , but also due to the complex storage and transport mechanisms of free and adsorbed gas [53, 58]. For these reasons, more difficulties and challenges arise in modelling CO<sub>2</sub>-EGR process in shale reservoirs. Considering both the cost of field injection tests and many uncertainties in the numerical simulation process, the conventional energy industry therefore requires a new developed tool/approach to evaluate the potential of applying CO<sub>2</sub> injection to shale gas reservoirs. The motivation behind this approach is to present a reliable and cost-effective tool to manage and predict the incremental enhanced CH<sub>4</sub> by CO<sub>2</sub> injection in shale gas reservoirs.

## 1.4 Research Objectives

The major objectives of this thesis are to clarify several aspects of adsorbed gas contribution to total shale production and thus provides practical screening tools to evaluate, manage and predict the efficiency of enhanced gas recovery and CO<sub>2</sub> sequestrations in shale gas reservoirs. In addition, the objectives of this work mainly are to obtain results and develop tools which will help address and remedy the research gaps in the area of CO<sub>2</sub>-EGR that previously mentioned in sections 1.2, 1.3.1, and 1.3.2 in the Introduction chapter. Furthermore, this study aims to offer significant contributions to reaching the target of net-zero CO<sub>2</sub> emissions for energy transitions.

Three major objectives of this thesis are listed as follows



Objective#1 – Investigate the effect of reservoir pressure and total organic content (TOC) on adsorbed gas production

Objective#2 - Identify the correlation between shale properties / engineering parameters and the efficiency of CO<sub>2</sub>-EGR

Objective#3 - Develop a reliable and cost-effective tool to accurately predict the incremental enhanced CH<sub>4</sub>

To achieve our research objectives, the methodological approach taken in this study is a combination of numerical reservoir simulation, statistical analysis, and machine learning modelling. This will be discussed in detail in chapter 3.

## 1.5 Thesis Organisation

The overall structure of the thesis takes the form of seven chapters including the Introductory Chapter. The layout of the thesis can be seen as below.

**Chapter 1 – Introduction and Background** – This chapter provides a high-level research introduction and background to shale gas production and CO<sub>2</sub>-EGR technique in shale gas reservoirs.

**Chapter 2 – Literature Review** This chapter gives a comprehensive literature review of previous research studies that have been carried out to investigate adsorbed gas production and contribution, as well as the feasibility and the controlling factors of enhanced shale gas recovery by CO<sub>2</sub> injection.

**Chapter 3 – Research Objectives and Methodologies** – This chapter gives a brief overview of our work objectives and methodologies.

**Chapter 4 – Effect of Reservoir Pressure and Total Organic Content on Adsorbed Gas Production in Shale Reservoirs: A Numerical Modelling Study** – This chapter presents and discusses the results of a detailed numerical simulation study performed to examine the effect of reservoir depth and TOC on the contribution of adsorbed gas to shale gas production.

**Chapter 5 – Statistical Analysis of Controlling Factors on Enhanced Gas Recovery by CO<sub>2</sub> Injection in Shale Gas Reservoirs** – In this chapter, the results of a correlation analysis

carried out to identify the strength of the relationship between shale properties and engineering design parameters, and the efficiency of CO<sub>2</sub>-EGR with a detailed discussion of the findings.

**Chapter 6 – Application of Supervised Machine Learning to Predict the Enhanced Gas Recovery by CO<sub>2</sub> Injection in Shale Gas Reservoirs** –This chapter presents and assess application of a developed Supervised Machine Learning (ML) based model to preliminary evaluate CO<sub>2</sub>-EGR efficiency. It also presents and evaluates the performance of the proposed model.

**Chapter 7 – Conclusion and Recommendations** – This final chapter draws upon the entire thesis, giving a summary of our results, implications, and recommendations for the future work.

# Chapter 2. Literature Review

## 2.1 Introduction

Over the past two decades, published studies have shown an increased interest in the promising technique of CO<sub>2</sub>-EGR to achieve enhanced CH<sub>4</sub> productivity and CO<sub>2</sub> sequestration. More recently, the dual benefits of CO<sub>2</sub>-EGR, the growing demand for natural gas, and the increased concerns about climate change has made the petroleum researchers continuously working to constrain the uncertainty about the process and to present a framework for field-scale applications. Although the same conceptual application, the research on CO<sub>2</sub> injection in shale reservoirs is less advanced than that for CO<sub>2</sub> injection in CBM [59]. These previous studies have sought to answer the raised questions about feasibility and the applicability of CO<sub>2</sub> injection in shale reservoirs. More specifically, desorption mechanism in both primary production and during CO<sub>2</sub> injection, the factor influencing the efficiency of the process, and prediction of the amounts of enhanced CH<sub>4</sub> and sequestration CO<sub>2</sub>.

Since the desorption phenomenon plays the key role in CO<sub>2</sub>-EGR, the desorption behavior has received considerable attention not only for CO<sub>2</sub> injection purposes, but also for the primary production of shale reservoirs. In literature, the desorption behavior has been studied by experimental investigations and numerical simulation. While most of the previous investigations were centered on quantifying the desorbed gas production, a few studies examined the factors influencing the contribution of adsorbed gas to the total shale gas production. In contrast, investigations on the desorption performance during CO<sub>2</sub>-EGR were mainly concerned with the influencing factors rather than quantifying the desorbed gas production. In literature, sensitivity studies have been the only approach taken for these previous investigations to examine the impact of shale petrophysical properties and engineering parameters on CO<sub>2</sub>-CH<sub>4</sub> displacement. However, numerical reservoir simulation has been widely used for quantifying the amounts of both enhanced CH<sub>4</sub> and sequestered CO<sub>2</sub>. Nevertheless, a wide range of modelling approaches has been presented in literature. For example, some studies have employed a multi-porosity and permeability model [28, 32] while other studies have considered a dual-porosity and permeability model [10, 57].

In this chapter, firstly, we present a review and identify the gap in knowledge on the work done concerning the adsorbed gas production in shale gas primary stage. In particular, highlight the previous studies that have attempted to identify the major contributing factors for adsorbed gas

production during the primary stage of production. Secondly and more broadly, we explore the studies that addressed the controlling factors of both enhanced CH<sub>4</sub> and sequestered CO<sub>2</sub>. Finally, previous attempts were made to predict the efficiency of CO<sub>2</sub>-CH<sub>4</sub>; additionally, the methodology taken and assumptions for each study are presented.

## 2.2 Adsorption-Desorption Behaviour

The adsorption and desorption phenomenon has been investigated in a growing body of literature. Although several studies have widely focused on adsorption behavior [60-62], few studies identified the factors governing desorption in shale gas production. While some studies focused on the impact of engineering design factors such as well pattern, hydraulic fracture, and well spacing, other studies investigated the influencing reservoir parameters on adsorbed gas production. However, the majority of the previous studies focused on the effect of reservoir parameters.

Several studies drew attention to the effect of hydraulic fractures configuration on adsorbed gas production in shale primary stage. In his study, [16] demonstrated that larger fractures possess higher pressure drop which facilitates the desorption process. Similarly, [15] concluded that longer and wider fractures are favorable for adsorbed gas production. A recent study by [63] presented the impact of well configuration, he stated that the desorption becomes minor with vertical wells if compared to horizontal well production. The effect of network fracture conductivity was presented by [64], the reduction in fracture conductivity reduces the cumulative production of both free and adsorbed gas. Although this work presented interesting findings, the work neglected the diffusion of desorbed gas to primary shale matrix and and/or the induced fractures.

Other studies investigated the effect of shale reservoir parameters on both free and adsorbed gas production. For example, as noted by [15, 65, 66], shale matrix permeability was found to have a significant impact on adsorbed gas production as higher matrix permeability results in releasing more adsorbed gas towards shale matrix. Moreover, [67] in his analysis he reported that higher the production of adsorbed gas tends to decrease with increasing the adsorption layers thickness. [15] concluded that high Langmuir volume and pressure lead to more production from adsorbed gas. However, the multi-porosity and diffusion models have not been considered in their studies. Obviously, neglecting the multi porosity and permeability effect of shales may lead to inaccurate capturing of desorbed gas transient within shale matrix. Another

study by [14] pointed out that longer and sustainable production promotes the production from the adsorbed gas. [17, 68] concluded very similar findings as their study highlighted the insignificant contribution of adsorbed gas at an early stage of production. Whilst further investigations considered the multi-porosity and permeability models such as [18, 19], the impact of TOC and reservoir pressure were not studied.

### 2.3 Factors Controlling the Efficiency of CO<sub>2</sub>-EGR

Even though CO<sub>2</sub>-EGR injection has not been commercialised yet, a considerable amount of laboratory tests and simulation studies and experimental investigations have been carried out on the feasibility of the technique. The concept of CO<sub>2</sub> injection was first extended to shale gas reservoirs by [23]. His experimental study has demonstrated that shales can react very similarly to coal-bed methane where organic matter CO<sub>2</sub> is preferentially adsorbed on organic surface over CH<sub>4</sub> at a ratio of 5:1. These remarkable observations have drawn attention to shales as potential geological traps for CO<sub>2</sub> permanent sequestration and EGR. Therefore, many numerical simulation and experimental investigations have been conducted to investigate CO<sub>2</sub> storage capacity and prove the viability of enhanced gas production from different shale reservoirs. In literature, shale reservoirs have been proven to be promising targets for EGR-CO<sub>2</sub> [31, 33, 44, 54].

Investigating reservoir parameters which govern the applicability of CO<sub>2</sub>-EGR has been extensively undertaken in literature. According to several studies, natural and induced fractures permeabilities are the key influencing parameters on the efficiency of EGR and CO<sub>2</sub> sequestration, where a higher fractures permeabilities results in high enhanced gas recovery and CO<sub>2</sub> thus likely to sequester [20, 34, 69, 70]. Additionally, matrix permeability has been recognised as the most significant factor in many studies [7]. In contrast to those findings, [26] demonstrated that EGR efficiency correlates negatively with matrix permeability due to higher pore fractal dimension. [20] demonstrated that reservoir pressure plays the key role in the process where low reservoir pressure facilitates CH<sub>4</sub> displacement by injected CO<sub>2</sub>. In addition to reservoir pressure effect, the TOC has been found as a significant parameter on CO<sub>2</sub> storage [26, 32]. Later in 2014, [55] pointed out the significance of matrix porosity on the incremental recovery.

A considerable amount of literature has investigated the effect of engineering design parameters on CO<sub>2</sub>-EGR. The injection pressure has been investigated. [31] highlighted that, despite the positive correlation between injection pressure and enhanced gas recovery, early

severe breakthrough of CO<sub>2</sub> is very likely to occur. Conversely, [71] reported no significant effect of increasing CO<sub>2</sub> injection rates on shale gas recovery. This view was supported by [72] in his numerical simulation study. In another investigation, the correlation between the production time and enhanced recovery has been addressed. [28] demonstrated that production time and pressure significantly affect CO<sub>2</sub> sequestration and shale gas recovery. On the other hand, [10] performed a comprehensive simulation work investigating a series of injection scenarios of CO<sub>2</sub> flooding (continuous injection) and huff and puff (injection-soaking cycle). Their simulation results showed that CO<sub>2</sub> flooding into shale reservoirs showed a significant increase in recovery with about 50% of injected stream being sequestered. In terms of well configuration, [33] reported in his study that 7% incremental recovery could be achieved at optimal wells pattern.

## 2.4 CO<sub>2</sub>-EGR Efficiency Prediction

The efficiency of CO<sub>2</sub>-EGR is represented by two main parameters. First, incremental RF which represents the amount and the additional CH<sub>4</sub> production due to CO<sub>2</sub> injection. Second, sequestered CO<sub>2</sub> which represents the amount of adsorbed CO<sub>2</sub>. Since CO<sub>2</sub>-EGR has been only tested once on a small field-scale, research on that subject has been mostly restricted to numerical simulation. Obviously, numerical reservoir simulation techniques are widely accepted as indispensable tools for realistic prediction and evaluation of reservoir performance [22]. Therefore, reservoir simulation studies have offered a preliminary stage of CO<sub>2</sub>-EGR efficiency evaluation on a field-scale. Thus, there has been a large volume of simulation studies investigating the applicability of CO<sub>2</sub>-EGR to several shale types and the effectiveness of different injection scenarios.

In literature, the previous studies were conducted using various modelling techniques and approaches. For example, some previous studies employed multi-porosity and permeability model to accurately simulate gas transport mechanisms within shale organic, inorganic, and fractures [28, 32], while other studies considered single and dual-porosity and permeability models [10, 31, 32, 57]. In recent simulation work, the multi-component effect of gas transport and adsorption was taken into consideration [44, 54]. Most recently, the effect of multi components was considered in many simulation studies [30, 44, 54, 73]. In his simulator, [73] considered pressure-dependent permeability associated with CO<sub>2</sub> injection into shale reservoirs. Along with modelling approaches, simulation models under different injection

scenarios were also considered. In literature, few studies have been made to evaluate the performance of huff-and-puff injection [7, 10, 28, 32, 55], while great attention was paid to flooding injection scenario such as studies done by [30, 33, 56, 57].

Since their revolution, machine learning applications have been broadly applied to various domains such as medical applications, biochemical, natural language processing, finance, and social media services [74]. Commonly, the processed datasets associated with the oil and gas industry are huge, complex in terms of correlation [75]. Thus, the applications of machine learning have also been extended to several areas in the oil and gas industry [76]. Recently, ML algorithms have been widely used to enhance and resolve several reservoir engineering aspects such as permeability prediction [77, 78]. Additionally, ML-based models have been created and employed for production estimation and optimization in several studies presented in literature [79, 80]. Furthermore, supervised machine learning models have demonstrated potential solution for several issues in the industry, for example the ML model presented by [81] for early fault prediction of centrifugal pump in the process engineering, and the ML based approach to monitor CO<sub>2</sub> geological sequestration and simulate CO<sub>2</sub> leakage [40].

Due to the complexity associated with shale gas modelling, ML applications have been also employed to help with shale gas production monitoring, and prediction [82]. In 2020, [79] presented a ML based predictive model to estimate the productivity of shale gas wells. Very similarly, [83] integrated ANNs based model with decline curve analysis to predict shale gas production curve. More recent studies introduced solutions for shale gas production optimization such as [84-87]. Methane adsorption capacity in shale gas was also studied, [88, 89] developed a supervised machine learning model to predict CH<sub>4</sub> adsorption in shale gas. Despite this, only a few studies concerned with the application of ML study the performance of CO<sub>2</sub> injection into shale gas reservoirs. As an example, ML-based approach was employed by [90] to simulate CO<sub>2</sub>-CH<sub>4</sub> displacement to predict CO<sub>2</sub> adsorption in fractured shale reservoirs. However, his ML model was incorporated with numerical simulation, and it was only utilized to expand the computational limits. Very similarly, [50] developed a Support Vector Machine (LSSVM) model which is able to estimate the adsorption capacities of both CO<sub>2</sub> and CH<sub>4</sub> in shale reservoirs. In another study, [91] investigated the factors controlling CO<sub>2</sub> sequestration in shale reservoirs using machine learning applications coupled with data analysis approaches. However, no previous study employed ML application to develop a predictive model to quantify the amount of enhanced CH<sub>4</sub> production in shale gas due to CO<sub>2</sub> injection.

## 2.5 Knowledge Gaps

### 2.5.1. The Effect of Reservoir Pressure and TOC on The Contribution of Adsorbed Gas Production.

Although several sensitivity studies have been carried out in the literature to investigate adsorbed gas production, few research works have been conducted to identify the controlling parameters on the contribution of adsorbed gas to shale gas production. From the above review in section 3.2, this lack in knowledge may be attributed to two main reasons:

- **The modelling approaches used.** Most previous numerical studies tended to employ conventional single or dual porosity and permeability models which resulted in inaccurate capture of the gas transit between shale matrix and fractures. Moreover, the diffusion model was not considered in much of the previous work. Since the desorbed and free gas are subjected to diffusion transport mechanisms within organic and inorganic shale matrix, it becomes essential to consider the diffusion model in shale gas prediction for accurate simulation of shale gas production performance.
- **The factors investigated.** Whilst extensive research has been carried out on the controlling factors of shale gas production, there is a very little understanding on how the reservoir depth (pressure) affects the contribution of adsorbed gas on shale gas production. Additionally, although TOC is one of the main characteristics of shale reservoirs and plays an important role in adsorbed gas storage, the effect of TOC coupled with reservoir depth has not been reported in literature.

From the foregoing, desorption behavior has not been completely elucidated, presenting a substantial impediment in the efficient management and performance predictions of shale gas reservoirs. Consequently, the uncertainty of adsorbed gas production has extended to CO<sub>2</sub>-EGR where the adsorbed gas plays the key role of the process. Therefore, there is a pressing need to constrain the uncertainty around desorption behavior and to present a better understanding of the factors controlling adsorbed gas during shale gas primary production. To the best of our knowledge, few works have been carried out with consideration of the multi-permeability and diffusion models to investigate the impact of reservoir depth on the production of adsorbed gas considering TOC. Therefore, in this work, we employ multi-porosity and multi permeability model incorporating diffusion model along with Langmuir isotherms and instant sorption models to quantify the contribution of adsorbed gas to total gas production. with respect to reservoir depth and TOC. The sensitivity analysis aims to provide



a greater understanding of transient and desorption behavior with respect to reservoir depth and TOC.

### 2.5.2. Factors Controlling the Efficiency of CO<sub>2</sub>-EGR

In the review of work done on studying CO<sub>2</sub>-EGR, the factors influencing the amounts of sequestered CO<sub>2</sub> and enhanced CH<sub>4</sub> have been extensively investigated by numerical simulation studies and experimental investigations. Nevertheless, no quantitative framework and accurate CO<sub>2</sub>-EGR modelling, and design process has been identified in literature. Thus, there are still uncertainties in determining the main factors that control CO<sub>2</sub> sequestration and enhanced CH<sub>4</sub> recovery in shale reservoirs. In the light of the literature review in section 3.3, three discrete reasons may account for this knowledge gap:

- **The complexity of shale gas reservoirs.** Shale reservoirs are widely characterized as heterogeneous formations in lithology, TOC, pore size, texture, and petrophysical properties [60]. Consequently, a complexity is presented whilst modelling and predicting shale gas performance. Furthermore, injecting CO<sub>2</sub> into shale matrix even presents more complexity in terms of predicting the behavior of CO<sub>2</sub>-CH<sub>4</sub> displacement behavior.
- **The approaches of previous studies.** Most researchers to date have tended to conduct sensitivity analysis to investigate the effect of a few parameters individually rather than treating the controlling parameters collectively in much detail.

Overall, this gap highlights the need for a new approach of investigation that presents a better understanding of the key factors controlling CO<sub>2</sub>-CH<sub>4</sub>. With regard to the sensitivity methods, previous studies were carried out by using a sensitivity analysis approach which does not take into account the magnitude of relationship between independent and dependent variables collectively. As a sequence, this indicates a need to employ the correlation analysis methods to study the effect of the parameters more broadly and effectively. Thus, this work provides a comprehensive investigation on the correlation between shale properties as well as engineering parameters and the efficiency of CO<sub>2</sub>-EGR. Our correlation analysis yields a direction and a magnitude of correlation which helps to conceptual understanding when designing and implementing CO<sub>2</sub>-EGR in shale reservoirs.

### 2.5.3. Prediction of CO<sub>2</sub>-EGR Efficiency

As previously discussed, numerical reservoir simulation techniques have been widely used to predict the amount of enhanced CH<sub>4</sub> in shale reservoirs due to CO<sub>2</sub> injection. Nevertheless,

challenges arise when employing the conventional simulating methods to predict CO<sub>2</sub> /CH<sub>4</sub> displacement within the complex pores system of shales. Moreover, the lack of a clear identification of the predictors (i.e., the features that have the most impact on enhanced CH<sub>4</sub>) adds even more challenges in quantifying the efficiency of CO<sub>2</sub>-EGR. Furthermore, with the high cost of field testing if compared to simulation costs, the petroleum industry therefore requires a cost-effective tool/approach to evaluate the potential of applying CO<sub>2</sub> injection to shale reservoirs.

Apart from the conventional simulation studies, no studies in literature have taken the advantages of ML applications to develop a new innovative model that enables the industry to predict the enhanced recovered CH<sub>4</sub>. ML models can predict preliminary and focused values based on input features or predictors. Additionally, the accuracy of prediction from supervised ML models can challenge the current uncertainties in the conventional numerical simulation methods. Despite this, the review presented in section 3.4 concludes that the previous studies that have utilized the ML application to study CO<sub>2</sub>-EGR, have been concerned only with the adsorption capacities prediction. Although the availability of data in literature that presents a wide range of input and output variables, data-driven approaches have not been considered for CO<sub>2</sub>-EGR efficiency prediction. For these reasons, more difficulties and challenges arise in modelling CO<sub>2</sub>-EGR process in shale reservoirs. Thus, this work provides a solution by the effective utilization of data available in literature to develop a Supervised Machine Learning (ML) based model to preliminary evaluate CO<sub>2</sub>-EGR efficiency.

# Chapter 3. Research Framework and Methodologies

## 3.1 Research Framework

Since the adsorbed gas plays a key role in shale gas primary production as well as in CO<sub>2</sub>-EGR, the first purpose of this study is to examine the effect of reservoir pressure (depth) and TOC on adsorbed gas production and test the hypothesis that shallow shale gas reservoirs are more adsorbed gas producer, hence favorable targets for CO<sub>2</sub>-EGR. Therefore, the second objective is to set out to prove this tested hypothesis and to determine what shale properties and engineering parameters affect both enhanced CH<sub>4</sub> and CO<sub>2</sub> sequestration. Thirdly, the strength of the relationship between the examined parameters and the efficiency of CO<sub>2</sub>-EGR are employed to adapt the best predictors (features) to develop a machine learning (ML) model which can predict the incremental enhanced CH<sub>4</sub> by CO<sub>2</sub> injection in shale gas reservoirs. To achieve our research objectives, the methodological approach taken in this study is a combination of numerical reservoir simulation, statistical analysis, and machine learning modelling. Figure 3.1 summarizes the research framework and methodologies.

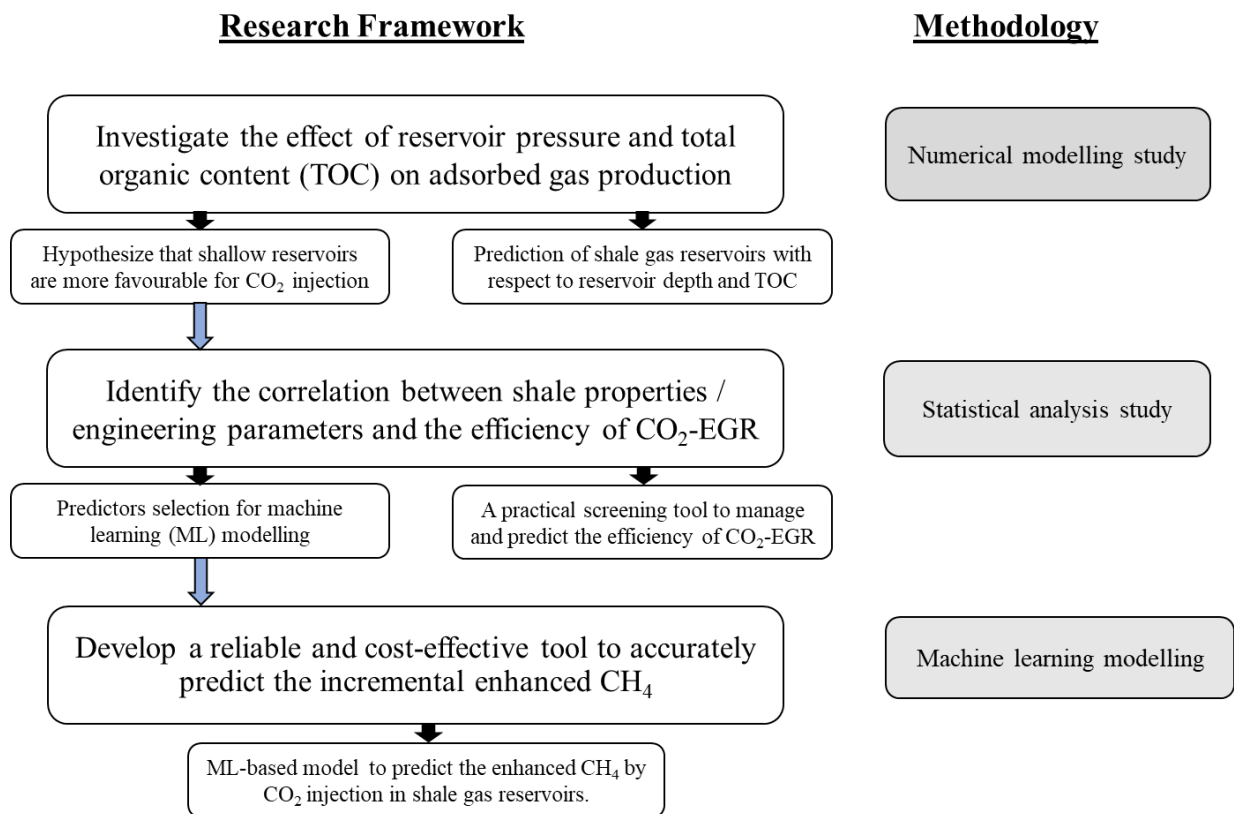


*Figure 3. 1 A summary of the research framework and methodology approach taken for each objective*

## 3.2 Research Methodologies

The research methodologies and the adopted methodologies can be described as follows:

1. Whilst several sensitivities studies have been carried out in the literature to evaluate the desorption behavior, to the best of our knowledge, few research work has considered the multi-permeability and diffusion models to investigate the impact of reservoir depth on the production of adsorbed gas considering TOC. Therefore, there is a pressing need to combine all these models to examine the impact of reservoir depth (i.e., pressure) coupled with TOC on adsorbed gas production performance in shale gas reservoirs. To achieve this objective, we employed a multi-porosity and multi permeability model incorporating Langmuir isotherms and instant sorption option to quantify the contribution of adsorbed gas to total gas production. The model was calibrated using core data analysis from literature for Barnett shales. Then, sensitivity analysis was performed on a range of reservoir depth and TOC to quantify and investigate the contribution of adsorbed gas to total gas production with respect to reservoir depth and TOC.
2. The efficiency of CO<sub>2</sub>-EGR is mainly dominated by several factors of shale properties and engineering design parameters. However, due to the heterogeneity of shale reservoirs and the complexity of modelling CO<sub>2</sub>-CH<sub>4</sub> displacement process, there are still uncertainties in determining the controlling factors. Therefore, in view of the previous sensitivity analysis studies, quantitative framework and accurate CO<sub>2</sub>-EGR modelling together with designing process remains unclear. Thus, this work aims to provide a screening tool of CO<sub>2</sub>-EGR efficiency and to delineate a practical framework of its application at field scale. To achieve this objective, we performed correlation analysis to identify the strength of the relationship between the examined shale properties and engineering design parameters and the efficiency of CO<sub>2</sub>-EGR. Data for this study was gathered across the publications that have examined the feasibility of CO<sub>2</sub> sequestration with potential of enhanced gas recovery in shale reservoirs. For the most generalizable results, we gathered data across the available studies in literature on a wide subset of numerical modelling studies and experimental

investigations. The sensitivity of these data was further improved by handling the missing values using imputation approaches. The methodological approach taken in this study is the Spearman correlation coefficient to identify the direction and the strength of correlation in the dataset.

3. Since enhanced shale recovery by CO<sub>2</sub> injection technology has not been commercialised yet, reservoir simulation studies have offered a preliminary stage of CO<sub>2</sub>-EGR efficiency evaluation on a field-scale. Thus, there has been a large volume of simulation studies investigating the applicability of CO<sub>2</sub>-EGR to several shale types and the effectiveness of different injection scenarios. Nevertheless, key challenges arise when simulating and predicting CO<sub>2</sub>/CH<sub>4</sub> displacement within the complex pore systems of shales. Therefore, the petroleum industry needs development of a cost-effective tool/approach to evaluate the potential of applying CO<sub>2</sub> injection to shale reservoirs. To achieve this objective, this work proposed a solution by employing Machine Learning (ML) based regression models for preliminary evaluation of CO<sub>2</sub>-EGR efficiency. The motivation behind our model is to present a reliable and cost-effective tool which can manage and accurately predict the incremental enhanced CH<sub>4</sub> by CO<sub>2</sub> injection in shale gas reservoirs.

# Chapter 4. Effect of Reservoir Pressure and Total Organic Content on Adsorbed Gas Production in Shale Reservoirs: A Numerical Modelling Study

## 4.1 Abstract

Adsorbed gas plays a key role in organic-rich shale gas production due to its potential to contribute up to 60% of the total gas production. The amount of gas potentially adsorbed on organic-rich shale is controlled by thermal maturity, total organic content (TOC), and reservoir pressure. While those factors have been extensively studied in literature, the factors governing desorption behavior have not been elucidated, presenting a substantial impediment in managing and predicting the performance of shale gas reservoirs. Therefore, in this paper, a simulation study was carried out to examine the effect of reservoir depth and TOC on the contribution of adsorbed gas to shale gas production.

The multi-porosity and multi-permeability model, hydraulic fractures, and local grid refinements were incorporated in the numerical modelling to simulate gas storage and transient behavior within matrix and fracture regions. The model was then calibrated using core data analysis from literature for Barnett shales. Sensitivity analysis was performed on a range of reservoir depth and TOC to quantify and investigate the contribution of adsorbed gas to total gas production.

The simulation results show the contribution of adsorbed gas to shale gas production decreases with increasing reservoir depth regardless of TOC. In contrast, the contribution increases with increasing TOC. However, the impact of TOC on the contribution of adsorbed gas production becomes minor with increasing reservoir depth (pressure). Moreover, the results suggest that adsorbed gas may contribute up to 26% of the total gas production in shallow (below 4,000 feet) shale plays.

These study findings highlight the importance of Langmuir isothermal behavior in shallow shale plays and enhance understanding of desorption behavior in shale reservoirs; they offer significant contributions to reaching the target of net-zero CO<sub>2</sub> emissions for energy transitions by exhibiting insights in the application of enhanced shale gas recovery and CO<sub>2</sub> sequestration – in particular, the simulation results suggest that CO<sub>2</sub> injection into shallow shale reservoirs,

rich in TOC, would give a much better performance to unlock the adsorbed gas and sequester CO<sub>2</sub> compared to deep shales.

## 4.2 Introduction

Shale gas resources have been identified as an important component in current clean ge-energy, which plays an important role in the energy transition to net-zero target of carbon dioxide emission. Therefore, in recent years, there has been increasing interest in the commercial development of shale gas resources worldwide; in 2018, shale gas accounted for nearly 65% of The United States (U.S.) total gas production [5], and 21% in China [92]. This significant breakthrough in the exploitation of shale gas resources has extended to other countries such as Canada and Australia. However, shale gas reservoirs have presented new challenges due to their ultra-low permeability and recovery factors [58]. Consequently, it is essential to enhance the matrix permeability to achieve economical production from shale reservoirs.

The advanced technologies of horizontal drilling and multi-stage hydraulic fracturing techniques create and establish the conductivity between fractures and matrix with induced fractures network. These technologies enable the oil and gas industry to achieve the shale gas reservoirs' potential with commercial production. Similar to coalbed methane, shale gas reservoirs hold a tremendous amount of gas on the surface of organic minerals which can be referred to as adsorbed gas [9]. The adsorbed gas has been a key parameter in shale gas reservoirs evaluation and development and may account for up to 60% of the total gas in place [12]. Unlocking adsorbed methane on organic-rich shale surface has attracted great attention in industry due to its potential to produce considerable amounts of gas.

The adsorption and desorption phenomenon has been investigated in a large, growing body of literature. Although several studies have widely focused on adsorption behavior [60-62], desorption behavior has not been completely elucidated, presenting a substantial impediment in the efficient management and performance predictions of shale gas reservoirs. Of the few studies identifying factors governing desorption in shale gas production, some have focused only on the impact of hydraulic fracture parameters on both free and adsorbed gas [15, 16]. Researchers have investigated the influencing reservoir parameters on shale production [14, 17]– however, the multi-porosity and diffusion models have not been considered in their

studies. Further investigations considering the aforementioned models [18, 19] have neglected the effect of TOC and the impact of reservoir pressure.

Currently, research regarding the parameters governing the contribution of adsorbed gas to shale production is lacking. Whilst several sensitivities studies have been carried out in the literature to evaluate the desorption behavior, however, to the best of our knowledge, no single study exists which has considered the multi-permeability and diffusion models to investigate the impact of reservoir depth on the production of adsorbed gas considering TOC. Therefore, there is a pressing need to combine all these models to examine the impact of reservoir depth (i.e., pressure) coupled with TOC on adsorbed gas production performance in shale gas reservoirs.

In this work, we employ multi-porosity and multi permeability model incorporating with Langmuir isotherms and instant sorption option to quantify the contribution of adsorbed gas to total gas production. In particular, this research seeks to investigate the factors influencing adsorbed gas production in shale reservoirs. The sensitivity analysis aims to provide a greater understating of transient and desorption behavior with respect to reservoir depth and TOC. The results of this paper could provide important insights into the selection of optimal depth to inject CO<sub>2</sub> in shale reservoirs which can potentially enhance both CH<sub>4</sub> recovery and CO<sub>2</sub> sequestration.

This study has been divided into five parts: the first part includes this introductory section. The second consists of a brief overview focusing on the key theory of shale gas reservoirs production and modelling. Thirdly, the methodology used for this study including model development and calibration will be covered. The fourth section presents the simulation results and discussion. Finally, the conclusion gives a summary of the findings and implications.

## 4.3 Theory

### 4.3.1. Shale Gas Production

Shale gas mainly exists in three different forms: (a) free gas in the fractures with various length scales and in the interconnected micro-pores of the organic content [59]; (b) adsorbed gas on the organic surfaces; (c) dissolved gas in the reservoir fluids [9]. The primary production profile of a single shale well dramatically declines after a few years of high initial production rate. As the reservoir pressure declines, adsorbed gas begins to be desorbed form the organic matter



surface contributing to the total production with a considerable amount accounting up to 60% of the total gas in [12]. This stage of production extends and contributes significantly to the cumulative production.

Figure 4.1 below shows the gas primary production profile for the base case from our simulation results. Therefore, the contribution of adsorbed gas in production has been considered as a pintail of shale reservoirs long term production [14]. However, challenges arise when quantifying and predicting the recoverable adsorbed gas due to complex transport of desorbed gas within organic and matrix micropores towards fractures and then to the producing wells. The production from the adsorbed gas has been found difficult to be produced compared with the free gas, as a result of different mechanisms of storage (adsorption) and the transport mechanism (surface diffusion) through the shale pores system [93]. Moreover, the adsorbed gas tends to behave differently in terms of density and accumulation [94, 95].

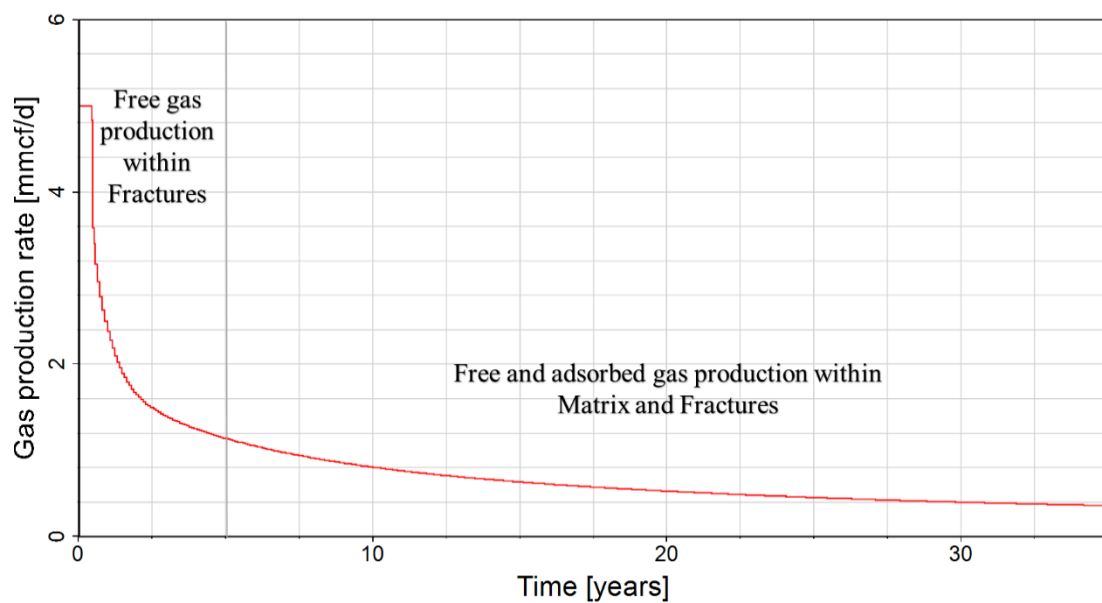


*Figure 4. 1 The production profile of free and adsorbed gas for Barnett shale reservoir calculated by our predictive simulation model.*

The prospective production from adsorbed gas is influenced by many factors such as reservoir permeability and the fracture network [15]. The initial reservoir pressure and the amount of total organic content are playing the main role in the adsorption capacities [96]. The adsorption capacities of shales and TOC show a direct linear correlation, where the adsorbed gas typically increases with increasing TOC [97]. With increasing the thermal maturation, the adsorption capacities are found to increase as a result of generated microporosity from the organic matter

[61]. In addition, it has been proven that clay minerals can also adsorb gases and vapors [98]. In respect to pressure, the adsorption capacity, hence the original adsorbed gas in place, yields a general trend of increasing with pressure. Figure 4.2 shows how the adsorbed CH<sub>4</sub> typically relates in a non-linear correlation to pressure in different shale samples. However, the adsorption capacity tends to increase slowly at high pressure. This observed change in adsorption behavior at high pressure environment could be attributed to the completion of mono-layer adsorption, which is typically followed by the equilibrium saturation [23].

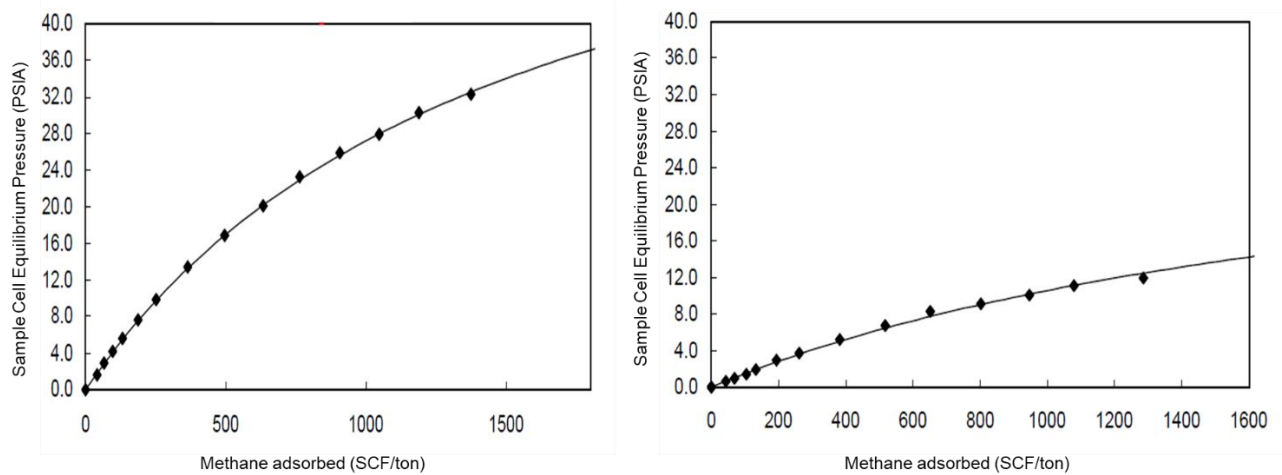


Figure 4. 2 Methane adsorption isotherms analysis at a range of pressure values calculated for New Albany Shale and Ohio Shale [23]

#### 4.3.2. Multi-Porosity and Multi-Permeability Model

Shale gas reservoirs have two distinct types of porosity, the fractures and matrix porosity. The matrix pores are in nano-scale and only occupied by free gas. The analysis of three-dimensional high-resolution imaging has recently shown a large and interconnected pores of organic pockets within the shale matrix [9]. The organic pores have a much smaller length compared to the inorganic matter (typically less than 10 nm) [99], and are more likely than matrix to be interconnected [100]. The contribution of organic pores lies in the range of 34 to more than 50% to the total pore volume [60, 101, 102]. According to the complex mechanisms by which gas is trapped in shale structure, in this work, a multi-porosity and multi- permeability model became essential to simulate gas transport behavior from sub-matrix cells to the primary matrix cells towards the natural and/or the induced fractures, and then to the wellbore.

### 4.3.3. Gas Adsorption Isotherm

In shale reservoirs, the original gas in place is estimated in terms of gas content for both free and adsorbed gas. The relative contribution of free vs adsorbed gas varies with the total organic content, reservoir pressure and temperature, pore size distribution, and rock texture [103]. The free gas reserve is defined using shale porosities (fractures, organic, and inorganic). In this study, Langmuir isotherm (monolayer molecules of the adsorbed gas) was used to define the shale gas adsorption and desorption process. Langmuir isotherms can be expressed as shown in Equation (4.1) [104]:

$$V_p = \frac{V_l P}{P_l + P} \quad \text{Equation (4.1)}$$

Where:

$V_p$  is the predicted amount of adsorbed gas at gas pressure  $P$ ,

$V_l$  is Langmuir's volume,

$P_l$  is Langmuir's pressure at which 50% of gas is adsorbed.

Commonly, Langmuir isotherm is the most applied kinetic model for shale gas adsorption and desorption process [105], it is a simple and practical model which is based upon two main assumptions. Firstly, molecules of free and adsorbed gas are in a state of dynamic equilibrium at constant temperature. Secondly, the adsorption thickness is a monolayer molecules of the adsorbed gas [25]. In contrast, Emmet and Teller (BET) isotherm is a model in which an infinite number of multi-layer adsorption is taken into account [106].

Whilst Langmuir isotherm has been proven in previous study to fit accurately over a range of pressure and temperature [106], it may not be always valid for organic-rich shale of a large effective pore size greater than 10 nm [107]. Therefore, in this work, it was decided not to consider the effect of multi-layer adsorption. The main reason for this is that organic porosity of 2 % was defined in our predictive model, which is an indication of small effective organic pore size typically < 10nm [9]. Consequently, multi-layer adsorption model consideration in this study will result in underestimating free gas volume occupying the organic pores. Moreover, in respect to surface diffusion, the upper layer may not necessarily contribute if the lower layer is not completely formed [108]. Hence, the formation of multi-layers of adsorption may not play a significant role in our undertaken investigation.

#### 4.3.4. Gas Transport Mechanism

Gas transport in shale reservoirs is a complex flow process as a result of different gas storage mechanisms and pore size distribution. Gas flow mechanism in shale reservoirs varies in organic from inorganic pores and significantly different from that in conventional gas reservoirs [93]. Typically, within the shale pores system, gas flow comes from the matrix region to fractures region to feed the wells [13]. With regard to the channel size, Darcy's law can be used to simulate the free gas flow within the fractures network [109]. In contrast, the capillary size is considerably much smaller in the matrix pores, therefore, the free gas transport is subjected to diffusion transport mechanism [18]. Finally, in inorganic pores, where the gas is adsorbed on the surface organic matter, the desorption process governs gas transport to fractures and to inorganic matrix pores. Consequently, accurate simulation of shale gas reservoirs needs to consider the effects of different flow and storage mechanisms associated with the different pore types described above. Therefore, a combination of desorption, diffusion, and Darcy flow mechanisms were considered in our simulation study.

### 4.4 Methodology of Reservoir Modelling

#### 4.4.1. Model Development

The Numerical reservoir simulation technique has been one of the effective tools used to analyse the realistic flow mechanism of free and desorbed shale gas. In this study, Eclipse-300 compositional reservoir simulator was used to simulate gas production for Barnett shale reservoir. The numerical simulation model of Barnett shale reservoir was generated using data in the public domain. The key input parameters were defined in the model within the range which consists with that presented in literature for the realistic shale. Tables 4.2 & 4.3 show the reservoir parameters and Langmuir constants of CH<sub>4</sub> for Barnett shale gas reservoir [13, 17, 54, 60, 95, 99, 110-114].

Many previous simulation studies used the traditional dual-porosity model which neglects the transient behavior within matrix regions [10, 55]. To accurately simulate the storage and transient behavior of the matrix region, multi-porosity and multi-permeability models were employed in our predictive model. Thus, our model can predict gas flow from sub-matrix cells to the primary matrix cells towards the natural and/or the induced fractures, and then to the wellbore.

Mass accumulation and flow within the matrix region is dominated by the adsorption and desorption process. Therefore, an accurate capture of adsorption-desorption behavior is of crucial importance for shale gas modelling. The instant sorption option was used in our model to offer an effective way to represent the gas volumes (free and adsorbed) simultaneously within the organic matrix pores.

In this model, a horizontally producer well and five stages of hydraulic fractures were generated in the middle of the reservoir segment intersecting. Table.4.1 shows the fracture parameters used for the simulation model. For more accurate gas flow simulation, a local grid refinement option was also generated around the fractures. Given that the gas is non-wetting phase in inorganic matter [115], conceptually, two relative permeability curves were assigned in this case study for shale bulk and organic matter separately.

*Table 4. 1 The fracture data for used for Barnett model*

<i>Parameter</i>	<i>Value</i>	<i>Unit</i>
Hydraulic fracture spacing	300	feet
Hydraulic fracture height	200	feet
Hydraulic fracture width	0.15	feet
Total number of fractures	25	
Fracture half length	350	feet
Number of Stages	5	

*Table 4. 2 The reservoir properties of Barnett shale reservoir.*

<i>Reservoir Parameter</i>	<i>Value, reference</i>	<i>Unit</i>
Matrix Porosity	2 – 6, [114]	%
Fracture Porosity	1 – 6, [111]	%
Organic Porosity	2, [60]	%
Matrix Permeability	0.0001 - 0.005, [110, 113]	mD

Fracture Permeability	0.001, [54]	mD
Organic Permeability	0.0015, [111]	mD
Adsorption Capacity	50 -200, [111]	scf/ton
TOC	4 – 8, [114]	%
Organic Density	166, [95]	lb/ft <sup>3</sup>
Bulk Density	156, [17]	lb/ft <sup>3</sup>
Pressure Gradient	0.43 - 0.52, [99]	psi/ft
Reservoir Temperature	200, [17]	F°
Depth	6000 – 9000, [114]	ft
Gross Thickness	100 – 1000 [114]	ft
Diffusion Coefficients	0.1116 [13]	ft <sup>2</sup> /day

*Table 4. 3 Langmuir constants of CH<sub>4</sub> for Barnett shale gas reservoir [17, 114]*

Langmuir constants of CH <sub>4</sub>	Value	Unit
V <sub>L</sub>	880	scf/ton
P <sub>L</sub>	400	psi

The shale reservoir of interest in this work is Barnett shale reservoir, which is a fine-grained and rich-organic sediments located in the USA. Barnett shale reservoir was discovered in 1981 [116]. Currently, it is one of the most prolific shale gas producers in USA. For numerical modelling, a segment of Barnett shale reservoir was simulated using a 3D reservoir model with dimensions of 1,750 × 1,100 × 200 feet. The multi- porosity model has a grid size of 40 × 13 cells in X, Y directions and 7 cells in Z direction. The cells in Z direction were subdivided into 1 + 1+ 5, representing fracture, matrix and sub-matrix cells respectively. Figure 4.3 shows by a 2D view the matrix and fractures for Barnett shale model represented by fluid in place region

1 and 2 respectively, the Figure also illustrates the induced fracture stages and the refined grid cells.

The first stage of prediction was carried out to compare the fractions of adsorbed gas to the total gas production at various reservoir depths ranging from 3,000 to 11,000 feet at a fixed value of TOC. Afterwards, sensitivity cases were generated for every reservoir depth with varying TOC from 4 to 8% to capture the contribution of produced adsorbed gas and the corresponding effect of TOC for each case.

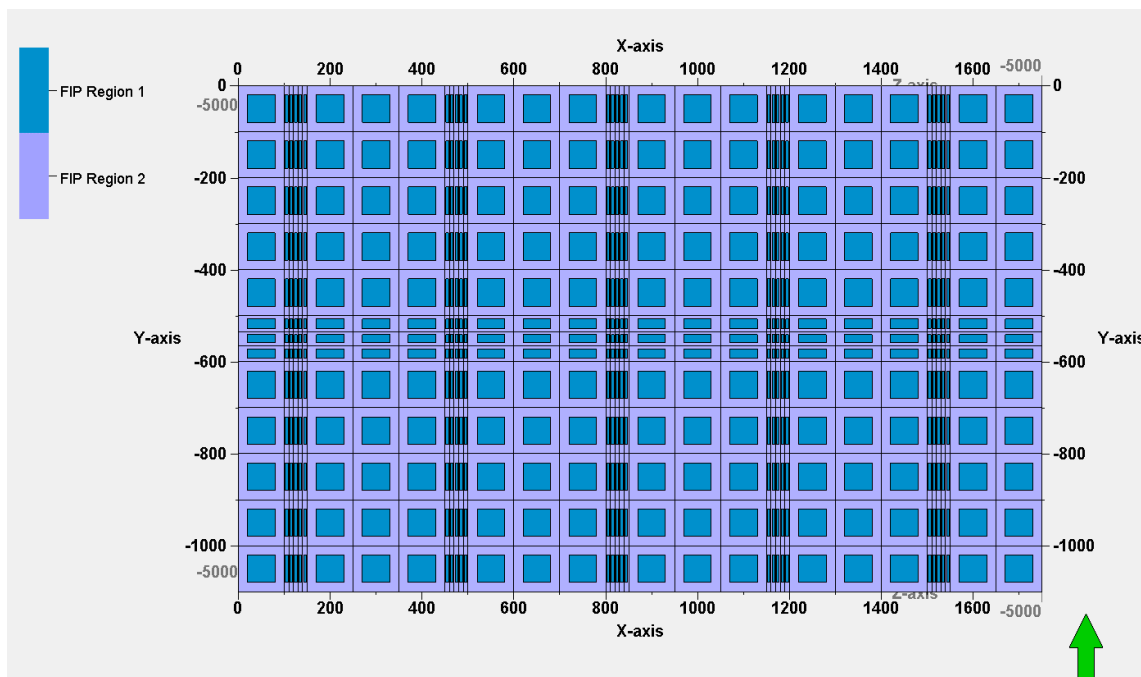


Figure 4. 3 2D view of the Barnett shale reservoir model

#### 4.4.2. Calibration of the Shale Mechanistic Model

In our simulation model, the initial conditions, adsorption capacities, the fractions of free, and adsorbed gas volumes to the total gas in place at given reservoir pressures, and the recoverable volume were adopted to match the typical data for Barnett shale reservoir.

To calibrate the shale mechanistic model, static and dynamic simulations were conducted to match the gas content and the recovery factor of Barnett Shale. The original gas in place is estimated in terms of gas content for both free and adsorbed gas. Shale porosities (fractures and inorganic) describe the free gas whereas Langmuir isotherms define the relation between the adsorption capacity and pressure at constant temperature. Overall, to estimate the total

original gas in place for our predictive model, the gas content (scf/ton) was estimated by Barnett shale reservoir data given in literature.

For model calibration and result robustness, our base simulation model was applied to couple Langmuir isotherms and volumetric calculations, estimating the gas content for free and adsorbed gas at different values of reservoir pressure. The estimation of adsorbed gas content was made by realistic Langmuir isotherms published in literature [17, 114].

In order to validate the predictive model, the simulated fractions of adsorbed and free gas volumes to the total gas in place against the fractions extracted from core data analysis were matched for Barnett shale reservoir. This is shown in Figure 4.4 [117].

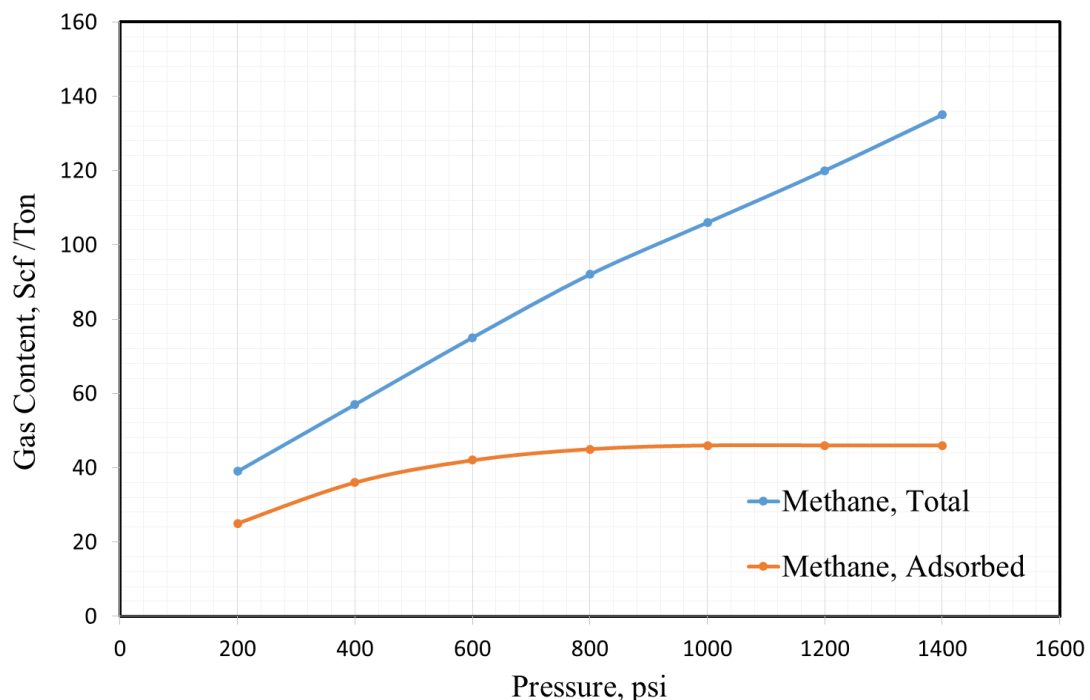


*Figure 4. 4 Typical gas content measured by core analysis for Barnett shale reservoirs at depth of 7640 feet and 4% of TOC reproduced from [117]*

To increase the reliability of validation, it was carried out in terms of volume fractions instead of gas, eliminating the effect of crushed porosities and in the measured samples. Figure 4.5 displays an accepted match between the estimated fractions from the calibrated model and by core analysis.



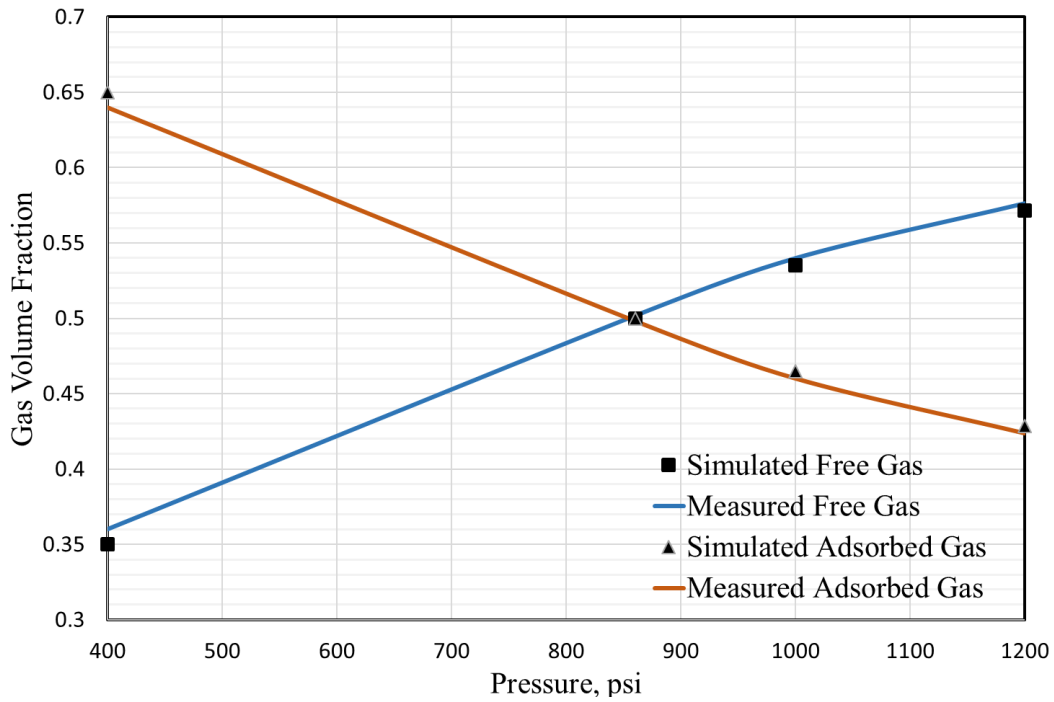


Figure 4. 5 The simulated fractions of adsorbed and free gas volumes are compared to fractions measured by core analysis for Barnett shale reservoirs at depth of 7640 feet and 4% of TOC

For further validations, the estimated recoverable reserves across the typical range of pressures and TOC resulted from the calibrated model were adopted to lie in the range of 10% and 20% as shown in Figure 4.6 which typically matches the reported recovery factors of Barnett shale [114].

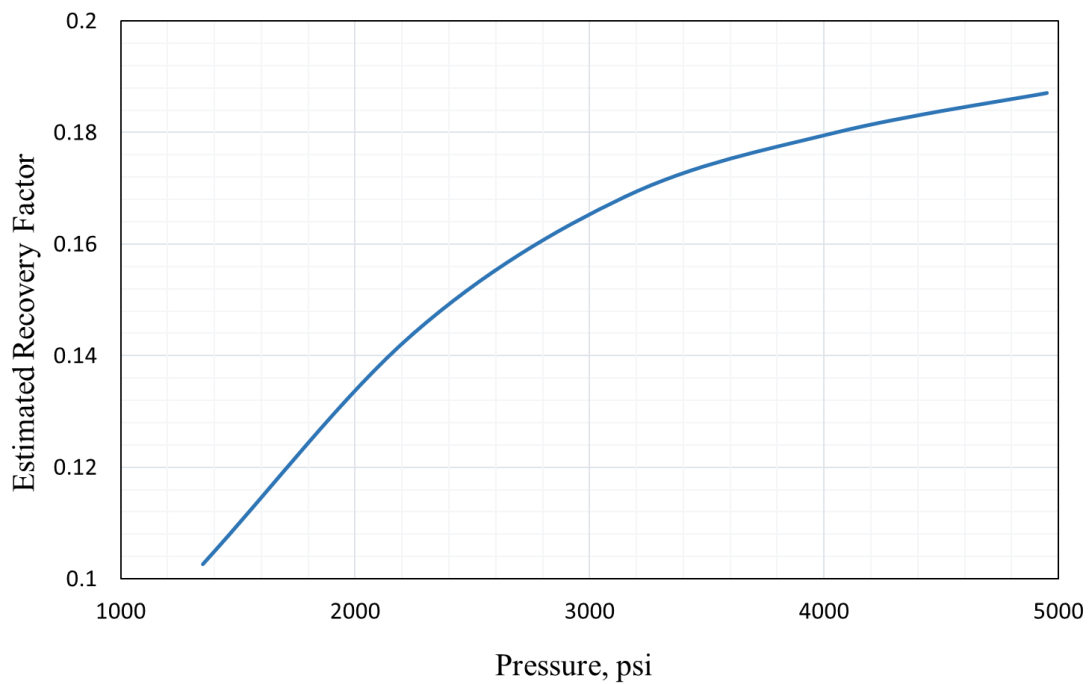


Figure 4. 6 The recovery factors estimated by our calibrated model at 8% of TOC

## 4.5 Results and Discussion

### 4.5.1. Effect of Reservoir Pressure on Adsorbed Gas Production

In order to investigate the impact of reservoir pressure on adsorbed gas production, our predictive model quantified the contribution of adsorbed and free gas for 40 years in regard to increasing in reservoir depth from 3,000 to 11,000 feet (i.e. pressure) within TOC range of 4 to 8%. The results obtained from the sensitivity runs show that adsorbed gas production strongly decreased with increasing reservoir depth regardless of TOC, as shown in Figure 4.7. For example, at a given TOC of 4%, the contribution of adsorbed gas production decreased from 18 to 1% with increasing reservoir depth from 3,000 to 11,000 feet. It is important to note that the gas volume fractions in this study are presented in surface conditions, as the software utilized, Eclipse, employs the use of a formation volume factor to convert the volumes from reservoir conditions to surface conditions.

Based on the simulation results, it can be concluded that the desorption phenomenon becomes an insignificant storage mechanism in deep shale reservoirs, particularly for low TOC shales. Our findings are also supported by the experimental results [96], who reported that adsorbed gas contributed by 21% of the total produced gas at 800 psi which is equivalent to 1,770 feet with Barnett shale pressure gradient. Their observations also suggest that the adsorbed gas likely contributes to 50% of total gas production at the abandonment pressure.

It is understandable that desorption process is mainly controlled by pressure decline in matrix pores [7], therefore, in high pressure shales (typically higher than 4500 psi) [29, 34] since very low pressure decline takes place due to ultra-low matrix permeability, the adsorbed gas is less likely to be desorbed from the organic matter surface. It can be seen from Figure 4.8 that the reservoir pressure declined approximately by only 30% from the initial pressure across 40 years of continuous production. As shown in Figure 4.7, for shale reservoirs deeper than 5,000 feet, the contribution of the adsorbed gas is less than 12% across 40 years production, hence, it can be concluded that the free gas flow within matrix pores to the induced fractures is the dominant contributor of this stage of production. This explains that fracture and matrix permeabilities have been found to be the key significant parameters at early and late time of shale gas production [7, 15, 66].

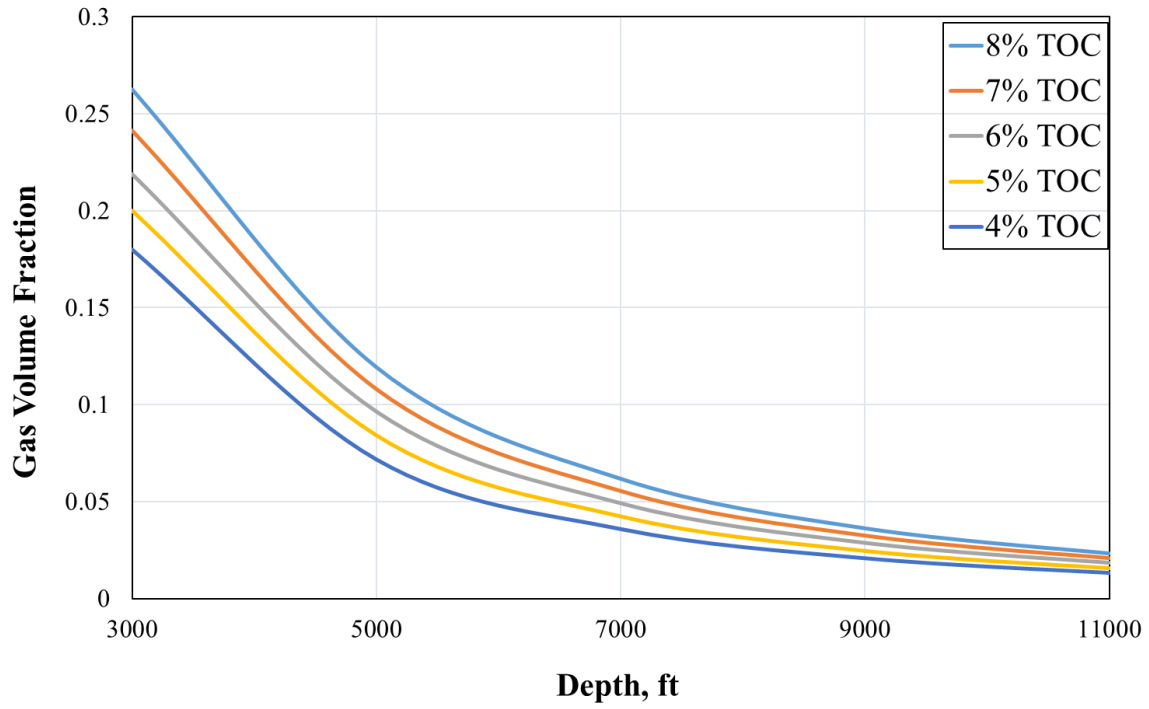


Figure 4. 7 Fractions of produced adsorbed gas to the total cumulative production at different reservoir depths at a range of 4 - 8% of TOC.

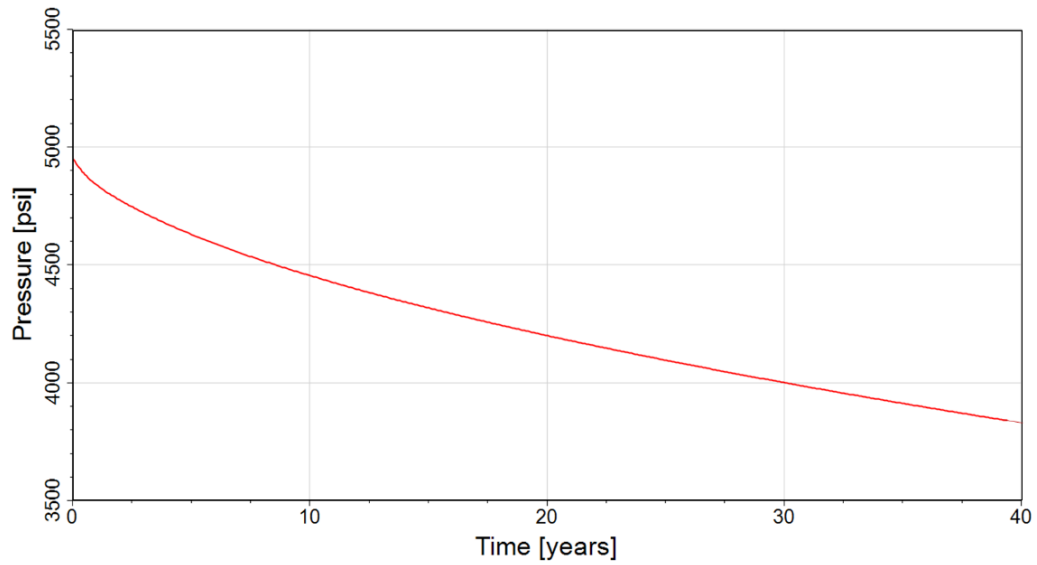


Figure 4. 8 The simulated pressure decline profile for 4% TOC and 4000 psi initial pressure.

Our results imply that adsorbed gas plays a minor role in deep shale reservoirs production. Consequently, this work underscores the importance of Langmuir isothermal behavior to manage and predict the performance of shale gas production in shallow shale plays. Moreover, the results prove that an enhancement in shale matrix permeability can lead to a higher adsorbed and free gas cumulative production since the pressure difference between the adsorbed and free gas increases.

#### 4.5.2. Effect of TOC on Adsorbed Gas Production

In this study, a range of 4 to 8% of total organic content (TOC) was considered to analyse the effect of increasing TOC on the adsorbed gas production within a range of 3,000 to 11,000 feet of reservoir depth. As shown in Figure 4.9, the predicted adsorbed gas from the simulation model shows that increasing TOC increases the contribution of adsorbed gas to the total gas production for a given reservoir depth. For example, increasing TOC from 4 to 8% results in increasing the cumulative adsorbed gas production from 195 to 335 MMSCF at the same reservoir depth of 5,000 feet.

The observed correlation between TOC and adsorbed gas production could be attributed to the fact that the amount of gas originally adsorbed on the surface of organic matter in rich-organic shale reservoirs is a function of the pressure and the volume of organic matter in the shale matrix. However, the impact of TOC on the contribution of adsorbed gas production becomes minor with increasing reservoir depth. This observation seems to be consistent with that presented in literature, for instance, the simulation results study presented by [15], which argued that the increase of adsorbed gas (i.e. total organic content) increases the cumulative production from both free and adsorbed gas. However, our study proves that the amount of the desorbed gas has less contribution to the total production in deep shale reservoirs compared to shallow reservoirs.

This combination of findings offers several contributions to the existing knowledge by providing insight into the characterisation, development, and prediction of shale gas reservoirs with respect to pressure and TOC. Also, this work has important implications related specifically to the application of enhanced shale gas recovery by CO<sub>2</sub> injection. Our results suggest that CO<sub>2</sub> injection in shallow shale (rich in TOC) reservoirs would give a much better performance to unlock adsorbed gas compared to deep shales, since the desorbed gas is more likely to be desorbed and the injected stream of CO<sub>2</sub> could be potentially sequestered.

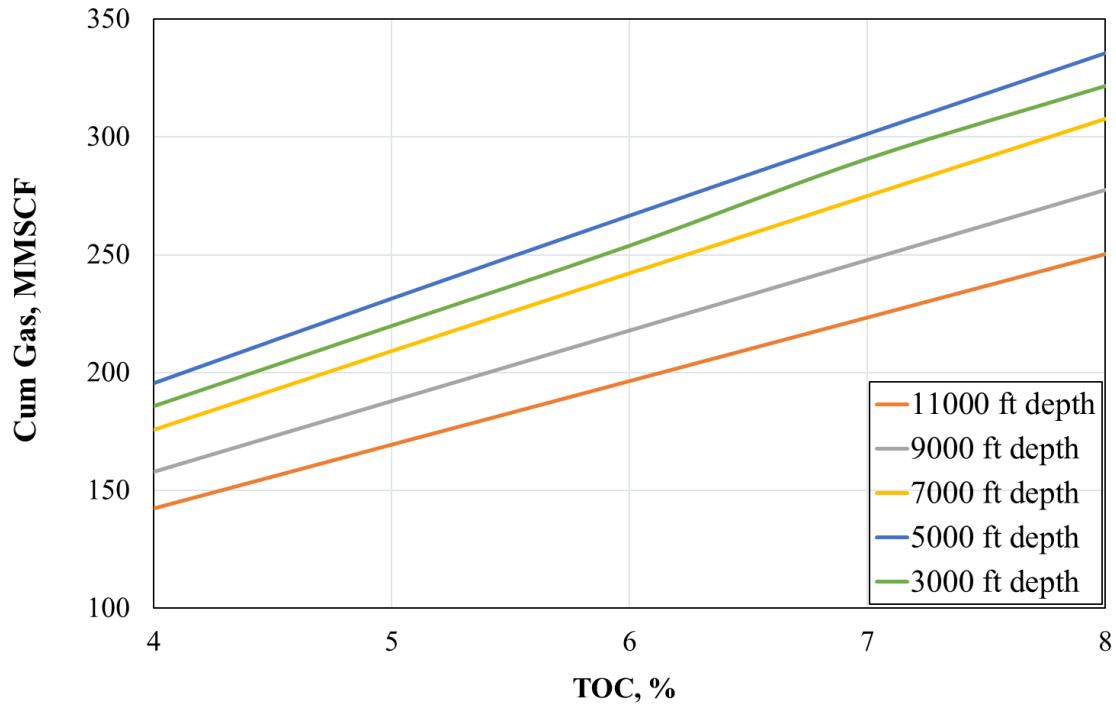


Figure 4. 9 The cumulative production from adsorbed gas volumes with range of 4 - 8% TOC.

#### 4.6 Conclusions and Implications

This work aimed to examine the effect of the reservoir depth coupled with TOC on the adsorbed gas production. A sensitivity study was performed to examine the desorption behaviour in shale reservoirs. The results of this study show that reservoir depth has a significant effect on the contribution of adsorbed gas to shale gas production. Regardless of TOC, adsorbed gas production decreases with increasing reservoir depth. Whilst this contribution increases with increasing TOC, the impact of TOC on the contribution of adsorbed gas production becomes minor with increasing reservoir depth. These results suggest that adsorbed gas may play an important role (12% - 26%) in total gas production in shallow shale plays below 4,000 feet.

This study highlights the importance of Langmuir isothermal behaviour in shallow shale plays and contributes to existing research by providing insight into characterisation, development, and prediction of shale gas reservoirs with respect to reservoir depth and TOC; it presents a significant contribution to the energy transition to net-zero target of CO<sub>2</sub> emissions by demonstrating important insights into the application of enhanced shale gas recovery and CO<sub>2</sub> sequestration. Based on the simulation results (shallow shale reservoirs have been proven in our study to produce more adsorbed gas compared to deep shales) injecting CO<sub>2</sub> into shallow

shale reservoirs (rich in TOC) would give an improved outcome to unlock the adsorbed gas and sequester CO<sub>2</sub>.

# Chapter 5. Statistical Analysis of Controlling Factors on Enhanced Gas Recovery by CO<sub>2</sub> Injection in Shale Gas Reservoirs

## 5.1 Abstract

Development of shale gas reservoirs is the fastest growing on a large scale globally due to their potential reserves. CO<sub>2</sub> has a great affinity to be adsorbed on shale organic surface over CH<sub>4</sub>. Therefore, CO<sub>2</sub> injection into shale reservoirs initiates a potential for enhanced gas recovery and CO<sub>2</sub> geological sequestration. The efficiency of CO<sub>2</sub> enhanced gas recovery (CO<sub>2</sub>-EGR) is mainly dominated by several shale properties and engineering design parameters. However, due to the heterogeneity of shale reservoirs and the complexity of modelling CO<sub>2</sub>-CH<sub>4</sub> displacement process, there are still uncertainties in determining the main factors that control CO<sub>2</sub> sequestration and enhanced CH<sub>4</sub> recovery in shale reservoirs. Therefore, in view of the previous sensitivity analysis studies, no quantitative framework and accurate CO<sub>2</sub>-EGR modelling, and design process has been identified. Thus, this work aimed to provide a practical screening tool to manage and predict the efficiency of enhanced gas recovery and CO<sub>2</sub> sequestrations in shale reservoirs. To meet our objectives, we performed correlation analysis to identify the strength of the relationship between the examined shale properties and engineering design parameters and the efficiency of CO<sub>2</sub>-EGR. Data for this study was gathered across the publications on a wide subset of numerical modelling studies and experimental investigations. The sensitivity of data was further improved by a hybrid approach adopted for handling the missing values to avoid bias in our dataset.

Our results indicate that CO<sub>2</sub> flooding might be the best applicable option for CO<sub>2</sub> injection in shale reservoirs, whereas the huff and buff scenario does not seem to be a viable option. The efficiency of CO<sub>2</sub>-EGR increases as the pressure difference between injection pressure and reservoir pressure increases. The results show that shallow shale reservoirs with high fractures permeability, total organic content, and CO<sub>2</sub>-CH<sub>4</sub> preferential adsorption capacity are favourable targets for CO<sub>2</sub>-EGR. Moreover, our results indicate that a successful hydraulic-fractures network with effective values of fractures permeability and conductivity is essential for a higher CO<sub>2</sub>-EGR efficiency. Well spacing and fractures half-length are crucial engineering features in CO<sub>2</sub>-EGR process design that must be carefully optimised due to their negative effect on CH<sub>4</sub> production and positive effect on CO<sub>2</sub> storage. Our statistical analysis

lays a foundation for efficient CO<sub>2</sub>-EGR design and implementation and presents an important contribution to the field of reaching the target of net-zero CO<sub>2</sub> emissions for energy transitions.

## 5.2 Introduction

The global energy markets have dramatically changed since the Covid-19 outbreak. Despite the global economy has been severely affected under lockdown measures, the global energy demand increased by 4% in 2021 and is expected to continue growing by 1.3% per year up to 2030 [1]. In the light of this fact, the clean energy has recently become the central focus of global investment and development to meet the accelerated demand in energy consumption. Natural gas, as one of cleanest fossil fuels, has become a significant contributor to the world energy market [54] and currently plays a key role in the energy transition to clean geo-energy. Over the past several years, due to the normal decline in conventional natural gas reserves, shale gas reservoirs have become an important alternative source for natural gas. In The United States (U.S.), shale gas production accounted for nearly two-thirds of the total gas production in 2018 [5]. Due to the revolution in shale gas exploitation since 2005, China has become the second largest gas producer [4]. Worldwide, according to the U.S Energy Information Administration, the expected production from shale gas resources will account for nearly 70% of the total production in 2050 [118].

The term ‘unconventional reservoirs’ refers to low reservoir quality formations where artificial stimulations are required to achieve production in commercial quantities [119, 120]. Following this definition, the recognised types of unconventional gas resources are; tight gas, coal -bed methane, gas hydrates, and shale gas reservoirs [121]. At present, development of shale gas reservoirs is the fastest-growing not only in North America, but it’s also growing on a large scale globally due to their potential reserve [122]. The key technologies of horizontal and multilateral drilling, and multi-stages hydraulic fracturing have been perceived techniques to achieve commercial development of shale resources [123]. However, despite the recent revolution of those technologies, shale gas recovery may account for up to only 30% of the original gas in place [13]. The expected low recovery factor (RF) from shale reservoirs attributes to a uniquely geological and petrophysical system which is characterised by ultra-low permeability and porosity, small pore size, high total organic content (TOC) , and complex gas storage and transport mechanisms [7]. Shale reservoirs are multi-permeabilities nature formations which typically have two distinct permeabilities, natural fractures permeability, and matrix permeability (for organic and inorganic matter). Typically, shale gas reservoirs have



permeabilities of nano to micro Darcy [124] and porosity ranging up to 10% [93, 125]. The typical focused two-dimensional images of rich-organic shale gas samples shown a finely organic materials dispersed within the inorganic shale matrix, the pore size of these organic pores is having a length much smaller if compared to the inorganic matter (typically less than 50 nm) [7]. Recently, the analysis of three-dimensional imaging has showed that interconnected pores of organic pockets are filled with a significant amount of gas with different density profiles as illustrated in Figure 5.1 [9].

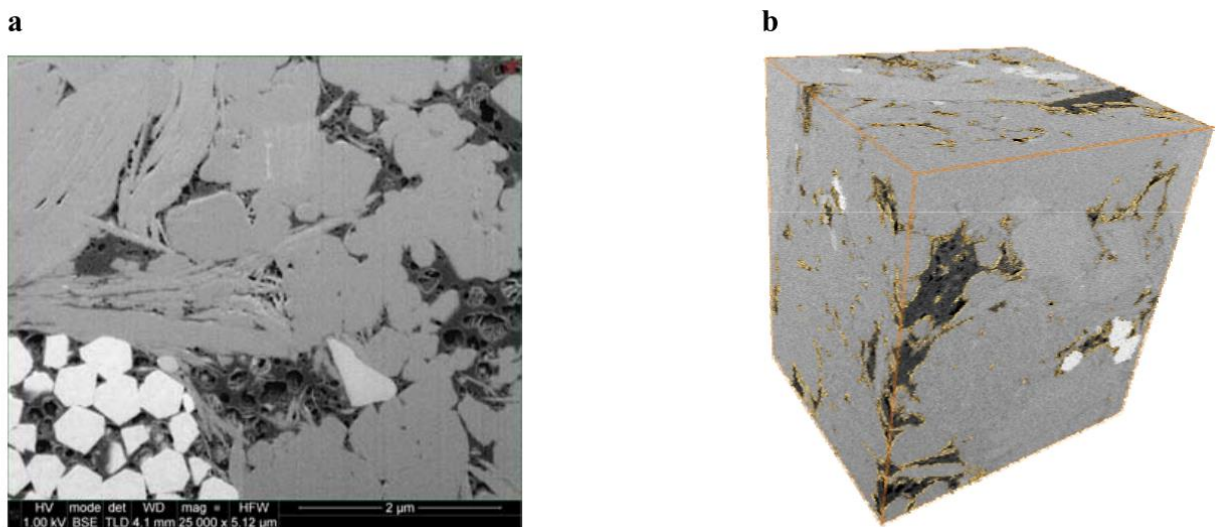


*Figure 5. 1 -a: 2-D image of shale gas sample showing the organic material in a dark gray dispersed in light gray inorganic materials. b: 3-D shale segmentation showing in light color the interconnected organic pockets [9]. [Copyright 2011, Society of Petroleum Engineers]*

### 5.3 Motivation of CO<sub>2</sub> Injection in Shale Gas Reservoirs

In organic-rich shale reservoirs, gas typically exists in different thermodynamic states as free gas in fractures and in the interconnected micro-pores of the organic materials, and adsorbed gas on the surface of organic materials, and dissolved gas in the reservoir fluids [9, 10]. Figure 5.2 depicts the pores system and different storage mechanisms within shale gas reservoirs. Very similar to coal-bed methane, shale reservoirs hold immense an amount of adsorbed gas accounting for up to 60% of the total gas in place [12]. As reservoir pressure naturally declines, desorption phenomena takes place and desorbed gas transports by diffusion mechanism towards matrix and fractures [126]. In a typical shale gas production profile, gas desorption occurs after the initial production of free gas in fractures and matrix pores [127] and plays the main role at late stage of reservoir life maintaining the long-term production plateau [14]. However, the adsorbed gas may contribute to the total production up to 26% in shallow

reservoirs [22]. [127] concluded the factors limit the production capacity of adsorbed gas as the ultra-tight nature of shale matrix and high bottom hole pressure. Since pressure is the key controller of the desorption capacity, adsorbed gas is very unlikely to desorb from the surface of organic matter due to very low-pressure decline occurring in shale pores as a result of ultra-low permeability. Despite the current challenges presented to shale production, unlocking the trapped adsorbed gas has attracted great attention in industry due to the potential to increase the productivity of shale at commercial rate. Thus, developing a cost-effective technique to enhance gas recovery from shale gas reservoirs has been recently in the centre of attention of reservoir engineers. The technique of injection CO<sub>2</sub> into shale reservoirs therefore becomes more considerable due to its dual benefit as a mechanism for enhanced shale recovery and CO<sub>2</sub> sequestrations.

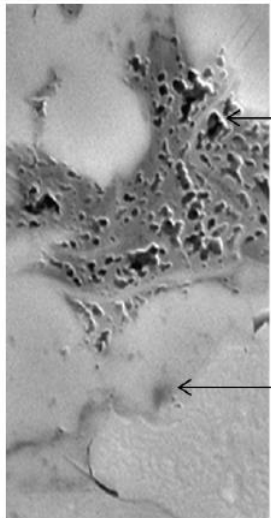
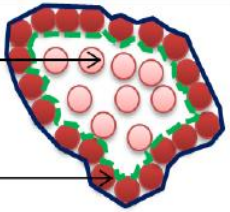
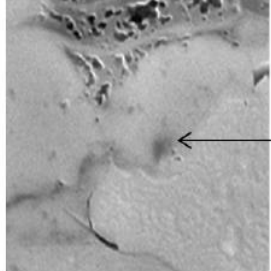
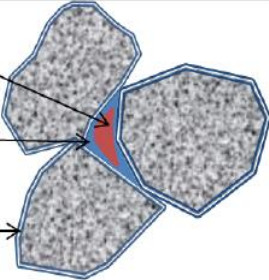
Shale Structure		Fluid in Shale	
	Kerogen	Free gas ( $\phi_{kff}$ )	
		Adsorbed gas ( $\phi_{kff}$ )	
	Inorganic matrix (clay + non-clay)	Free gas ( $\phi_{bff}$ )	
		Pc bound water ( $\phi_{pcbww}$ )	
		Clay bound water ( $\phi_{clbw}$ )	

Figure 5. 2 Typical shale gas pores system and storage mechanism [110][Copyright 2013, Society of Petroleum Engineers]

### 5.3.2. CO<sub>2</sub> Sequestration

Since the industrial revolution, the increased emission of greenhouse gases (GHG) has been recognised as a factor strongly related to the global climate changes [128]. The major portion of anthropogenic GHGs emissions is mainly released from the consumption of fossil fuel [36].

As a result of the intensive consumption in fossil fuels due to global energy demand, emissions from GHGs, in particular CO<sub>2</sub>, have sparked sharp and historical rises in emission levels in the past decade [129]. In 2020, despite the reduction gained due to COVID-19 pandemic, global energy-related CO<sub>2</sub> emission is on track to increase by 1.2 billion tonnes in 2021, recording a historical level [1]. Figure 5.3 depicts the change in consumption trend for fossil fuels by fuel from 1900 -2021.

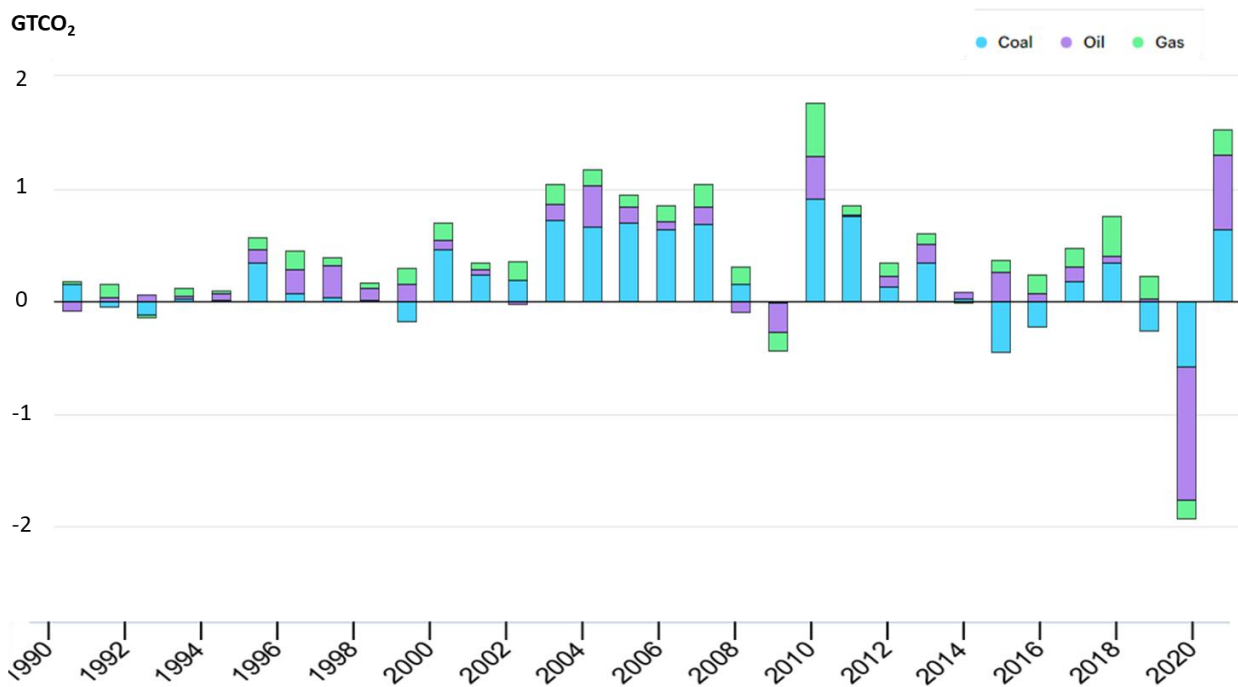


Figure 5. 3 Global CO<sub>2</sub> emission from fossil fuels [1]

Therefore, global agreements have been launched to initiate mechanisms needed for a sharp reduction in GHGs. Typically, emissions could be reduced either by switching to alternate cleaner energies such as solar and wind or mitigating the effects of GHGs using capturing and storage technologies. Geological sequestration has been considered as a potential mechanism for a large-scale and effective CO<sub>2</sub> subsurface storage. CO<sub>2</sub> geological sequestration is injecting CO<sub>2</sub> into deep geologic formation in which CO<sub>2</sub> could be safely stored underground for thousands of years [130]. Depleted oil and gas reservoirs, coal-beds, shale, and deep saline formation have the potential to store CO<sub>2</sub> permanently [131] [40]. Among these geological sites, shale is the safest for CO<sub>2</sub> sequestration due to its ultra-low permeability [131]. In

literature, laboratory work and simulation studies revealed that up to 95% of the injected CO<sub>2</sub> into shale reservoirs could be potentially stored [9, 57, 132, 133].

### 5.3.2. Enhanced Gas Recovery

It is well-known that shale reservoirs are characterised by high organic content which ranges from 2% to 10% of the total weight of organic-rich shales and mainly controlled by thermal maturity [60]. Significant amounts of gas are stored in shale reservoirs as an adsorbed gas on the surface of finely dispersed organic matter [52, 72, 134]. Thus, unlocking adsorbed gas has brought more attention to shale reservoirs as a promising target for enhanced gas recovery and has recently been the major area of interest within the exploitation of shale gas resources [8]. One such method is Carbon dioxide (CO<sub>2</sub>) injection within shale fracture and matrix system. Laboratory tests have proven that CO<sub>2</sub> has a great affinity to be adsorbed on organic surface over methane and thus initiates the potential not only for enhanced gas recovery (EGR), but also for CO<sub>2</sub> sequestration [23, 24, 26, 104, 135, 136]. This allows CO<sub>2</sub> to release CH<sub>4</sub> under subsurface conditions which can be referred to the desorption process. As desorption takes place, desorbed gas transports by diffusion mechanism from micro pores of organic materials (primary porosity system) to macropores of matrix and fractures (secondary porosity system) [34]. Theoretically, pressure in the secondary porosity system is dominated by an injection effect which drives gas (free and resorbed) by Darcy flow mechanism towards fracture and then well bores [12]. In addition, it is believed that desorption process enhances matrix permeability as a sequence of increasing in effective diameter [137]. However, CO<sub>2</sub>-EGR is a complex geophysical process as the effectiveness of EGR is governed by many physical process such as the diffusion capacity of CO<sub>2</sub> into shale matrix [45] and CO<sub>2</sub>-CH<sub>4</sub> competitive adsorption [46]. When CO<sub>2</sub> presents in the shale pores system, counter diffusion, and competitive adsorption between CO<sub>2</sub> and CH<sub>4</sub> takes place in the shale matrix. Multi-component effect is a well-recognised process that modifies gas transport mechanism, particularly, the surface diffusion of desorbed gas [44].

Previous studies in literature have proved that injection of CO<sub>2</sub> into organic-rich shale reservoirs can lead up to 59% additional recovery from original gas in place (OGIP) whereas up to 100% of the injected CO<sub>2</sub> could be permanently sequestered [31, 33, 44, 54]. Even though, EGR-CO<sub>2</sub> injection has not been commercialised yet, a considerable amount of laboratory tests and simulation studies have been carried out on the feasibility of the technique. The concept of CO<sub>2</sub> injection was first extended to shale gas reservoirs by [23]. His

experimental study has demonstrated that shales can react very similarly to coal-bed methane where organic matter  $\text{CO}_2$  is preferentially adsorbed on organic surface over  $\text{CH}_4$  at a ratio of 5:1. The adsorption ratio depends on shale type and reservoir pressure and temperature [20]. These remarkable observations have drawn attention to shales as potential geological traps for  $\text{CO}_2$  permanent sequestration and EGR. Therefore, many studies have been conducted to investigate  $\text{CO}_2$  storage capacity and prove the viability of enhanced gas production from different shale reservoirs. [10] performed a comprehensive simulation work investigating a series of injection scenarios of  $\text{CO}_2$  flooding (continuous injection) and huff and puff (injection-soaking cycle). Their simulation results showed that  $\text{CO}_2$  flooding into shale reservoirs showed a significant increase in recovery with about 50% of injected stream being sequestered. Similarly, [33] reported in his study that 7% incremental recovery could be achieved at optimal wells pattern. In another study, [57] [32] employed dual-porosity and dual-permeability models in their studies that showed the feasibility of  $\text{CO}_2$  injection to increase shale recovery.

Investigating the controlling factors which govern the applicability of  $\text{CO}_2$ -EGR has been also undertaken in literature. According to several studies, the induced and natural fractures permeabilities are the key influencing parameters on the efficiency of EGR and  $\text{CO}_2$  sequestration, where a higher fractures permeabilities results in high enhanced gas recovery and  $\text{CO}_2$  thus likely to be sequestered [20, 34, 69, 70]. In contrast to those findings, [26] demonstrated that EGR efficiency correlates negatively with matrix permeability due to higher pore fractural dimension. In addition to fractures permeability effect, the TOC has been found as a significant parameter on  $\text{CO}_2$  storage [26, 32]. Later in 2014, [55] pointed out the significance of matrix porosity on the incremental recovery. Recently, the effect of multi components have been considered in many simulation studies [30, 44, 54, 73]. The results of these studies concluded the functionality of  $\text{CO}_2$  injection to increase shale recovery by indicating the importance of surface diffusion as a key driving mechanism in  $\text{CO}_2$ -EGR process. The effect of injection pressure has been also investigated. [31] highlighted that, despite the positive correlation between injection pressure and enhanced gas recovery, early severe breakthrough of  $\text{CO}_2$  is very likely to occur. Conversely, [71] reported no significant effect of increasing  $\text{CO}_2$  injection rates on shale gas recovery. This view was supported by [72] in his numerical simulation study. [20] demonstrated that reservoir pressure plays the key role in the process where low reservoir pressure facilitates  $\text{CH}_4$  displacement by injected  $\text{CO}_2$ . Matrix permeability has been recognised as the most significant factor in many studies [7]. In

another investigation, the correlation between the production time and enhanced recovery has been addressed. [28] demonstrated that production time and pressure significantly affect CO<sub>2</sub> sequestration and shale gas recovery.

From the foregoing, no quantitative framework and accurate CO<sub>2</sub>-EGR modelling, and design process has been identified. Thus, there are still uncertainties in determining the main factors that control CO<sub>2</sub> sequestration and enhanced CH<sub>4</sub> recovery in shale reservoirs. Two discrete reasons could explain this gap in knowledge. First, shale reservoirs are widely characterised as heterogeneous formations in lithology, TOC, pore size, texture, and petrophysical properties [53]. As a result of this complexity, the previous studies have been conducted using various modelling techniques and approaches. A notable example of this, some authors employed single-porosity and single-permeability models, while others considered dual and multi-porosity and multi-permeability models. Second, most researchers to date have tended to conduct sensitivity analysis to investigate the effect of a few parameters individually rather than treating the controlling parameters collectively in much detail.

This study therefore seeks to remedy this gap in knowledge by providing a comprehensive investigation on the correlation between shale properties as well as engineering parameters and the efficiency of CO<sub>2</sub>-EGR and helps the industry to conceptual understanding when designing and implementing CO<sub>2</sub>-EGR in shale reservoirs. To meet these objectives, data for this work were extracted from previous publications that have examined the feasibility of CO<sub>2</sub> sequestration with potential of enhanced gas recovery in shale reservoirs. For most of the generalizable results, we gathered data across the available studies in literature on a wide subset of numerical modelling studies and experimental investigations. The sensitivity of these data was further improved by handling the missing values using imputation approaches. Previous studies have been carried out by using a sensitivity analysis approach which does not take account of the relationship between independent and dependent variables, Unlike the previous studies, this is the first study to employ correlation to identify the strength of the relationship between the examined parameters and the efficiency of CO<sub>2</sub>-EGR. In this study, we provide a broader perspective from the collected data on the correlation of factors which have a significant impact on enhanced gas recovery and CO<sub>2</sub> sequestration in shale gas reservoirs. The methodological approach taken in this study is Spearman correlation coefficient to further analyse 63 injection cases. Our statistical analysis provides a practical screening tool to manage and predict the efficiency of both enhanced gas recovery and CO<sub>2</sub> sequestrations in shale

reservoirs. Moreover, this study lays a foundation for efficient CO<sub>2</sub>-EGR design and implementation.

## 5.4 Correlation Coefficient for Factors Analysis

### 5.4.1. Exploratory Data Analysis

The performance of enhancing shale recovery by CO<sub>2</sub> injection is a direct function of shale properties and engineering features of design and operational parameters. Therefore, to systematically examine the correlation between parameters, in this work totally data for 63 injection scenarios were collected from literature spanning the years 2009 – 2019. To ensure the reliability, our dataset was gathered from two main sources: results obtained from validated simulation models (54 simulation cases) and experimental investigations (9 experimental cases). Although this extensive range of sources offers a unified correlation for CO<sub>2</sub>-EGR, one of the limitations was the occurrence of unbalance as our dataset heavily relied on simulation studies which accounted for about 85% of our dataset. Table 5.1 illustrates the breakdown of the studies and shale types used in our dataset.

*Table 5. 1 Simulation studies and shale types used for dataset.*

<i>Shale Type</i>	<i>Study</i>	<i>No of injection Cases</i>	<i>Methodologies/Assumptions</i>	<i>Author</i>
Devonian	Numerical Simulation	6	<ul style="list-style-type: none"> <li>• Huff-n-puff</li> <li>• Dual porosity and permeability model</li> </ul>	[10]
Synthetic	Numerical Simulation	4	<ul style="list-style-type: none"> <li>• Flooding</li> <li>• Discrete fracture network model</li> <li>• Multi porosity and permeability model</li> </ul>	[34]
Marcellus	Numerical Simulation	9	<ul style="list-style-type: none"> <li>• Flooding</li> <li>• Multi porosity and permeability model</li> </ul>	[33]

Synthetic	Numerical Simulation	2	<ul style="list-style-type: none"> <li>• Flooding</li> <li>• Dual porosity and permeability model</li> <li>• Diffusion model</li> </ul>	[57]
New Albany	Numerical Simulation	2	<ul style="list-style-type: none"> <li>• Flooding / huff-n-puff</li> <li>• Dual porosity and permeability model</li> <li>• Diffusion model</li> <li>• CO<sub>2</sub> dissolution</li> </ul>	[32]
Barnett	Numerical Simulation	3	<ul style="list-style-type: none"> <li>• Flooding</li> <li>• Dual porosity and permeability model</li> </ul>	[31]
Barnett	Numerical Simulation	4	<ul style="list-style-type: none"> <li>• Flooding / huff-n-puff</li> </ul>	[7]
Barnett	Numerical Simulation	14	<ul style="list-style-type: none"> <li>• Flooding / huff-n-puff</li> <li>• Multi porosity and permeability model</li> <li>• CO<sub>2</sub> dissolution</li> <li>• Stress-dependent model</li> </ul>	[30]
Yanchang	Numerical Simulation	4	<ul style="list-style-type: none"> <li>• Flooding</li> <li>• Diffusion model</li> </ul>	[72]
Silurian Longmaxi	Numerical Simulation	1	<ul style="list-style-type: none"> <li>• Huff-n-puff</li> <li>• Multi porosity and dual permeability model</li> <li>• Diffusion model</li> </ul>	[28]
Synthetic	Numerical Simulation	3	<ul style="list-style-type: none"> <li>• Flooding</li> <li>• Non-Darcy effect</li> <li>• Instant sorption model</li> </ul>	[29]
Yanchang	Numerical Simulation	2	<ul style="list-style-type: none"> <li>• Flooding</li> <li>• Geochemical interaction effect.</li> </ul>	[27]
Silurian Longmaxi	Experimental Study	9	<ul style="list-style-type: none"> <li>• Flooding</li> <li>• New NMR experimental approach</li> </ul>	[26]



Missing values is one of the most common problems frequently occurring in real-world data recording or processing [138]. The most popular handling methods for missing values is either deleting rows or columns having null values or imputing the missing values using mean or categorical imputing techniques [139]. For the two treatment methods, there is no preferred solution, but each method becomes the preferable under certain conditions [140].

In this study, therefore a hybrid approach was adopted for handling the missing values to avoid producing the issue of bias in our dataset. However, there are some parameters that we could not technically impute such as reservoir thickness.

Our approach categorises the missing values and treats it accordingly as follows:

1. Following ‘missingness mechanism’ [139], variables missing at random (MAR) were dropped from data. For example, missing values of reservoir thickness.
2. Impute Missing Not at Random (MNAR) that can be predicted using shale data. For example, missing petrophysical values for Barnett shale (e.g., TOC and pressure gradient) could be imputed from the typical data for the Barnett shale listed in our databank.

Table 5.2 illustrates the wide range of petrophysical data used in our original dataset. Table 5.3 shows the operating parameters of different injection cases including flooding scenarios denoted by 1, and huff and buff scenario denoted by 0.

*Table 5. 2 The range of petrophysical parameters used in dataset*

Parameter	Mean	Standard deviation	Minimum	Percentile 25%	Percentile 50%	Percentile 75%	Maximum
<b>Pressure, psi</b>	6792.673	10886.48	780	1396.603	2140	4582.783	48643.61
<b>Temperature, F°</b>	120.8826	41.2604	85	90.82959	106	150	302
<b>Reservoir thickness, ft</b>	255.3311	411.2362	3.28084	100	200	300	2913
<b>Depth, ft</b>	4770.73	1766.632	1378	3720	4102.761	5670	9842.52
<b>Matrix permeability, md</b>	0.002199	0.005642	5E-20	5.7E-07	0.000236	0.00052	0.018
<b>Organic permeability, md</b>	0.002293	0.005607	0.000005	0.000228	0.00038	0.00052	0.018
<b>Natural fracture Permeability, md</b>	2.130345	14.42826	5E-10	0.00227	0.00321	0.00712	100
<b>TOC, %</b>	3.92	0.252982	3.2	4	4	4	4
<b>Matrix porosity, %</b>	4.677407	2.421882	1	2.9	4.1	6.875	10
<b>Organic porosity, %</b>	2.024052	3.097961	0.0352	0.0505	0.06	4.125	10

<b>Natural fracture porosity, %</b>	1.966663	3.717878	0.00004	0.029	0.0352	0.7075	14
<b>CH<sub>4</sub> Langmuir volume, scf/ton</b>	91.22467	120.5147	38.9	39.2	51	90.05	741.615
<b>CO<sub>2</sub> Langmuir volume, scf/ton</b>	287.4234	481.5702	10.2	74.375	183.6	232.98	2189.53
<b>CH<sub>4</sub> Langmuir pressure, psi</b>	1302.016	420.1904	145	1000	1458.705	1596	1765.537
<b>CO<sub>2</sub> Langmuir pressure, psi</b>	36257.35	248008.9	493	973.4727	1253.13	1254	1754870
<b>Injection scenario</b>	0.698113	0.46347	0	0	1	1	1
<b>Sequestrated CO<sub>2</sub>, %</b>	0.350409	0.378015	0	0	0.2	0.7	1
<b>Incremental RF, %</b>	0.086263	0.094658	-0.047	0.0105	0.07	0.1385	0.34

Table 5. 3 The range of engineering parameters used in dataset

Parameter	Mean	Std deviation	Minimum	Percentile 25%	Percentile 50%	Percentile 75%	Maximum
<b>well spacing, ft</b>	597.9574	401.636	49.2126	249.3438	498.6877	1000	1280
<b>Fracture conductivity, md-ft</b>	50.3772	45.49276	3.28084	10	31	99	100
<b>Fracture half length, ft</b>	276.3678	162.3138	82	100	250	425	541
<b>Hydraulic fracture permeability, md</b>	14321.43	37780.7	1E-07	50	50	50	100000
<b>Injection scenario</b>	0.692308	0.466041	0	0	1	1	1
<b>overpressure injection, psi</b>	667	430.1395	0	580	725	870	1160
<b>Injected CO<sub>2</sub>, ton</b>	3466.761	4336.405	300	300	1204.603	9291.306	13430.42
<b>sequestrated CO<sub>2</sub>, ton</b>	906.2089	2217.973	0	0	274	300	8953.614
<b>Recovered CO<sub>2</sub>, %</b>	38.20695	41.57038	0	1.5	14.75	82.29167	100
<b>Primary RF, %</b>	41.87746	33.81309	2.2	9.897114	51.65	73.75	85.1
<b>Injection RF, %</b>	44.49178	36.57873	2	9.502762	48.4	80	95.3
<b>Incremental RF, %</b>	8.979585	9.548676	-4.7	1.05	7.5	13.9	34

### 5.4.2. Spearman Correlation Coefficient

Correlation analysis methods are the most common statistical approaches which are widely used for several applications such as exploratory data analysis and structural modelling [141] [142]. The main objectives of the correlation analysis tests are to identify whether there is a statistically negative or positive relationship between variables, and to determine the statistical strength of relationship [141]. The term ‘correlation’ is often referring to a linear relationship between two or more continuous variables. In most of the cases, the conventional correlation methods may not be suitable for the non-linearity correlations.

In statistics, the most common correlation methods are Pearson coefficient, Spearman coefficient, and Analysis of Variance (ANOVA) [143] [144]. The application of each method highly depends on the types of the examined dataset. Pearson coefficient is typically used for normally distributed and large observation data [145]. Although Pearson correlation works best if the correlation between two variables is a linear relationship, the main limitation of Pearson method is that a significant correlation between two variables can result in a non-significant [146]. On the other hand, Spearman coefficient can be used for non-normally distributed data or for data with relevant outliers to measure the monotonic relationship of variables whether linear or non-linear [145]. Analysis of variance (ANOVA) is a statistical technique used to analyse the variation in responses between several group means [147]. Currently, ANOVA continues to be one of the most widely used forms of statistical analysis in many areas of science. Nevertheless, ANOVA is a general linear model that quantifies the correlation in only parametric and normally distributed data [147].

The main reason for choosing Spearman correlation for this study is that it does not require the assumption that the relationship between the variables in our dataset is linear since it determines the monotonic relationship of variables whether linear or non-linear. Additionally, Spearman correlation is the most fitting for datasets with nonnormality as previously discussed. Consequently, Spearman correlation was a preferred method in our study than Pearson and ANOVA if taking into consideration the wide range of resources and shale types in our dataset. However, a potential limitation of using Spearman correlation is that the significance in Spearman correlation may lead to significance and insignificance in other correlation methods as presented in previous studies in literature [144].

Spearman correlation coefficient can be expressed by formulation (5.1) [148] which yields a value that varies from  $-1$  that represents a negative correlation to  $+1$ , that represents a positive correlation between variables [149].

$$\rho = \frac{\sum_i(x_i-\bar{x})*(y_i-\bar{y})}{\sqrt{\sum_i(x_i-\bar{x})*(y_i-\bar{y})}} \quad \text{Equation (5.1)}$$

Python is widely used in data science and engineering fields for technical computing and modelling purposes. In our study, some Python libraries and functions have been written to take advantage of spearman correlation computing.

## 5.5 Results and Discussion

### 5.5.2. The Effect of Shale Petrophysical Parameters on CO<sub>2</sub>-EGR

The results obtained from correlation analysis are summarized in Figure 5.4 and 5.5 which capture the intercorrelation among the whole variables across our dataset as shown in the horizontal and vertical axis. However, this work focuses only on the parameters affecting the efficiency of CO<sub>2</sub>-EGR as the intercorrelation between the shale and engineering is beyond the scope of this study (e.g., the correlation between TOC and shale porosity or the correlation between well spacing and hydraulic fracture conductivity). The visualisation techniques of Figures 5.4 and 5.5 are that they illustrate the direction of the correlation (positive or negative), and they depict the magnitude (strength) as colour where darker colours indicate stronger correlation.

In this section, we will discuss in detail the statistical results and the interpretation on the correlation between shale properties and the efficiency of CO<sub>2</sub>-EGR. In our analysis, the efficiency of CO<sub>2</sub>-EGR is represented by two main parameters. First, incremental RF which represents the amount and the additional CH<sub>4</sub> production due to CO<sub>2</sub> injection. Second, sequestered CO<sub>2</sub> which represents the amount of adsorbed CO<sub>2</sub>. In the below discussion, interpretation on the observed correlation between each single parameter and both incremental RF and sequestered CO<sub>2</sub> will be provided. For example, the explanation on why fracture permeability has a negative impact of incremental RF while it has a negative impact on CO<sub>2</sub> sequestration.

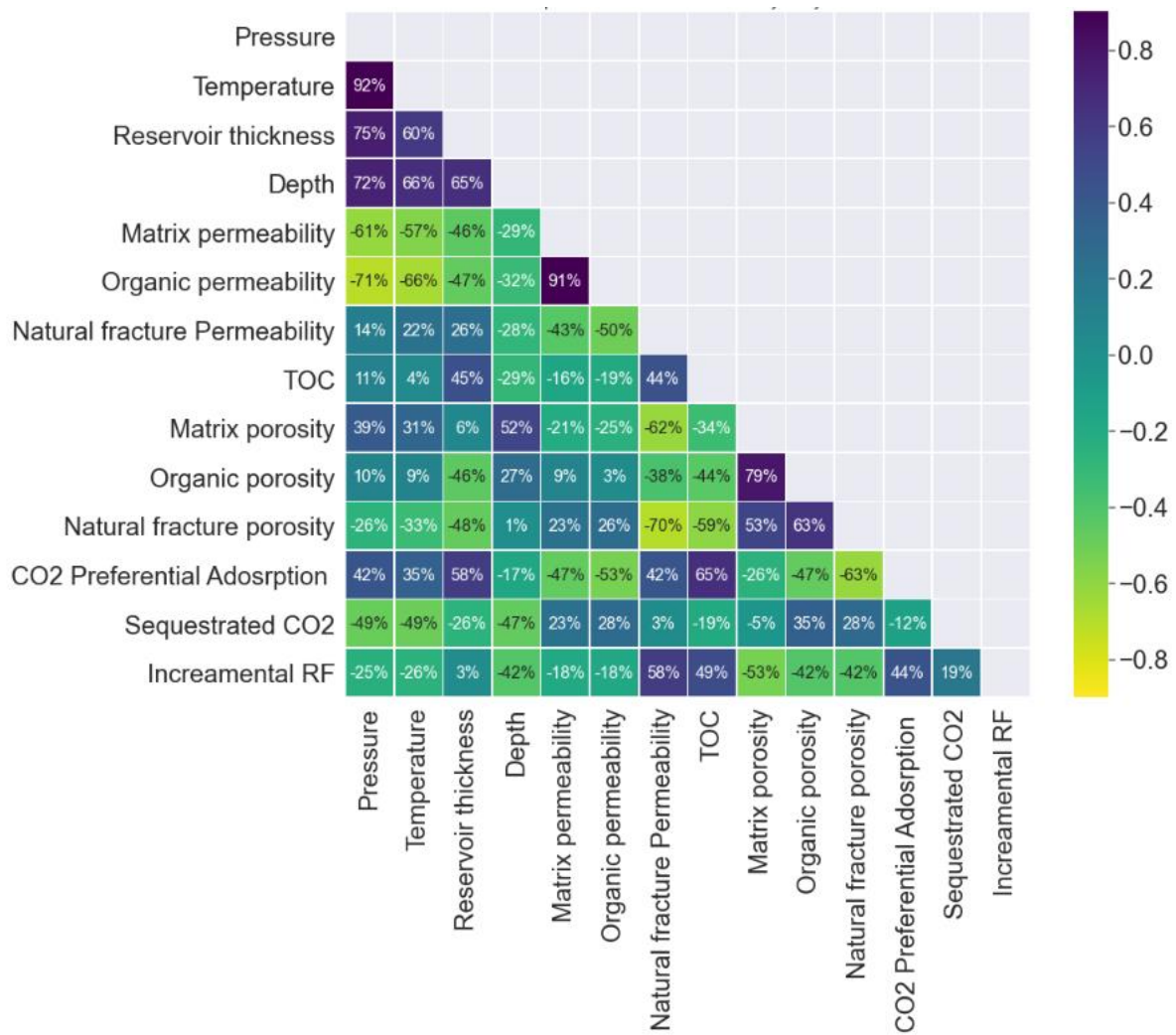


Figure 5.4 Spearman correlation for shale properties

### 5.5.1.1. The Effect of Permeability

Clearly, natural fracture permeability was found to be the most influential parameter on EGR. Figure 5.4 shows that natural fracture permeability has a positive correlation to both CH<sub>4</sub> production and CO<sub>2</sub> storage. It is worth to mentioning that higher natural fracture permeability could increase the possibilities of CO<sub>2</sub> re-production which explains the very low correlation of fractures permeability to CO<sub>2</sub> storage (3%) compared to CH<sub>4</sub> production (58%). These results match those observed in earlier studies which clearly demonstrated the pronounced effect of fractures permeability on EGR efficiency [20, 34, 69, 70]. This observation could be attributed to that higher fracture permeability causes larger pressure drop in natural fractures which facilitates free and desorbed gas transport from shale matrix to fractures network.

Turning now to matrix permeability, our results demonstrate that shale reservoirs in low inorganic matrix permeability are good candidates for EGR by CO<sub>2</sub> injection. By contrast, our results also showed a positive effect of matrix (inorganic) and organic permeabilities on CO<sub>2</sub> storage. A similar phenomenon observed by [26, 69] who argued in their studies that EGR efficiency tends to decrease with increasing matrix permeability. They attributed their finding to the possible negative effect of matrix permeability on CO<sub>2</sub>-CH<sub>4</sub> competitive adsorption; additionally, a higher permeability could promote CH<sub>4</sub> leakage away from the production area. There are, however, other possible explanations: injection CO<sub>2</sub> into a low matrix permeability does not significantly affect the pressure drawdown within shale matrix, consequently, the continuous pressure decline expedites methane desorption from shale surface; in addition, ultra-low matrix permeability leads to high partial pressure of CO<sub>2</sub> which increases CO<sub>2</sub> adsorption rate and in turn increases the desorption rate of CH<sub>4</sub> from shale matrix.

Organic permeability is found in our study to have the same magnitude of correlation as inorganic permeability. This could be attributed to the consideration of the dual-permeability model in most previous simulation studies in our dataset, which ignores the effect of sub-cells of organic permeabilities such as studies in references [10, 31, 32, 57].

#### 5.5.1.2. The Effect of TOC

In our analysis, a significant positive correlation of 49% is found between TOC and enhanced CH<sub>4</sub> production by CO<sub>2</sub> injection as illustrated in Figure 5.4. This is obviously because that the key mechanism of enhanced shale recovery is releasing of CH<sub>4</sub> from the surface of organic matter due to greater affinity of shale to adsorb CO<sub>2</sub>. Given the adsorbed CH<sub>4</sub> may account up to 60% of the total shale gas in place [12], the greater TOC increases competitive adsorption of CO<sub>2</sub>-CH<sub>4</sub> and hence increases the contribution of desorbed CH<sub>4</sub> to the total shale production. Although CO<sub>2</sub> adsorption on shale organic materials is the main trapping mechanism of CO<sub>2</sub>, what is unanticipated is that our results showed that less CO<sub>2</sub> tends to be trapped on the surface of shale with a greater TOC. This result does not support the previous studies [26, 32] that have examined the effect of TOC. However, this finding seems to be consistent with those of [150], this phenomenon could be attributed to the induced swelling response of shale matrix due to the simultaneous desorption of CH<sub>4</sub>, permeability decreases and the effective stress increases which results in inefficient CO<sub>2</sub> sequestration.

#### 5.5.1.3. The Effect of Adsorption Capacities

In literature, laboratory tests have proved that CO<sub>2</sub> is preferentially adsorbed over CH<sub>4</sub> at a ratio of 5:1 [23]. The adsorption ratio across our collected dataset lies in the range of 0.1 to 4.7 as shown in Table 5.1. The analytical approach taken in our study was to examine the preferential adsorption capacity rather than adsorption capacities of CO<sub>2</sub> and CH<sub>4</sub> separately to provide a more realistic perspective of CO<sub>2</sub>-CH<sub>4</sub> displacement. Figure 5.4 clearly shows that the preferential adsorption is an important factor that has a substantial positive effect on CO<sub>2</sub>-EGR efficiency. Our study indicates that the higher affinity of rich-organic shales to adsorb CO<sub>2</sub> will promote the release of CH<sub>4</sub> from organic surface and increase.

#### 5.5.1.4. The Effect of Reservoir Depth (Pressure)

As shown in Figure 5.4, our results reveal that deep shale reservoirs are not favourable targets for both enhanced shale recovery and CO<sub>2</sub> sequestration. As shown in Figure 5.4, the enhanced recovery and CO<sub>2</sub> storage are negatively correlating to reservoir depth at coefficients of 42% and 47% respectively. Those results further support our previous simulation study [22] which demonstrated that desorption of CH<sub>4</sub> becomes insignificant with the increase in reservoir depth regardless of shale organic volume. Typically, the adsorbed gas relates in a non-linear correlation to pressure yielding a general trend of increasing with pressure [23]. Clearly, unlocking adsorbed gas which is basically controlled by pressure drop within the shale matrix plays key role in both shale primary production and CO<sub>2</sub>-EGR. For this reason, in deep shale reservoirs (i.e., higher reservoir pressure), with taken into consideration the ultra-low permeability nature of the shale matrix, adsorbed CH<sub>4</sub> is less likely to desorb and transport towards fractures network. The results indicate that shallow shale reservoirs are most favourable targets for CO<sub>2</sub>-CH<sub>4</sub> displacement, particularly shales with high TOC.

#### 5.5.1.5. The Effect of Porosity

Usually, shale matrix porosity has a pronounced effect on free gas storage and production. Hence CO<sub>2</sub> injection basically enhances adsorbed gas production, previous studies reported no clear correlation between porosity and both enhanced shale recovery and sequestered CO<sub>2</sub> [54]. Other studies, however, found a minor positive correlation between shale porosity and CO<sub>2</sub>-EGR efficiency [34]. Contrary to expectations, however, organic and natural fracture porosities are showing in our analysis a positive correlation to CO<sub>2</sub> storage. Our study also shows that any increases in shale porosities (organic, in organic, and natural fractures

porosities) will noticeably decrease the incremental CH<sub>4</sub> production. This finding is found to be consistent with those of Yu and Al-Shalabi [7].

To further explain our observation, it is essential to understand that CO<sub>2</sub>-CH<sub>4</sub> displacement results from CO<sub>2</sub>-CH<sub>4</sub> competitive adsorption. The competitive adsorption takes place within organic pores due to CO<sub>2</sub> injection into the shale matrix which is dominated by diffusion/dispersion gas transport mechanisms [44, 110]. According to Equation 5.2 [24], molecular diffusion coefficient (D<sub>a</sub>) of CO<sub>2</sub> decrease with increasing shale porosity (ϕ) which in return mitigates desorbed gas transport towards shale matrix and fractures.

$$K_d = \frac{D_a}{N\phi} + \gamma \quad (5.2)$$

Where:

K<sub>d</sub> : dispersion coefficient

D<sub>a</sub>: molecular diffusion coefficient

N: formation resistivity factor

ϕ: porosity

γ: dispersity

#### 5.5.1.6. The effect of Reservoir Temperature

In accordance with previous studies, a remarkable negative correlation between reservoir temperature and both enhanced CH<sub>4</sub> and CO<sub>2</sub> sequestration is observed in our analysis as shown in Figure 5.4. As discussed before, a successful CO<sub>2</sub>-EGR process results from efficient CO<sub>2</sub>-CH<sub>4</sub> competitive adsorption within the shale matrix. At high-temperature shale reservoirs, less quantities of adsorbed CH<sub>4</sub> and thus is less likely to capture CO<sub>2</sub>. For further explanation, Langmuir isotherms are commonly the most applied model for shale gas adsorption and desorption behaviours. Langmuir isotherms are based upon the assumption of monolayer adsorption thickness at constant temperature [25]. Several studies that examined CH<sub>4</sub> adsorption revealed that the amount of adsorbed CH<sub>4</sub> significantly decreases with increased temperature [151].

#### 5.5.1.7. The Effect of Reservoir Thickness

Based on our results, the effect of reservoir thickness on incremental CH<sub>4</sub> production is negligible. However, as shown in Figure 5.4 a negative correlation is found between the



sequestered CO<sub>2</sub> and reservoir thickness. This phenomenon could be attributed to lower CO<sub>2</sub> saturation of fractures and matrix due to large reservoir thickness, if compared to saturation in a smaller thickness, which may result in a limited amount of injected CO<sub>2</sub> displacing adsorbed CH<sub>4</sub>. However, more in-depth investigations are required to further confirm this observation.

### 5.5.2. The Effect of Engineering Parameters on CO<sub>2</sub>-EGR

Even though the significance impact of shale properties on CO<sub>2</sub>-EGR efficiency is undisputed, engineering parameters also play a considerable role in the process of enhanced shale recovery by CO<sub>2</sub> injection. In this section of our analysis, several engineering parameters are analysed as shown in Figure 5.5.

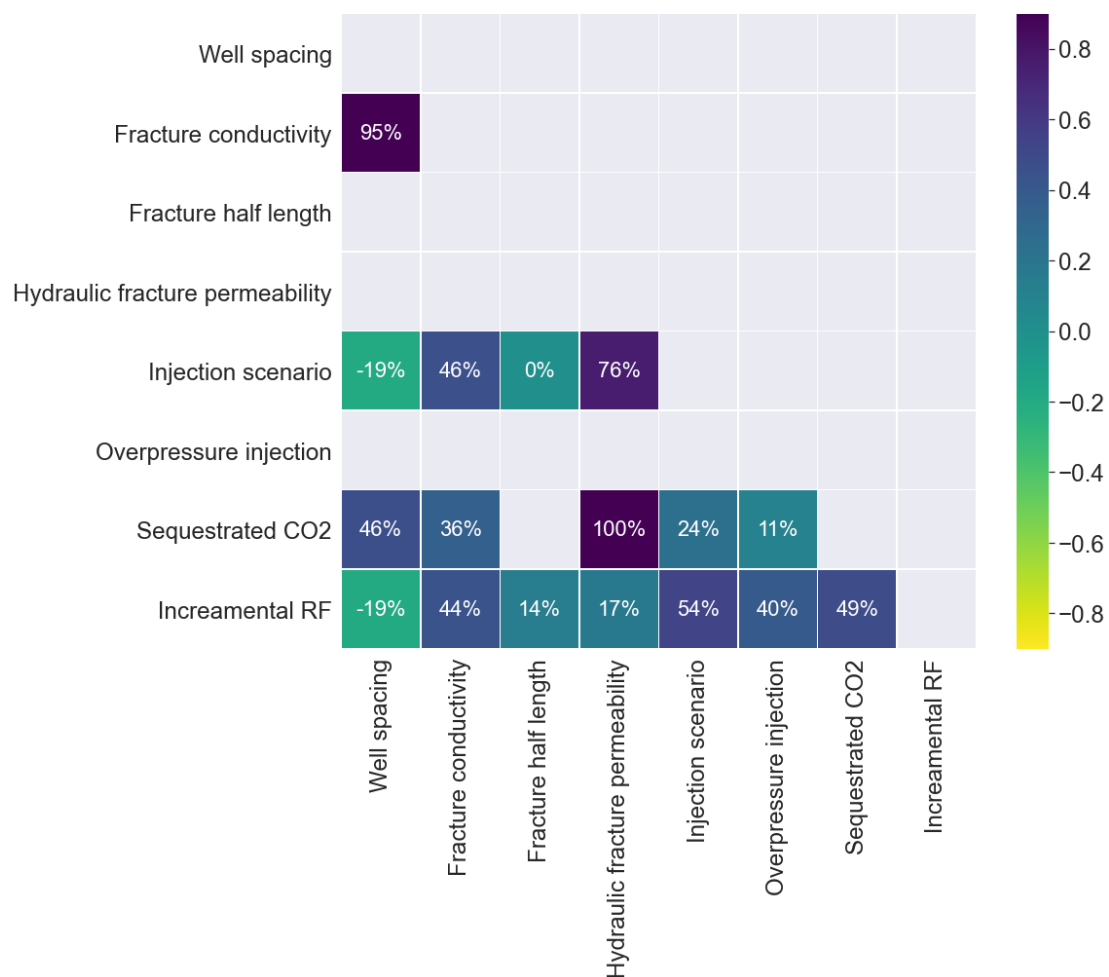


Figure 5. 5 Spearman correlation for injection engineering parameters

#### 5.5.2.1. The Effect of Injection Scenario

In our analysis we aimed to investigate the efficiency of enhanced CH<sub>4</sub> recovery and sequestered CO<sub>2</sub> in shale gas under two injection scenarios of CO<sub>2</sub>, flooding and huff and buff. Our analysis clearly shows that huff-buff injection scenario is not the best option for CO<sub>2</sub> injection into shale reservoirs regardless of the effect of the soaking period as illustrated in Figure 5.5. Due to the typical cycle of soaking-production, the injected CO<sub>2</sub> cannot efficiently migrate to the extension of shale reservoirs which significantly reduces the effect of CO<sub>2</sub>-CH<sub>4</sub> competitive adsorption, and injected CO<sub>2</sub> is consequently re-produced very quickly. However, a noticeable amount of CO<sub>2</sub> is simultaneously sequestered which may explain the less effect of huff and buff on CO<sub>2</sub> sequestration.

These results further agree with the findings of previous simulation studies which agreed that huff and buff injection may not be a viable option for shale production enhancement and sequestration of CO<sub>2</sub> [10, 30, 32, 55]. Moreover, the huff and buff scenario was found to reduce methane recovery if compared to no-injection scenario due the rapid backflow of injected CO<sub>2</sub> [7]. Our Study indicates that continuous injection might be the best applicable option for CO<sub>2</sub> injection in shale reservoirs.

#### 5.5.2.2. The Effect of Fracture Conductivity and Permeability

In our analysis, the conductivity and permeability of the hydraulic-fractures network are found to have substantial positive effect on enhanced CH<sub>4</sub> production as well as CO<sub>2</sub> storage as depicted in Figure 5.5. For example, fracture conductivity correlates positively by 44% to incremental recovery, and by 36% to CO<sub>2</sub> storage. Theoretically, the fracture network promotes Darcy flow of free gas (free and desorbed) at an early stage of production and causes a larger pressure drop in the shale matrix. As a result, any increase in fractures conductivity will noticeably increase the rate of CH<sub>4</sub> desorption. This obviously reduces adsorbed gas concentration around fractures and facilitates surface diffusion within shale matrix not only for desorbed CH<sub>4</sub>, but also for injected CO<sub>2</sub>, thus leads to faster and higher CO<sub>2</sub>-CH<sub>4</sub> displacement rate. Therefore, a successful hydraulic-fractures network with effective values of permeability and conductivity is essential for CO<sub>2</sub>-EGR efficiency in shale reservoirs.

#### 5.5.2.3. The Effect of Injection Pressure

According to our results, it is clearly shown that higher injection pressure increase the total enhanced CH<sub>4</sub> production. Obviously, as the pressure difference between injection pressure

and reservoir pressure increases, more driving forces are initiated within the shale matrix [24]. As discussed earlier, surface diffusion is the key gas transport mechanism within organic nanopores where CO<sub>2</sub>-CH<sub>4</sub> competitive adsorption takes place. Although surface diffusion coefficient is independent on pressure [12], higher injection pressure reduces the flowing fraction leading more CO<sub>2</sub> to diffuse and displace adsorbed CH<sub>4</sub> towards producers [24]. However, to some extent, injecting CO<sub>2</sub> at high pressure increases dispersion coefficient (mechanical mixing of CO<sub>2</sub>-CH<sub>4</sub>) [24], consequently, early CO<sub>2</sub> break-through of injected stream may occur. Therefore, the injection pressure effect on CO<sub>2</sub> storage capacity is not significant as in enhancing CH<sub>4</sub> production as shown in Figure 5.5, this finding was also obtained by Li, X. and D. Elsworth [31].

#### 5.5.2.4. The Effect of Well Spacing

Figure 5.5 depicts that the enhanced CH<sub>4</sub> production decreases with increasing the space between CO<sub>2</sub> injectors and CH<sub>4</sub> producers. The results are expected because with increasing well spacing, more pressure is maintained around CO<sub>2</sub> injectors and less pressure transient extended into organic volumes due to the ultra-low matrix permeability, which results in a limited amount of CO<sub>2</sub> migrating to the zone of CH<sub>4</sub> producers. Although this phenomenon reduces CO<sub>2</sub>-CH<sub>4</sub> displacement, it significantly mitigates CO<sub>2</sub> breakthrough and increases CO<sub>2</sub> storage as shown in Figure 5.5.

In summary, our results indicate that well spacing is a critical parameter that has a pronounced dual-effect on enhanced production as well as CO<sub>2</sub> storage, if the distance between injectors and producers becomes far, the amount of stored CO<sub>2</sub> increases while the cumulative CH<sub>4</sub> production decreases. Therefore, an optimal injector-producer spacing is essential for achieving the highest possible CH<sub>4</sub> incremental production and minimizing CO<sub>2</sub> reproduction. Also, our study presents thus far strong evidence that even though continuous injecting of CO<sub>2</sub> has been proven to unlock CH<sub>4</sub> from shale organic surface, some of the desorbed CH<sub>4</sub> flows towards producers while the remaining amount is trapped as free gas within matrix and fractures pores.

#### 5.5.2.5. The Effect of Fracture Half-Length

In literature, fracture half-length has been identified as one of the most important parameters that has significant impact on primary shale production [19]. However, with enhancing shale production by CO<sub>2</sub> injection, fracture half-length is found in our analysis to have a minor

positive effect on EGR as Figure 5.5 illustrates. The cumulative CH<sub>4</sub> production tends to increase as fracture half-length increases. Despite no correlation between fracture half-length and CO<sub>2</sub> storage is observed in our study, increasing fractures length could result in CO<sub>2</sub> early breakthrough [54]. Therefore, fractures half-length remains an optimal parameter that must be considered in CO<sub>2</sub>-EGR design.

## 5.6 Conclusions and Implications

The goal of this work is to present a screening tool of CO<sub>2</sub>-EGR efficiency and to delineate a practical framework of its application on a field scale. By further analysis of the previous CO<sub>2</sub> injection studies in literature, a statistical analysis of the comprehensive correlations among shale properties, engineering parameters, and CO<sub>2</sub>-EGR efficiency is presented. Our results offer some important insights into the selection criteria on the physical properties of the shale reservoirs and engineering parameters to yield maximum efficiency of CO<sub>2</sub>-EGR process.

In reviewing the previous laboratory work and simulation studies, CO<sub>2</sub> has proven to have an obvious preferential adsorption on shale organic materials over CH<sub>4</sub>. This result has made shale reservoirs potential targets for enhancing gas production and CO<sub>2</sub> long-term geological sequestration, as one of the alternatives to CO<sub>2</sub>-EOR in sandstone oil reservoirs. The amount of adsorbed CO<sub>2</sub> and the amount of recovered CH<sub>4</sub> in shale reservoirs are mainly dominated by several parameters of shale properties and engineering design. Therefore, we employed Spearman correlation analysis to identify the strength of the relationship between the examined parameters and the efficiency of CO<sub>2</sub>-EGR. Our statistical analysis lays a foundation for efficient CO<sub>2</sub>-EGR design and implementation and presents an important contribution to the field of reaching the target of net-zero CO<sub>2</sub> emissions for energy transitions. The observations can be summarized as follows:

- 1) Among shale properties, natural fractures permeability followed by TOC and the capacity of shale to preferentially adsorb CO<sub>2</sub> over CH<sub>4</sub> are the most significant shale parameters that have a positive effect on the recovered CH<sub>4</sub>, while shale porosities are found to have a negative impact. On the other hand, shale porosities and matrix permeabilities are found to have the most positive impact on CO<sub>2</sub> storage.

- 2) Deep shale reservoirs are not favourable targets for both enhanced shale recovery and CO<sub>2</sub> sequestration because desorption of CH<sub>4</sub> becomes insignificant with the increase in reservoir depth.
- 3) CO<sub>2</sub> flooding might be the best applicable option for both enhanced CH<sub>4</sub> recovery and CO<sub>2</sub> sequestration in shale reservoirs, whereas huff and buff scenario does not seem to be a viable option because the injected CO<sub>2</sub> cannot efficiently migrate into shale matrix and consequently the injected CO<sub>2</sub> is then more likely to be re-produced very quickly.
- 4) Successful hydraulic-fractures network with effective values of permeability and conductivity is essential to achieve the maximum CO<sub>2</sub>-EGR efficiency in shale reservoirs.
- 5) Higher injection pressure is favourable to increase the total enhanced CH<sub>4</sub> production. However, to some extent, injecting CO<sub>2</sub> at high pressure increases mechanical mixing of CO<sub>2</sub>-CH<sub>4</sub> which may result in early CO<sub>2</sub> break-through.
- 6) Well spacing and fracture half-length are crucial optimal features in CO<sub>2</sub>-EGR process design. As the distance between injectors and producers becomes far, the storage capacity of CO<sub>2</sub> increases while the cumulative CH<sub>4</sub> production decreases.
- 7) Within the range of investigated parameters, the effect of reservoir temperature, thickness, and organic permeability are negligible.

The results obtained from our correlation analysis provide more demonstration necessary to manage and predict and predict the efficiency of CO<sub>2</sub>-EGR. In our future work, the strength and the direction of the relationship between the examined will be the criteria for features selection to adapt the best predictors for machine learning (ML) modelling. The findings should make an important contribution to ML-based modelling which will enable the industry to accurately predict the incremental enhanced CH<sub>4</sub> by CO<sub>2</sub> injection in shale gas reservoirs.

# Chapter 6. Application of Supervised Machine Learning to Predict the Enhanced Gas Recovery by CO<sub>2</sub> Injection in Shale Gas Reservoirs

## 6.1 Abstract

The technique of Enhanced Gas Recovery by CO<sub>2</sub> injection (CO<sub>2</sub>-EGR) into shale reservoirs has brought increasing attention in the recent decade. CO<sub>2</sub>-EGR is a complex geophysical process that is controlled by several parameters of shale properties and engineering design. Nevertheless, more challenges arise when simulating and predicting CO<sub>2</sub>/CH<sub>4</sub> displacement within the complex pore systems of shales. Therefore, the petroleum industry is in need of developing a cost-effective tool/approach to evaluate the potential of applying CO<sub>2</sub> injection to shale reservoirs. In recent years, machine learning applications have gained enormous interest due to their high-speed performance in handling complex data and efficiently solving practical problems. Thus, this work proposes a solution by developing a Supervised Machine Learning (ML) based model to preliminary evaluate CO<sub>2</sub>-EGR efficiency. Data used for this work was drawn across a wide range of simulation sensitivity studies and experimental investigations. In this work, Linear Regression and Artificial Neural Networks (ANNs) implementations were considered for predicting the incremental enhanced CH<sub>4</sub>. Based on the model performance in training and validation sets, our accuracy comparison showed that (ANNs) algorithms gave 15% higher accuracy in predicting the enhanced CH<sub>4</sub> compared to the linear regression model. To ensure the model is more generalizable, the size of hidden layers of ANNs was adjusted to improve the generalization ability of ANNs model. Among ANNs models presented, ANNs of 100 hidden layer size gave the best predictive performance with the coefficient of determination ( $R^2$ ) of 0.78 compared to the linear regression model with  $R^2$  of 0.68. Our developed ML-based model presents a practical, reliable, and cost-effective tool which can accurately predict the incremental enhanced CH<sub>4</sub> by CO<sub>2</sub> injection in shale gas reservoirs.

## 6.2 Introduction

Global energy demand for natural gas has been continuously growing in the last decade and is expected to continue growing due to the forecasted exponential demand of recovered economics after Covid-19 outbreak [1]. Against this trend, global energy has been exhausting fossil fuel natural gas supply and therefore the conventional gas resources are currently unable to meet the accelerated demand. The recent emerging technologies of hydraulic fracturing and horizontal drilling have shifted attention towards shale gas reservoirs and made their reserves commercially achievable [152]. According to [1], shale gas is the fastest growing component of natural gas resources and is projected to account for 22% of global natural gas production by the end of 2050. Moreover, the continuous growing technologies in shale gas development are anticipated to encourage shale gas exploitation in more counties such as Mexico and Algeria. Figure 6.1 depicts natural gas production in bcf/d from shale and other natural gas resources for the big six counties in 2015 and 2040.

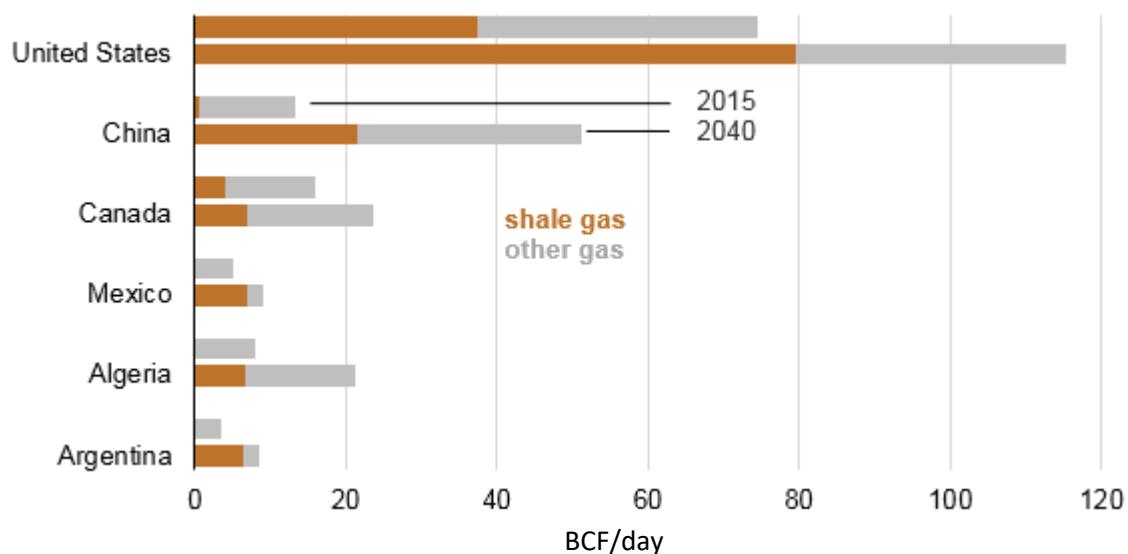


Figure 6. 1 Shale gas production from shale and other resources in selected counties in 2015 and 2040 [153]

Shale formations are considered as self-contained reservoirs that contain considerable amounts of natural gas [154]. These shales are extremely low in permeabilities, therefore, the primary shale gas production shows a very low recovery factor (up to 30%) caused by the dramatic decline during the early stage of development [123]. This highlights the essential need to develop methods to improve shale gas recovery. Thus, the techniques of enhanced shale gas

production such as gas injection and re-fracturing have brought increasing attention in the recent decade [3].

In gas shales, during thermal maturation, shales generate hydrocarbons and organic matter which can be referred to the total organic content (TOC) [60]. Typically, gas content in shale gas reservoirs is composed of free gas stored in nanopores, adsorbed gas on the surface of organic matter, and dissolved gas in formation liquids [114]. Since dissolved gas is negligible, adsorbed gas has been considered as the key component in shale recovery as it may account for up to 85% of total gas content [155]. Therefore, in organic-rich shales, releasing the adsorbed gas has been an increasingly important area in enhancing shale gas recovery. In literature, CO<sub>2</sub> injection into shale gas reservoirs has been perceived as an effective technique to unlock the adsorbed CH<sub>4</sub> and hence enhance shale recovery [10, 23, 34, 156]. Experimental investigations have shown that CO<sub>2</sub> has a greater adsorption affinity than CH<sub>4</sub> at a ratio of 5:1 when both co-exist within shale organic matter [23]. In other words, the preferential adsorption capacity has initiated a mechanism not only for enhanced shale recovery, but also for CO<sub>2</sub> geological sequestration. As a result, shale reservoirs have become potential targets for long-term geological CO<sub>2</sub> sequestration. Clearly, CO<sub>2</sub>-EGR technology offers a mechanism for CO<sub>2</sub> storage at a reasonable cost to mitigate the adverse effect of anthropogenic CO<sub>2</sub> emissions which are strongly related to the global concern of climate change [24, 25].

Enhanced shale recovery by CO<sub>2</sub> injection (CO<sub>2</sub>-EGR) is a displacement process which is mainly controlled by pressure and competitive adsorption between CH<sub>4</sub> and CO<sub>2</sub> [157]. Upon injecting, competitive adsorption phenomenon takes place where CO<sub>2</sub> molecules start to release adsorbed CH<sub>4</sub> from organic surface, and desorbed CH<sub>4</sub> transports by surface diffusion towards fractures and producers diffusion, the desorption process provides additional recovery accounting for up to nearly 59% [33] with a potential of permanent sequestration up to 100% of the injected CO<sub>2</sub> [10, 72].

Numerical reservoir simulation techniques are widely accepted as indispensable tools for realistic prediction and evaluation of reservoir performance [22]. Since enhanced shale recovery by CO<sub>2</sub> injection technology has not been commercialised yet, reservoir simulation studies have offered a preliminary stage of CO<sub>2</sub>-EGR efficiency evaluation on a field-scale. Thus, there has been a large volume of simulation studies investigating the applicability of CO<sub>2</sub>-EGR to several shale types and the effectiveness of different injection scenarios. In literature, few studies have been made to evaluate the performance of huff-and-puff injection



[7, 10, 28, 32, 55], while great attention was paid to flooding injection scenario such as studies done by [30, 33, 56, 57]. Moreover, some of previous studies have employed multi-porosity and permeability model to accurately simulate gas transport mechanism within shale organic, inorganic, and fractures [28, 32]. In recent simulation work, multi-components effect of gas transport and adsorption has been taken into consideration [44, 54]. Nevertheless, challenges arise when simulating CO<sub>2</sub>/CH<sub>4</sub> displacement within the complex pores system of shales and quantifying the efficiency of CO<sub>2</sub>-EGR. It is widely accepted that numerical modelling of shale reservoirs has presented unique challenges not only for the heterogeneity nature of shale petrophysical properties, texture, and TOC, but also for the complex storage and transport mechanisms of free and adsorbed gas [53, 58]. However, CO<sub>2</sub>-EGR is a more complex geophysical process that is controlled by several parameters of shale properties [20, 45] and engineering design [7, 54]. For these reasons, more difficulties and challenges arise in modelling CO<sub>2</sub>-EGR process in shale reservoirs. Considering both the cost of field injection test and many uncertainties in the numerical simulation process, the petroleum industry therefore requires a cost-effective tool/approach to evaluate the potential of applying CO<sub>2</sub> injection to shale reservoirs. Thus, this work proposes a solution by employing Machine Learning (ML) based regression models for preliminary evaluation of CO<sub>2</sub>-EGR efficiency. In this study, we used correlation analysis and different ML algorithms to provide a new approach for CO<sub>2</sub>-EGR efficiency prediction. To the best of our knowledge, this is the first study so far considering ML applications to predict and evaluate the process of CO<sub>2</sub> injection in shale gas reservoirs. The Motivation behind our model is to present a reliable and cost-effective tool which can manage and accurately predict the incremental enhanced CH<sub>4</sub> by CO<sub>2</sub> injection in shale gas reservoirs.

## 6.3 Methodology

### 6.3.1. Machine Learning Methods

Machine-Learning (ML) is the field that gives computers the ability to learn without being explicitly programmed [158]; in other words, a set of algorithms that use data or past experience to optimise a performance criterion [159]. Typically, the provided dataset is known as a ‘training set’ which is structured into pairs of input and outputs. In literature, the input variables are called “features” or “predictors”, and usually defined as ‘independent variables’, while the terms ‘dependent variables’ and ‘responses’ refer to the output variables [160]. Hence, the main purpose of learning is to infer a function to model the dependency between inputs and

outputs. The statistical learning framework distinguishes two types of outputs: quantitative outputs when the prediction is ‘regression’ task, and qualitative outputs when the prediction is ‘classification’ task [160].

Compared to human learning, ML handles large and complex data easier and learns much faster [161]. In recent years, ML applications have gained enormous interest due to their high-speed performance in handling complex data and efficiently solving practical problems. Since their revolution, ML applications have been broadly applied to various domains such as medical applications, biochemical, natural language processing, finance, and social media services [74]. Commonly, the processed datasets associated with the oil and gas industry are huge, complex in terms of correlation [75]. Thus, the applications of ML have also been extended to several areas in the oil and gas industry [76]. Recently, ML algorithms have been widely used to enhance and resolve several reservoir engineering aspects such as permeability prediction [77, 78]. Additionally, ML-based models have been created and employed for production estimation and optimization in several studies presented in literature [79, 80]. Furthermore, supervised ML models have demonstrated potential solution for several issues in the industry, for example the ML model presented by [81] for early fault prediction of centrifugal pump in the process engineering, and the ML based approach to monitor CO<sub>2</sub> geological sequestration and simulate CO<sub>2</sub> leakage [40].

Since the purpose of ML is to learn from data and employ different algorithms to solve the problem, there are many kinds of ML algorithms. The selection of algorithm used is basically depending on the kind of the problem, variables, and the suitable model to solve the problem [158]. The commonly used algorithms in ML are:

### **Supervised Learning**

In broad data scientist terms, supervised learning can be defined as learning a mapping between input variables (features) and output variable (target) based on provided data, and then applying this map for unseen data to predict the target [162]. Figure 6.2 illustrates the standard workflow of supervised ML.

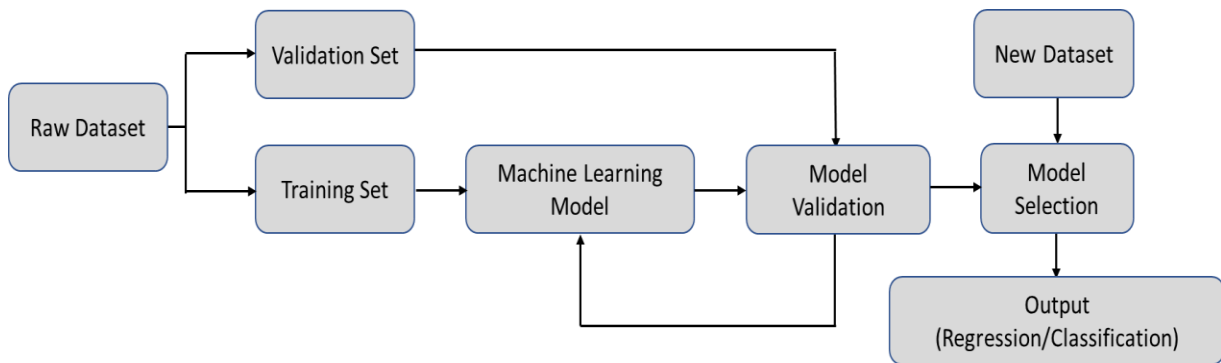


Figure 6. 2 The standard workflow of supervised ML

There are many supervised ML methods for both classification and regression problems. Brief descriptions of commonly employed supervised learning methods are given below:

a) Support Vector Machine SVMs

SVMs method was firstly introduced to solve classification and non-linear problems [163]. Currently, SVM algorithms are using kernel complex mathematical functions including linear, polynomial, splines and radial basis [74]. The basic role of SVM classification methods is formulating functions to find the optimal hyperplanes to separate the different classes in training data [162]. Such ways in solving problems can be expressed as ‘optimization’ where the larger margin between various classes in the training data gives the best hyperplanes (smaller SVM optimization) [164]. Since SVM can adopt generalization properties, overfitting is effectively avoided in the training phase [165]. However, the main disadvantage of SVM is the high computational burden and long training time associated with large datasets [77].

b) Artificial Neural Networks (ANNs)

Artificial Neural Networks (ANNs) is a widely used ML method which is based on simulating the human brain in processing data [166]. ANNs Are typically represented by layers, each layer consisting of many neurons or nodes [167]. Input layers are connected to the output layer through one or more hidden layers [164]. ML by ANNs is obtained by updating the weights between nodes after every success training iterations to ensure the performance of the network is improved [168]. ANNs method has applications in various industry segments in particular performing segmentation tasks in finance and business domain [74].

c) Decision Tree (DT)

Decision Tree mechanism works through sequential models which originally composed of smaller subsequent tests [169]. From the set of tests results, the model finally develops a decision tree which is constructed of two types of nodes; branch nodes and leaf nodes [170]. DT is one of the most powerful methodologies of classification and regression problems which has been widely used in chemical and medical fields [171]. It is widely accepted that DT technique is found to present best performance when performing classification tasks [172].

d) Random Forests (RF)

Random Forest (RF) method is an ensembled classification approach which utilize a group of classifiers and aggregate their results [173]. As the name suggests, RF is a combination of tree predictors. However, unlike normal DT, the best randomly chosen classifiers are used to split each node [174]. Therefore, it is a simply-applied technique since it has mainly two parameters; the number of variables at the random subset of classifiers at each node, and the number of trees [175].

### **Unsupervised Learning**

Unsupervised learning algorithms are basically used for clustering and dimension reduction [176]. Unlike supervised learning, the labels are not provided, hence the task of unsupervised algorithms is to identify the correct patterns in the data and present features [177]. The previously recognized patterns and features are then used to solve clustering problems in new raw data [176]. Therefore, due to the proliferation of unlabeled data, unsupervised ML methods have numerous applications as they are capable of automatically discovering and presenting patterns in the dataset [178]. However, compared to supervised learning, unsupervised learning techniques are less powerful since the answers in the training data enable an obvious criteria for model optimisation [162]. Figure 6.3 depicts a simple workflow for unsupervised learning to solve clustering problems.

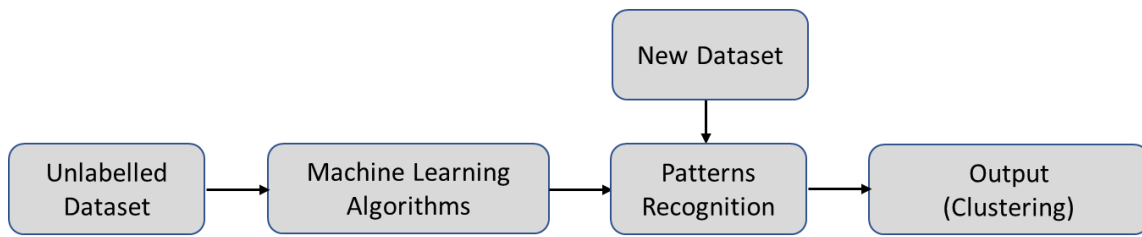


Figure 6. 3 A simple workflow for unsupervised learning to solve clustering problems.

### Reinforcement Learning

The concept of Reinforcement Learning is significantly different from supervised and unsupervised learning. Reinforcement learning is a goal-directed approach aimed at learning the best way to fulfil a task which is obtained through the repeated interactions with its environment [179]. As illustrated in Figure 6.4, reinforcement learning algorithms receive interaction (observations) from the environment as well as reward which measures the behavior response in accomplishing the task [180].

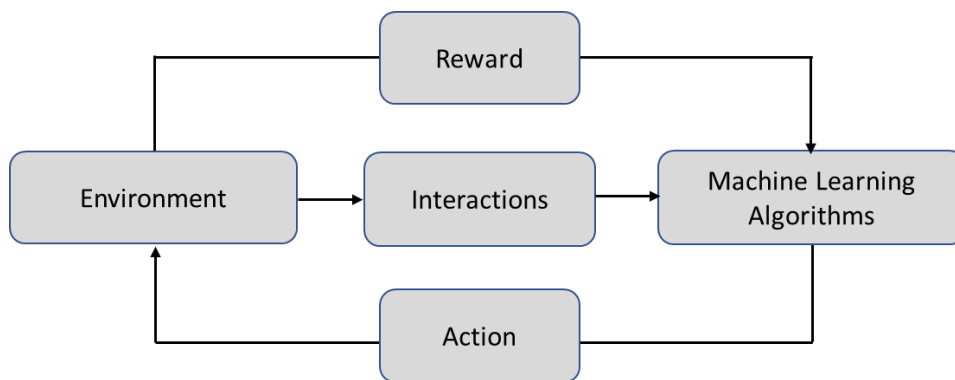


Figure 6. 4 Represents a basic workflow reinforcement learning

Since there are numerous studies in literature investigating CO<sub>2</sub>-EGR and providing an extensive range of resources which contain independent and dependent variables, a supervised ML approach was employed in this study to further investigate the potential of enhanced shale recovery in unseen data of shale reservoirs. In this work, the input dataset for our ML-based model consists of 63 injection scenarios data presented in literature spanning the years 2009 - 2019. Dataset for this work was constructed by shale properties and engineering parameters

(independent variable or features), and incremental recovery factor due to CO<sub>2</sub> injection (dependent variable or target). Among those independent variables, the variables that have the most effect on the target were selected as the best predictive for our model. Afterwards, the data was normalized, and several supervised ML models' performance were tested and compared. In this work, Linear Regression and Artificial Neural Networks (ANNs) implementations were considered for predicting the incremental enhanced CH<sub>4</sub>. As previously described, by training the model and selecting the best performance based on validation outcomes, our predictive model was able to perform prediction (regression) task for accurately predicting the efficiency of CO<sub>2</sub>-EGR.

### 6.3.2. Exploratory Data Analysis

The efficiency of applying CO<sub>2</sub> injection into shale reservoirs is mainly controlled by shale properties and engineering parameters. To increase the reliability of the model, data used for this work aimed to cover flooding and huff and puff injection scenarios that have been applied to various shale types under different engineering parameters such as well spacing, injection pressure, and injection rate. Table 6.1 illustrates the wide range of shale properties and engineering design parameters in our dataset. The boxplots in Figure 6.5 show the range of the main shale properties, incremental RF, and sequestered CO<sub>2</sub> in our dataset. Moreover, the dataset in this work is drawn across a wide range of resources available in literature with data being gathered from two main sources: simulation sensitivity studies and experimental investigations. In this work, total data for 63 CO<sub>2</sub> injection scenarios were collected which consist of: 9 experimental cases and 54 simulation cases. Table 6.2 shows the breakdown of the studies and shale types used in our dataset.

*Table 6. 1 The wide range of shale properties and engineering design parameters in our dataset*

<i>Parameter</i>	<i>Mean</i>	<i>Standard deviation</i>	<i>Minimum</i>	<i>Percentile 25%</i>	<i>Percentile 50%</i>	<i>Percentile 75%</i>	<i>Maximum</i>
Pressure, psi	6792.673	10886.48	780	1396.603	2140	4582.783	48643.61
Temperature, F°	120.8826	41.2604	85	90.82959	106	150	302
Reservoir thickness, ft	255.3311	411.2362	3.28084	100	200	300	2913
Depth, ft	4770.73	1766.632	1378	3720	4102.761	5670	9842.52
Matrix permeability, md	0.002199	0.005642	5E-20	5.7E-07	0.000236	0.00052	0.018

Organic permeability, md	0.002293	0.005607	0.000005	0.000228	0.00038	0.00052	0.018
Natural fracture Permeability, md	2.130345	14.42826	5E-10	0.00227	0.00321	0.00712	100
TOC, %	3.92	0.252982	3.2	4	4	4	4
Matrix porosity, %	4.677407	2.421882	1	2.9	4.1	6.875	10
Organic porosity, %	2.024052	3.097961	0.0352	0.0505	0.06	4.125	10
Natural fracture porosity, %	1.966663	3.717878	0.00004	0.029	0.0352	0.7075	14
CH <sub>4</sub> Langmuir volume, scf/ton	91.22467	120.5147	38.9	39.2	51	90.05	741.615
CO <sub>2</sub> Langmuir volume, scf/ton	287.4234	481.5702	10.2	74.375	183.6	232.98	2189.53
CH <sub>4</sub> Langmuir pressure, psi	1302.016	420.1904	145	1000	1458.705	1596	1765.537
CO <sub>2</sub> Langmuir pressure, psi	36257.35	248008.9	493	973.4727	1253.13	1254	1754870
Injection scenario	0.698113	0.46347	0	0	1	1	1
Sequestrated CO <sub>2</sub> , %	0.350409	0.378015	0	0	0.2	0.7	1
Incremental RF, %	0.086263	0.094658	-0.047	0.0105	0.07	0.1385	0.34

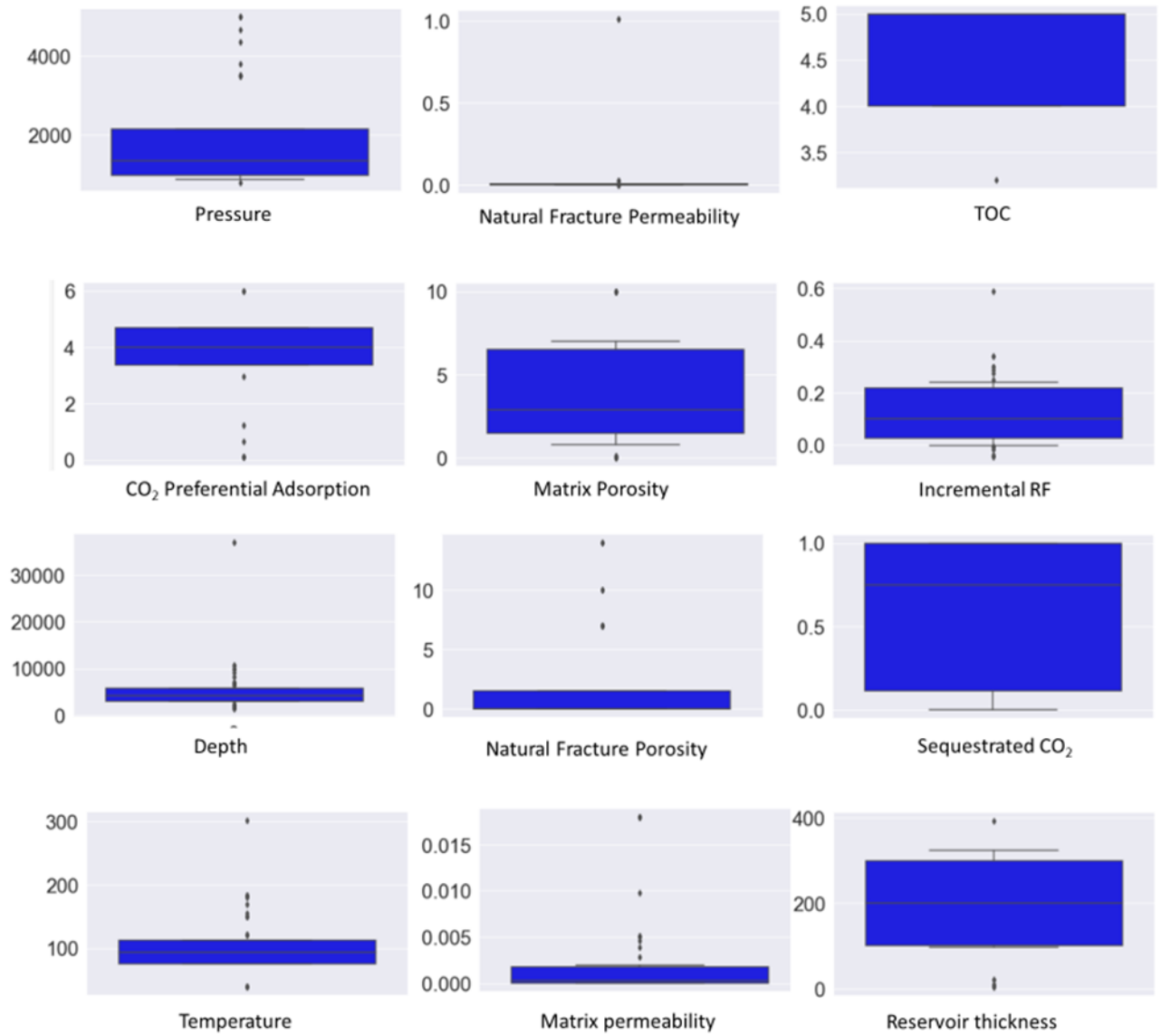


Figure 6. 5 Boxplots show the range of the main shale properties, incremental RF, and sequestered CO<sub>2</sub> in our dataset



Table 6. 2 The breakdown of shale types and number of cases for each study used in our dataset

Shale Type	Study	No of injection Cases	Methodologies/Assumptions	Author
Devonian	Numerical Simulation	6	<ul style="list-style-type: none"> <li>• Huff-n-puff</li> <li>• Dual porosity and permeability model</li> </ul>	[10]
Synthetic	Numerical Simulation	4	<ul style="list-style-type: none"> <li>• Flooding</li> <li>• Discrete fracture network model</li> <li>• Multi porosity and permeability model</li> </ul>	[34]
	Numerical Simulation	2	<ul style="list-style-type: none"> <li>• Flooding</li> <li>• Dual porosity and permeability model</li> <li>• Diffusion model</li> </ul>	[57]
	Numerical Simulation	3	<ul style="list-style-type: none"> <li>• Flooding</li> <li>• Non-Darcy effect</li> <li>• Instant sorption model</li> </ul>	[29]
Marcellus	Numerical Simulation	9	<ul style="list-style-type: none"> <li>• Flooding</li> <li>• Multi porosity and permeability model</li> </ul>	[33]
New Albany	Numerical Simulation	2	<ul style="list-style-type: none"> <li>• Flooding / huff-n-puff</li> <li>• Dual porosity and permeability model</li> <li>• Diffusion model</li> <li>• CO<sub>2</sub> dissolution</li> </ul>	[32]
Barnett	Numerical Simulation	3	<ul style="list-style-type: none"> <li>• Flooding</li> <li>• Dual porosity and permeability model</li> </ul>	[31]
	Numerical Simulation	4	<ul style="list-style-type: none"> <li>• Flooding / huff-n-puff</li> </ul>	[7]
	Numerical Simulation	14	<ul style="list-style-type: none"> <li>• Flooding / huff-n-puff</li> <li>• Multi porosity and permeability model</li> <li>• CO<sub>2</sub> dissolution</li> </ul>	[30]

			• Stress-dependent model	
Yanchang	Numerical Simulation	4	• Flooding • Diffusion model	[72]
	Numerical Simulation	2	• Flooding • Geochemical interaction effect.	[27]
Silurian Longmaxi	Numerical Simulation	1	• Huff-n-puff • Multi porosity and dual permeability model • Diffusion model	[28]
	Experimental Study	9	• Flooding • New NMR experimental approach	[26]

The occurrence of missing values in real-world data arise frequently when recording or processing data [138]. According to [181], the main categories of missing data are:

1. Missing Completely at Random (MCAR) when the missing data is unrelated to any observation in dataset.
2. Missing at Random (MAR) when the missing data are related to the dataset, but the actual missing values are random.
3. Missing at Random (MNAR) when the missing data are related to the dataset, but the actual missing values are not random.

Typically, removing rows or columns that have null values, and imputing methods are the common techniques for handling missing data problems. Typically, there is no preferred method of handling the missing data, but the applicability of each technique becomes more fitting under a specific condition [140]. The common methodology of handling the missing values with examples from our dataset are shown in Table 6.3 below:

Table 6. 3 The methodology used for handling the missing values in our dataset

<i>Type of missing data</i>	<i>Solution</i>	<i>Example</i>
Missing Completely at random (MCR)	Deleting	Not present in our dataset
Missing at Random (MAR)	Deleting	Missing reservoir thickness
Missing Not at Random (MNAR) that can be predicted using shale data	Imputation	Missing TOC- Pressure

Imputation approach taken in handling (MNAR) in our dataset is the median method using the typical data for shale type. For example, missing petrophysical values for Barnett shale such as TOC were imputed from the typical data for the Barnett shale listed in our dataset. However, if a value is missing for a synthetic shale type, the variable was imputed using the data of all shale types.

### 6.3.3. Feature Selection

Correlation analysis is one of the most widely used approaches to denote the relationship between two or more quantitative variables. The result of correlation analysis is known as “Correlation Coefficients” which identify the strength and the direction of the linear relationship between variables [182]. The values of correlation coefficients range from -1 to +1, where -1 indicates a strong negative correlation, and +1 indicates a strong positive correlation. In ML based modelling, the end results of correlation analysis are important not only for understanding the dependency between input and output variable, but also for features (predictors) selection. Features selection is commonly used in data pre-processing to reduce data size and adapt the best predictors for modeling. Reducing the features set is significant because a high number of features typically causes model overfitting which in return reduces model validation accuracy [183].

In this study, Spearman correlation coefficient method [148] was used to identify the relationship between the features and target in our dataset. The features in our data set can be categorized into two sets: shales properties and engineering parameters. The approach taken in this study aimed to use the properties of shale reservoirs to predict the incremental CH<sub>4</sub> recovery by CO<sub>2</sub> injection, rather than using engineering parameters of induced fractures and

injection. Therefore, shale gas properties and injection scenario (flooding or huff-puff) were only considered as the features set in our prediction. As shown in Figure 6.6, Spearman coefficient summarizes the direction (positive or negative) and the strength (0- +100% or -100%) of correlation between shale properties and enhanced methane recovery across our dataset. The results obtained from correlation analysis indicate that natural fractures permeability followed by the injection scenario, total organic content (TOC) and the capacity of shale to preferentially adsorb CO<sub>2</sub> over CH<sub>4</sub> are the most significant shale parameters that have a positive effect on CO<sub>2</sub>-EGR efficiency, while a significant negative correlation was found between shale porosities and enhanced CH<sub>4</sub> production. Reservoir depth and pressure were found to have a negative impact. In addition, our results also showed a minor impact of reservoir depth, pressure, and temperature on the enhanced CH<sub>4</sub> production. It can also be concluded from our results that the effect of matrix and organic permeabilities, and reservoir thickness is negligible.

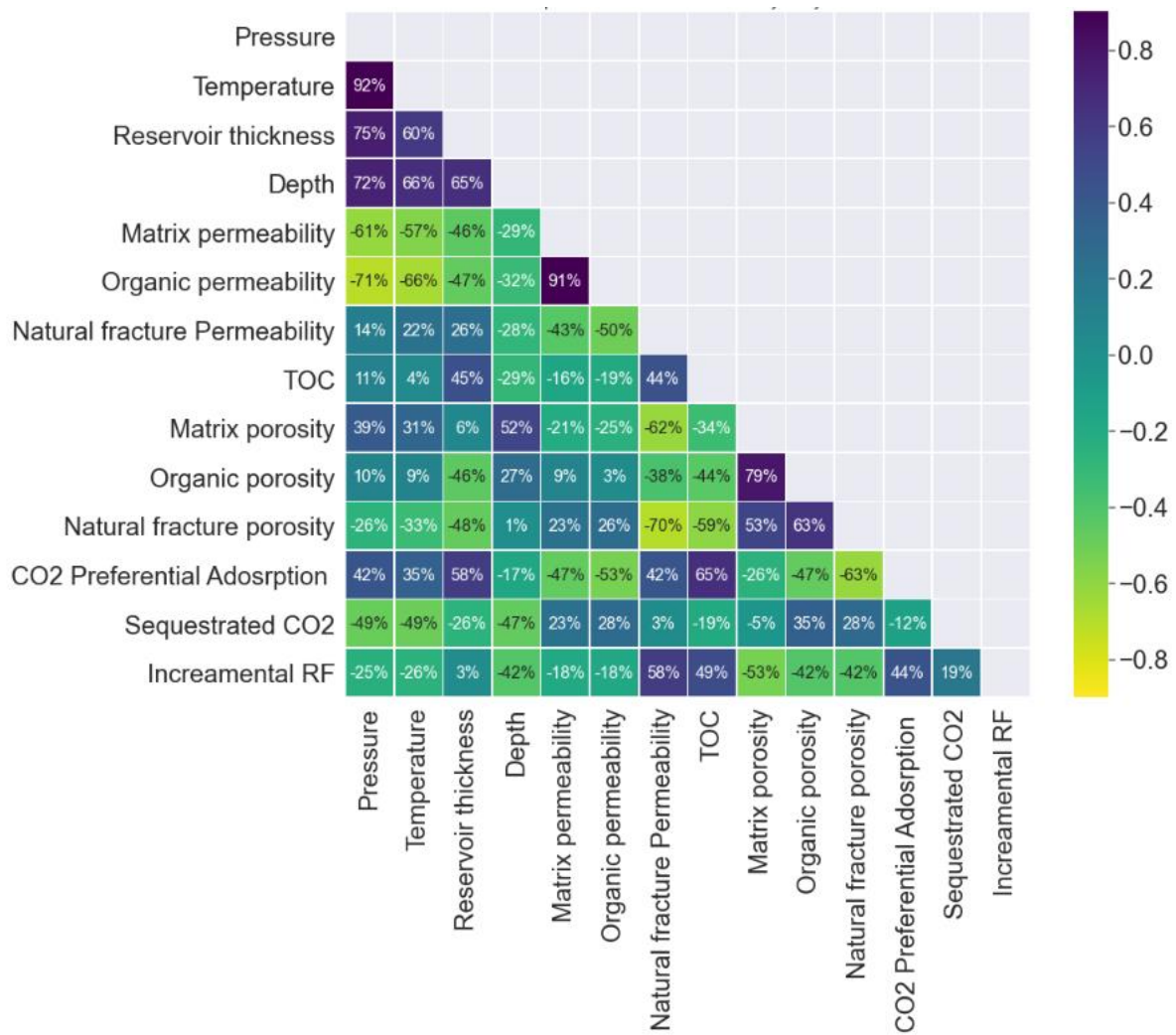


Figure 6.6 Spearman correlation between shale properties and incremental CH<sub>4</sub>

Hence, we have based our criteria for features selection upon the end results of correlation coefficient analysis shown in Figure 6.6 and assuming the chosen threshold for correlation coefficient is  $\pm 40\%$ , the selected predictors for our model were to be natural fracture permeability, injection scenario, TOC, matrix porosity, and CO<sub>2</sub> preferential adsorption. Figure 6.7 shows the correlation analysis between the selected features only and the incremental CH<sub>4</sub> recovery.

To further explain the impact of the selected predictors on incremental CH<sub>4</sub> recovery, it is worth to mention that natural fracture permeability is the most influential parameter since higher fracture permeability causes larger pressure drop in natural fractures which facilitates free and desorbed gas transport from shale matrix to fractures network. Obviously, TOC and CO<sub>2</sub> preferential adsorption have also a significant impact because the key mechanism of enhanced shale recovery is releasing CH<sub>4</sub> from the surface of organic matter, therefore, the greater TOC

increases competitive adsorption of CO<sub>2</sub>-CH<sub>4</sub> and hence increases the contribution of desorbed CH<sub>4</sub> to the total shale production. On the other hand, matrix porosity shows a strong negative impact on CH<sub>4</sub> production. The main reason for that is molecular diffusion of CO<sub>2</sub> decreases with increasing shale porosity which in return mitigates desorbed gas transport towards shale matrix and fractures. In terms of the injection scenario, CO<sub>2</sub> flooding might be the best applicable option for CO<sub>2</sub> injection in shale reservoirs, whereas the huff and buff scenario does not seem to be a viable option. Due to the typical cycle of soaking-production, the injected CO<sub>2</sub> cannot efficiently migrate to the extension of shale reservoirs which significantly reduces the effect of CO<sub>2</sub>-CH<sub>4</sub>.

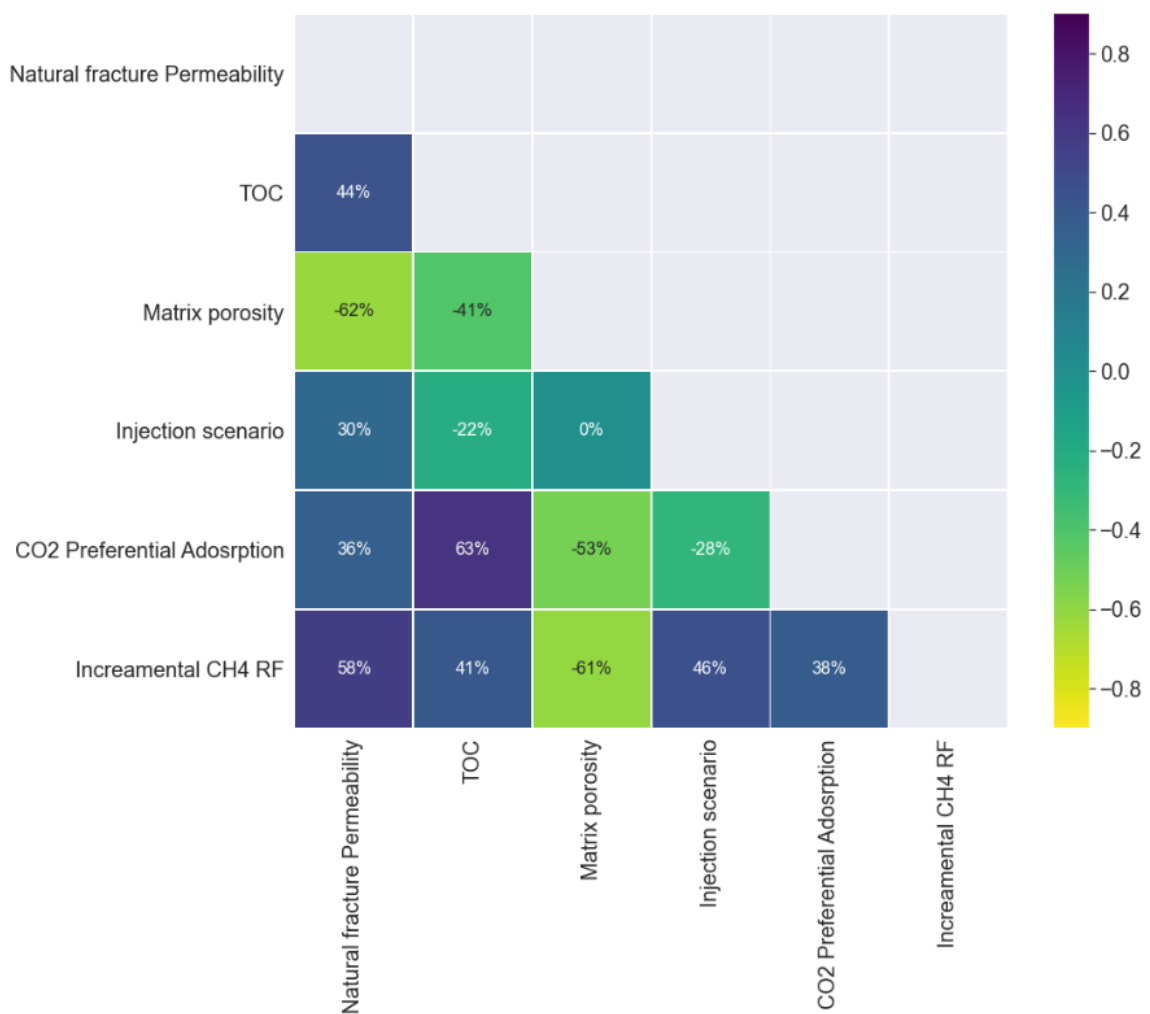


Figure 6. 7 Spearman correlation between the selected features and incremental CH<sub>4</sub>

### 6.3.3. Model Training and Validation

To estimate the predictive performance of our model, Scikit-learn train-test-split was used to randomly split our dataset into train and validation subsets. Training subset is a sample of data from which ML algorithms learn and discover the pattern between predictors and target(s). On the other hand, a validation subset is a sample of data not used in training where ML algorithms apply the identified pattern, and the model is then tuned to the best predictive performance. In our dataset, the ratio of training/validation was selected to be 80/20 which is very common in small datasets.

After the models are proposed, an evaluation criterion must be adopted for comparison. Therefore, for both training and validation, R-squared ( $R^2$ ) was employed to assess the degree of model-accuracy. R-squared is a statistical measure of fit which indicates how much variation in the response is explained in a regression model [184]. Practically, R-squared ( $R^2$ ) values range from  $-\infty$  which indicates no relationship between the predicted variables and the observed data, to 1 which indicates all the variance are explained in the model. R-squared can be mathematically expressed as:

$$R^2 = 1 - \frac{\text{sum squared regression}}{\text{total sum of squares}} \quad \text{Equation (6.1)}$$

## 6.4 Model Selection

In this work, Linear Regression and Artificial Neural Networks (ANNs) implementations are considered for predicting the incremental enhanced  $\text{CH}_4$  by  $\text{CO}_2$  injection. We used the available libraries of Python which is an open-source programming language to support the process of modelling and calculations. As mentioned earlier, the ratio of training/validation was kept the same for both models. In order to produce the same results across the runs, the Random State parameter was fixed and specified to 42 which corresponds to the seed of randomness. Technically, a fixed value of Random State is essential to allow a model to use the same training and validation sets for each run. Afterwards, each set was uniformly normalized. In the training and validation figures below, the observed data were represented by the dotted line and the predicted values were represented by the solid line. Finally, the

performance of these two models was evaluated by comparing R-squared ( $R^2$ ) values for the validation runs.

#### 6.4.1. Linear Regression Model

First, the effect of applying a Linear Regression model for prediction was examined. Figure 6.8 shows the prediction obtained for the training set while Figure 6.9 shows the validation results by using linear regression model. The value of R-squared ( $R^2$ ) obtained for the linear regression model was 0.68 which indicates that the variance explained by the model was about 68%.

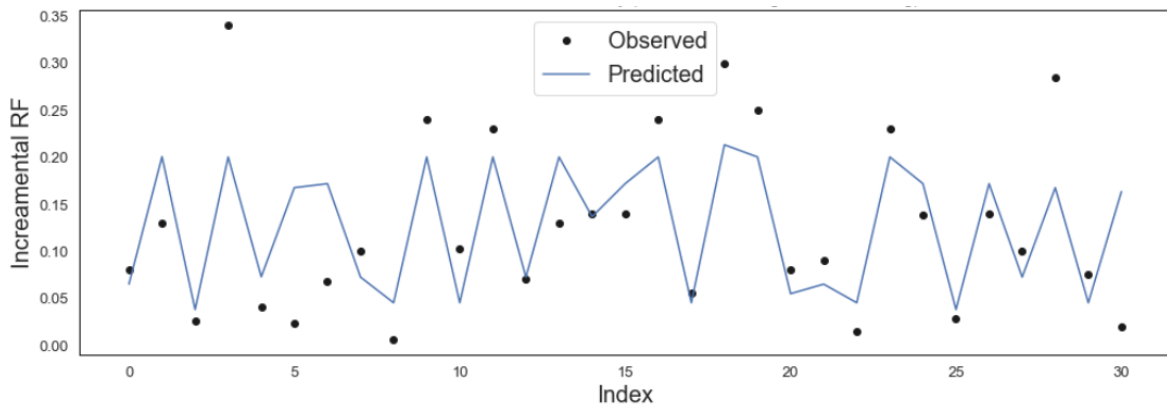


Figure 6. 8 Prediction of enhanced gas recovery- training set for linear regression model

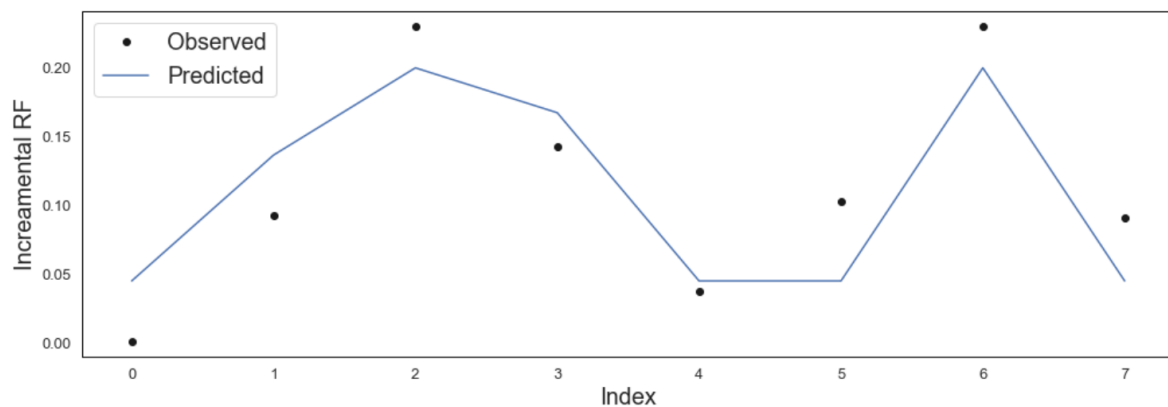
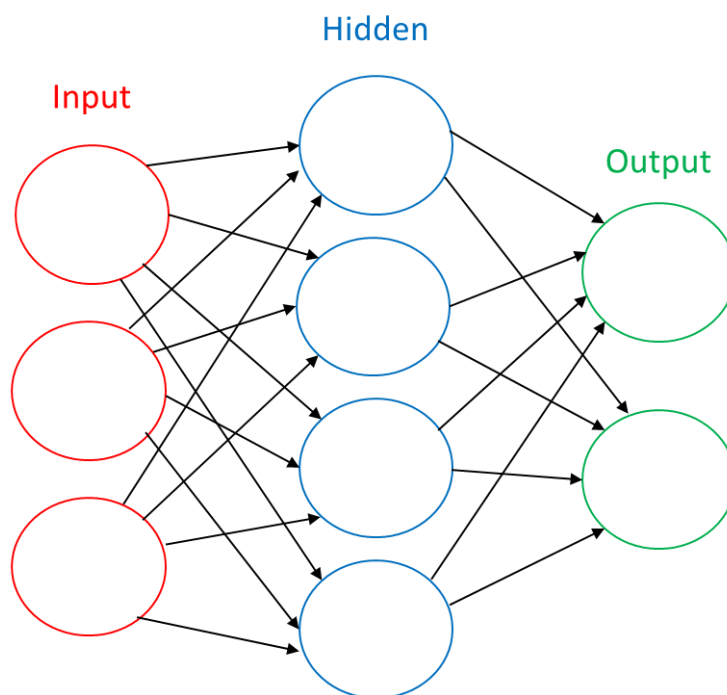


Figure 6. 9 Prediction of enhanced gas recovery- validation set for linear regression model



#### 6.4.2. Artificial Neural Networks (ANNs)

Artificial Neural Networks (ANNs) method was considered and compared to the linear regression model. In the theory as mentioned earlier, ANNs are typically represented by layers, each layer consists of many neurons or nodes where the input layers are connected to the output layer through more hidden layers as shown in Figure 6.10.



*Figure 6. 10 ANNs connected layers and outputs [185]*

Similarly, Figure 6.11 shows the prediction obtained for the training set while Figure 12 shows the validation results by using ANNs model with a hidden layer's size of 100. The value of R-squared ( $R^2$ ) obtained from ANNs model was 0.78 which indicates that the performance of prediction has been significantly improved compared to Linear regression model. However, the generalization ability of ANNs can be improved by adjusting the weights of layers connection. Therefore, we attempted to obtain a better performance by updating the hidden layer size. The first run, the hidden layer size was increased to the range of (110-130), while the second run, the hidden layer size was decreased to the range of (3-20). The summary of the size of hidden layers used and the corresponding R-squared ( $R^2$ ) are summarized as shown in Table 6.4.

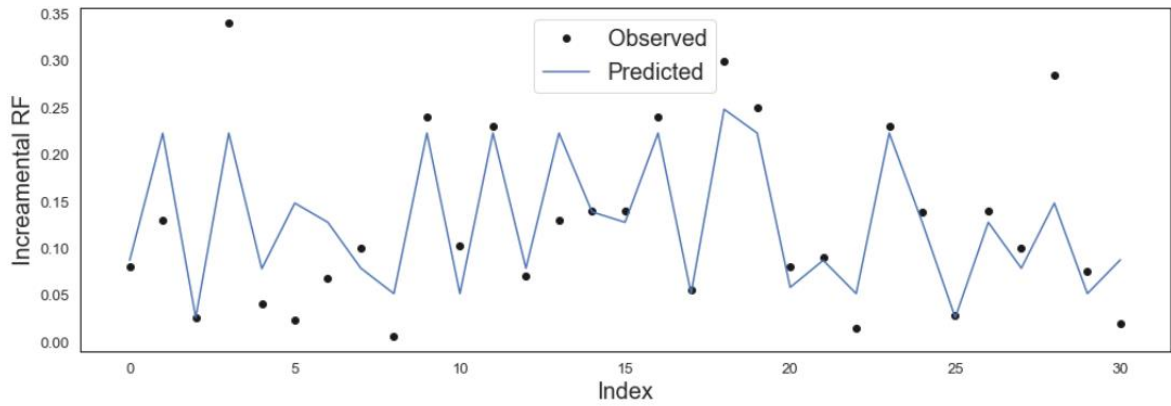


Figure 6.11 Prediction of Enhanced Gas Recovery- Training Set for Neural Network Regression Model

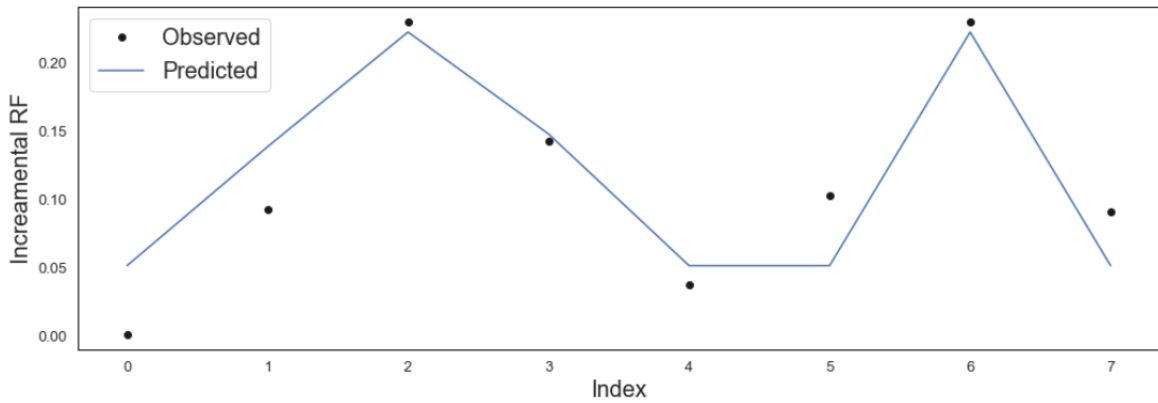


Figure 6.12 Prediction of Enhanced Gas Recovery- Validation set for Neural Network Regression Model

Table 6.4 Overall performance comparison of linear regression and ANNs models

Model	R-squared ( $R^2$ )	Configurations
Linear Regression	0.68	NA
Artificial Neural Networks (ANNs)	0.78	Hidden layer sizes = 100

Artificial Neural Networks (ANNs)	0.69	Hidden layer sizes = 3-20
Artificial Neural Networks (ANNs)	0.67	Hidden layer sizes = 110-130

It can be seen in Table 6.4 that using ANNs resulted in increasing R-squared ( $R^2$ ) value compared to the linear regression model which reflects about 15% improvement in the prediction accuracy. As shown in the same table, adjusting the layer size has significantly reduced the model accuracy. Among ANNs models presented, ANNs of 100 hidden layer size had the best predictive performance with R-squared ( $R^2$ ) of 78%. Nevertheless, the highest possible accuracy of our model seems to be not ideal. The main explanation for that is, in simplistic terms, the high heterogeneity of shale gas coupled with the complexity of factors driving  $CH_4$ - $CO_2$  displacement, can lead to wider uncertainty and difficulties in predicting the enhanced  $CH_4$ . Additionally, model accuracy is not only dependent on the features of prediction, but also on the volume of the training and validation sets. Therefore, it is generally believed that a larger dataset will result in a better predictive performance.

The best model which performed more accurately and gave better generalization ability is ANNs model with the hyper-parameters shown in Table 6.5.

*Table 6. 5 Hyper-parameters for the selected ANNs regression model*

<i>Parameter</i>	<i>Value</i>
Alpha_1	0.0001
Alpha_2	0.999
Hidden layer sizes	100
Momentum	0.9
Initial learning rate	0.001
Random state	42
Validation fraction	0.1

Epsilon	1e-08
Power t	0.5
Tol	0.0001

## 6.5 Conclusion

ML applications have been broadly applied to various domains due to their high-speed performance in handling complex data and efficiently solving practical problems. CO<sub>2</sub>-EGR is a complex geophysical process that is controlled by several parameters of shale properties and engineering design of injection which raises difficulties and challenges in modelling and predicting CO<sub>2</sub>-EGR in shale reservoirs. Thus, this work presents a ML based regression model to preliminary evaluate CO<sub>2</sub>-EGR efficiency. Our features selection concludes that our ML model based on natural fractures permeability, TOC, matrix porosity, and the CO<sub>2</sub> preferential adsorption ratio can effectively predict the enhanced CH<sub>4</sub> recovery in shale reservoirs due to CO<sub>2</sub> injection.

In this work, Linear Regression and Artificial Neural Networks (ANNs) implementations were considered for predicting the incremental enhanced CH<sub>4</sub>. For both models, R-squared (R<sup>2</sup>) was employed to assess the degree of model-accuracy. Based on the model performance in training and validation, our accuracy comparison showed that (ANNs) algorithms gave 15% higher accuracy in predicting the enhanced CH<sub>4</sub> compared to the linear regression model. To ensure the model is more generalizable, the size of hidden layers of ANNs was adjusted to improve the generalization ability of ANNs model. Among ANNs models presented, ANNs of 100 hidden layer size gave the best predictive performance with the coefficient of determination (R<sup>2</sup>) of 0.78 compared to the linear regression model with R<sup>2</sup> of 0.68.

Our results demonstrated that the high heterogeneity of shale gas coupled with the complexity of factors driving the process CH<sub>4</sub>-CO<sub>2</sub> displacement, can lead to wider uncertainty and difficulties in predicting the enhanced CH<sub>4</sub>. Additionally, model accuracy is not only dependent on the features of prediction, but also on the volume of the training and validation sets. Therefore, it is generally believed that a larger data set will result in better predictive performance. Our developed ML-based model presents a practical and reliable and cost-

effective tool which can accurately predict the incremental enhanced CH<sub>4</sub> by CO<sub>2</sub> injection in shale gas reservoirs.

# Chapter 7. Conclusions and Recommendations

## 7.1 Conclusions

The technique of Enhanced Gas Recovery by CO<sub>2</sub> injection (CO<sub>2</sub>-EGR) has drawn great attention to shale reservoirs as potential targets for enhancing gas production and CO<sub>2</sub> long-term geological sequestration. The adsorbed gas is an important component in shale primary production as it contributes significantly to maintaining the long-term production plateau and plays the key role in CO<sub>2</sub>-EGR which is mainly driven by the desorption process. However, the factors governing the desorption behavior have not been elucidated, presenting a substantial impediment in managing and predicting the performance of shale gas reservoirs. On the other hand, upon injection, a complex geophysical process takes place which is controlled by several parameters of shale properties and engineering design. Due to this complexity and the heterogeneity of shale reservoirs, there are still uncertainties in determining the main factors that control CO<sub>2</sub>-EGR process. Moreover, more challenges arise when simulating and predicting CO<sub>2</sub>/CH<sub>4</sub> displacement within the complex pore systems of shales. Therefore, this thesis aims to clarify several aspects of adsorbed gas contribution to total shale primary production and presents tools to evaluate, manage and predict the efficiency of enhanced gas recovery and CO<sub>2</sub> sequestrations in shale reservoirs. In addition, this thesis provides a comprehensive investigation on the correlation between shale properties as well as engineering parameters and the efficiency of CO<sub>2</sub>-EGR which helps the industry to conceptual understanding when designing and implementing CO<sub>2</sub>-EGR in shale reservoirs. Furthermore, this thesis develops for the first time a ML model which can predict the incremental enhanced CH<sub>4</sub> by CO<sub>2</sub> injection in shale gas reservoirs.

The methodological approach taken in this study is a combination of numerical reservoir simulation, statistical analysis, and ML modelling. For numerical simulation study, a predictive model of Barnett shale reservoir was generated using data in the public domain. The key input parameters were defined in the model within the range which consists with that presented in literature for the realistic shale data. The model then employed multi-porosity and multi permeability model incorporating Langmuir isotherms and instant sorption option. Furthermore, the model was calibrated using core data analysis from literature for Barnett shales. Then, sensitivity analysis was performed on a range of reservoir depth and TOC to

quantify and investigate the contribution of adsorbed gas to total gas production with respect to reservoir depth and TOC. A statistical analysis was performed to identify the strength of the relationship between shale properties and engineering design parameters and the efficiency of CO<sub>2</sub>-EGR. For most of the generalizable results, we gathered data across the available studies in literature on a wide subset of numerical modelling studies and experimental investigations. The approach taken in this analysis study is Spearman correlation coefficient to identify the direction and the strength of correlation in the dataset. Finally, the obtained results from the statistical analysis were employed to adapt the best predictors (features) to develop a ML model. The developed model is a supervised ML based regression model which can predict the incremental enhanced CH<sub>4</sub> by CO<sub>2</sub> injection in shale gas reservoirs.

The main findings to emerge from this thesis are summarized below:

## 7.2 Effect of Reservoir Pressure and Total Organic Content on Adsorbed Gas Production in Shale Reservoirs: A Numerical Modelling Study

From a shale gas primary production perspective, our results show that reservoir depth has a significant effect on the contribution of adsorbed gas to shale gas production. The sensitivity outcomes prove that regardless of TOC, adsorbed gas production decreases with increasing reservoir depth. Furthermore, the results suggest that adsorbed gas may contribute up to 26% of the total gas production in shallow (below 4,000 feet) shale plays.

On the other hand, as expected, TOC is found to have a substantial positive impact on the contribution of adsorbed gas to total shale production. For example, increasing TOC from 4 to 8% at a given reservoir depth results in increasing the cumulative adsorbed gas production by about 70%. However, the impact of TOC on the contribution of adsorbed gas production becomes minor with increasing reservoir depth.

This study highlights the importance of Langmuir isothermal behavior in shallow shale plays where the adsorbed gas plays a key role in total shale production. These findings also have important implications for characterisation, development, and prediction of shale gas reservoirs with respect to reservoir depth and TOC. Since our simulation results revealed that shallow shale reservoirs are found to produce more adsorbed gas compared to deep shales, injecting CO<sub>2</sub> into shallow shale reservoirs (rich in TOC) would give an improved outcome to unlock the adsorbed gas and sequester CO<sub>2</sub>. This significant finding has been studied and tested and proved using the statistical analysis approach in Chapter. 5. Moreover, the results present a

significant contribution to the energy transition to the net-zero target of CO<sub>2</sub> emissions by demonstrating important insights into the application of enhanced shale gas recovery and CO<sub>2</sub> sequestration.

### 7.3 The Controlling Factors on Enhanced Gas Recovery by CO<sub>2</sub> Injection in Shale Gas Reservoirs

Since the efficiency of CO<sub>2</sub>-EGR is mainly dominated by several parameters of shale properties and engineering design, this study applies a statistical analysis approach to quantify the strength and the direction of each factor on both enhanced CH<sub>4</sub> and sequestered CO<sub>2</sub>. In this study, shale reservoirs are found to be potential targets for enhancing gas production and CO<sub>2</sub> long-term geological sequestration. Compared to primary production (no injection scenario), CO<sub>2</sub> injection can lead up to 59% additional recovery from original gas in place (OGIP) whereas up to 100% of the injected CO<sub>2</sub> could be sequestered.

In terms of shale properties, our results show that natural fractures permeability is the most significant shale parameter that has a positive effect on CO<sub>2</sub>-EGR efficiency. Additionally, TOC followed by the capacity of shale to preferentially adsorb CO<sub>2</sub> over CH<sub>4</sub> have a pronounced positive impact on CO<sub>2</sub>-CH<sub>4</sub> displacement, while shale porosities are found to have a negative impact. As previously hypothesized, our statistical analysis proves that deep shale reservoirs are not favorable targets for both enhanced shale recovery and CO<sub>2</sub> sequestration because desorption of CH<sub>4</sub> becomes insignificant with the increase in reservoir depth.

In terms of engineering parameters, this study reveals that CO<sub>2</sub> flooding might be the best applicable option for CO<sub>2</sub> injection in shale reservoirs, whereas huff and buff scenario does not seem to be a viable option because the injected CO<sub>2</sub> cannot efficiently migrate into shale matrix and consequently the injected CO<sub>2</sub> is then more likely to be re-produced very quickly. On the other hand, the hydraulic-fractures network plays an important role as a successful hydraulic-fractures network with effective values of permeability and conductivity is essential for CO<sub>2</sub>-EGR efficiency in shale reservoirs. Moreover, the results indicate that higher injection pressure is favorable to increase the total enhanced CH<sub>4</sub> production. However, to some extent, injecting CO<sub>2</sub> at high pressure increases mechanical mixing of CO<sub>2</sub>-CH<sub>4</sub> which may result in early CO<sub>2</sub> break-through. Well spacing and fracture half-length are also crucial optimal features in CO<sub>2</sub>-EGR process design. As the distance between injectors and producers becomes far, and the



length of fracture increases, the storage capacity of CO<sub>2</sub> increases while the cumulative CH<sub>4</sub> production decreases.

Our results offer some important insights into the selection criteria on the physical properties of the shale reservoirs and engineering parameters to yield maximum efficiency of CO<sub>2</sub>-EGR process. These findings help to lay a foundation for efficient CO<sub>2</sub>-EGR design and implementation. Furthermore, the results obtained from our correlation analysis provide more demonstration necessary to manage and predict the efficiency of CO<sub>2</sub>-EGR as the correlation between the examined will be the criteria for features selection to adapt the best predictors for ML modelling.

#### 7.4 Application of Supervised Machine Learning to Predict the Enhanced Gas Recovery by CO<sub>2</sub> Injection in Shale Gas Reservoirs

Given that CO<sub>2</sub>-EGR is a complex geophysical process that presents difficulties and challenges in modelling and predicting, this work applies ML based regression model to preliminary predict and evaluate CO<sub>2</sub>-EGR efficiency. One of the key findings on this work is that the enhanced CH<sub>4</sub> recovery in shale reservoirs due to CO<sub>2</sub> injection can be effectively predicted using the features of natural fractures permeability, TOC, matrix porosity, and the CO<sub>2</sub> preferential adsorption ratio.

In this work, Linear Regression and Artificial Neural Networks (ANNs) implementations were considered for predicting the incremental enhanced CH<sub>4</sub>. As a result of comparison, Artificial Neural Networks (ANNs) algorithms gave a higher accuracy in predicting the enhanced methane. Based on the model performance in training and validation, our accuracy comparison showed that (ANNs) algorithms gave 15% higher accuracy in predicting the enhanced CH<sub>4</sub> compared to the linear regression model. Furthermore, to ensure the model is more generalizable, the size of hidden layers of ANNs was adjusted to improve the generalization ability of ANNs model. Among ANNs models presented, ANNs of 100 hidden layer size gave the best predictive performance with the coefficient of determination ( $R^2$ ) of 0.78 compared to the linear regression model with  $R^2$  of 0.68.

This work extends for the first time the application of to EGR-CO<sub>2</sub> and provides some conceptual contribution for field-scale applications. In addition, our developed model presents

a practical, reliable and cost-effective tool which predicts the incremental enhanced CH<sub>4</sub> by CO<sub>2</sub> injection in shale gas reservoirs.

## 7.5 Recommendations for Future Work

While our work clarifies several aspects of the desorption phenomenon in both shale primary production and CO<sub>2</sub>-CH<sub>4</sub> displacement process, further research should be done for better understanding and more accurate prediction of CO<sub>2</sub>-EGR efficiency. Obviously, field-scale tests, new approaches of modelling, and further experimental investigation will provide deeper insights into CO<sub>2</sub>-EGR to yield maximum efficiency of both enhanced production and CO<sub>2</sub> sequestration.

It is generally believed that the lack of field-scale data for CO<sub>2</sub> injection into shale gas reservoirs has been one of the current major sources of uncertainty about the process. Therefore, having such actual data will help not only for numerical modelling history matching validation purposes, but also for evaluation of CO<sub>2</sub> injection at field scale. In future investigations, it might be also possible to couple the history matched numerical models with new approaches-based experimental investigations for further sensitivity and statistical analysis.

As previously discussed, the high heterogeneity of shale gas coupled with the complexity of factors driving CH<sub>4</sub>-CO<sub>2</sub> displacement, can lead to wider uncertainties and difficulties in predicting the enhanced CH<sub>4</sub>. In ML based modelling, model accuracy is not only dependent on the strength of correlation between features and target(s), but also on the volume of the training and validation sets. Therefore, future work on ESGR prediction needs to take into account a larger dataset which will result in a better predictive performance. Additionally, future ML modelling which takes the volume dataset into account will also need to consider the balance in both training and validation sets.

## References

1. IEA, World Energy Outlook 2021. 2021.
2. Yuan, J., D. Luo, and L. Feng, A review of the technical and economic evaluation techniques for shale gas development. *Applied Energy*, 2015. **148**: p. 49-65.
3. Huang, Evaluation of CO<sub>2</sub> injection into shale gas reservoirs considering dispersed distribution of kerogen. *Applied Energy*, 2020. **260**: p. 114285.
4. Gao, S., et al., Experiences and lessons learned from China's shale gas development: 2005–2019. *Journal of Natural Gas Science and Engineering*, 2021. **85**: p. 103648.
5. IEA, World Energy Outlook 2019. 2019.
6. Wang, S., Shale gas exploitation: Status, problems and prospect. *Natural Gas Industry B*, 2018. **5**(1): p. 60-74.
7. Yu, W., E.W. Al-Shalabi, and K. Sepehrnoori, A Sensitivity Study of Potential CO<sub>2</sub> Injection for Enhanced Gas Recovery in Barnett Shale Reservoirs, in SPE Unconventional Resources Conference. 2014, Society of Petroleum Engineers: The Woodlands, Texas, USA. p. 16.
8. Louk, K., et al., Monitoring CO<sub>2</sub> storage and enhanced gas recovery in unconventional shale reservoirs: Results from the Morgan County, Tennessee injection test. *Journal of Natural Gas Science and Engineering*, 2017. **45**: p. 11-25.
9. Kang, S.M., et al., CO<sub>2</sub> Storage Capacity of Organic-Rich Shales, in SPE Annual Technical Conference and Exhibition. 2010, Society of Petroleum Engineers: Florence, Italy. p. 17.
10. Schepers, K.C., et al., Reservoir Modeling and Simulation of the Devonian Gas Shale of Eastern Kentucky for Enhanced Gas Recovery and CO<sub>2</sub> Storage, in SPE International Conference on CO<sub>2</sub> Capture, Storage, and Utilization. 2009, Society of Petroleum Engineers: San Diego, California, USA. p. 20.
11. Kang, S.M.M., et al., Carbon Dioxide Storage Capacity of Organic-Rich Shales. *SPE Journal*, 2011. **16**(04): p. 842-855.
12. Wu, K., et al., Apparent Permeability for Gas Flow in Shale Reservoirs Coupling Effects of Gas Diffusion and Desorption[in SPE/AAPG/SEG Unconventional Resources Technology Conference. 2014, Unconventional Resources Technology Conference: Denver, Colorado, USA. p. 18.
13. Shi, J., et al., Diffusion and Flow Mechanisms of Shale Gas through Matrix Pores and Gas Production Forecasting, in SPE Unconventional Resources Conference Canada. 2013, Society of Petroleum Engineers: Calgary, Alberta, Canada. p. 19.
14. Bumb, A.C. and C.R. McKee, Gas-Well Testing in the Presence of Desorption for Coalbed Methane and Devonian Shale. *SPE Formation Evaluation*, 1988. **3**(01): p. 179-185.
15. Pan, Z. and L.D. Connell, Reservoir simulation of free and adsorbed gas production from shale. *Journal of Natural Gas Science and Engineering*, 2015. **22**: p. 359-370.
16. Freeman, C.M., et al., A numerical study of performance for tight gas and shale gas reservoir systems. *Journal of Petroleum Science and Engineering*, 2013. **108**: p. 22-39.
17. Mengal, S.A. and R.A. Wattenbarger, Accounting For Adsorbed Gas in Shale Gas Reservoirs, in SPE Middle East Oil and Gas Show and Conference. 2011, Society of Petroleum Engineers: Manama, Bahrain. p. 15.
18. Wasaki, A. and I.Y. Akkutlu, Dynamics of Fracture-matrix Coupling during Shale Gas Production: Pore Compressibility and Molecular Transport Effects, in SPE Annual Technical Conference and Exhibition. 2015, Society of Petroleum Engineers: Houston, Texas, USA. p. 24.
19. Zhang, X., et al., Sensitivity Studies of Horizontal Wells with Hydraulic Fractures in Shale Gas Reservoirs, in International Petroleum Technology Conference. 2009, International Petroleum Technology Conference: Doha, Qatar. p. 9.

20. Huang, L., et al., Molecular Simulation of CO<sub>2</sub> Sequestration and Enhanced Gas Recovery in Gas Rich Shale: An Insight Based on Realistic Kerogen Model, in Abu Dhabi International Petroleum Exhibition & Conference. 2017, Society of Petroleum Engineers: Abu Dhabi, UAE. p. 9.
21. Yuan, W., et al., Experimental study and modelling of methane adsorption and diffusion in shale. *Fuel*, 2014. **117**: p. 509-519.
22. Mansi, M., et al., Effect of reservoir pressure and total organic content on adsorbed gas production in shale reservoirs: a numerical modelling study. *Arabian Journal of Geosciences*, 2022. **15**(2): p. 134.
23. Nuttal, B.C., et al., - Analysis of Devonian black shales in Kentucky for potential carbon dioxide sequestration and enhanced natural gas production, in *Greenhouse Gas Control Technologies 7*, E.S. Rubin, et al., Editors. 2005, Elsevier Science Ltd: Oxford. p. 2225-2228.
24. Du, X., et al., The Influences of CO<sub>2</sub> Injection Pressure on CO<sub>2</sub> Dispersion and the Mechanism of CO<sub>2</sub>-CH<sub>4</sub> Displacement in Shale. *Journal of Energy Resources Technology*, 2017. **140**(1): p. 012907-012907-9.
25. Yu, W., K. Sepehrnoori, and T.W. Patzek, Modeling Gas Adsorption in Marcellus Shale With Langmuir and BET Isotherms. *SPE Journal*, 2016. **21**(02): p. 589-600.
26. Liu, J., et al., Preliminary study of influence factors and estimation model of the enhanced gas recovery stimulated by carbon dioxide utilization in shale. *ACS Sustainable Chemistry & Engineering*, 2019. **7**(24): p. 20114-20125.
27. Liu, D., Y. Li, and S. Yang, Evaluation of the role of water-shale-gas reactions on CO<sub>2</sub> enhanced shale gas recovery. *Energy Procedia*, 2018. **154**: p. 42-47.
28. Xu, R., et al., Assessing the feasibility and CO<sub>2</sub> storage capacity of CO<sub>2</sub> enhanced shale gas recovery using Triple-Porosity reservoir model. *Applied Thermal Engineering*, 2017. **115**: p. 1306-1314.
29. Mahdi, S., X. Wang, and N. Shah, Interactions between the Design and Operation of Shale Gas Networks, Including CO<sub>2</sub> Sequestration. *Engineering*, 2017. **3**(2): p. 244-256.
30. Kim, T.H., S.S. Park, and K.S. Lee, Modeling of CO<sub>2</sub> Injection Considering Multi-Component Transport and Geomechanical Effect in Shale Gas Reservoirs, in *SPE/IATMI Asia Pacific Oil & Gas Conference and Exhibition. 2015*, Society of Petroleum Engineers: Nusa Dua, Bali, Indonesia. p. 17.
31. Li, X. and D. Elsworth, Effect of CO<sub>2</sub> Injectivity on Enhanced Shale Gas Recovery, in *48th U.S. Rock Mechanics/Geomechanics Symposium. 2014*, American Rock Mechanics Association: Minneapolis, Minnesota. p. 10.
32. Liu, F., et al., Assessing the feasibility of CO<sub>2</sub> storage in the New Albany Shale (Devonian–Mississippian) with potential enhanced gas recovery using reservoir simulation. *International Journal of Greenhouse Gas Control*, 2013. **17**: p. 111-126.
33. Godec, M., et al., Potential for enhanced gas recovery and CO<sub>2</sub> storage in the Marcellus Shale in the Eastern United States. *International Journal of Coal Geology*, 2013. **118**: p. 95-104.
34. Dahaghi, A.K., Numerical Simulation and Modeling of Enhanced Gas Recovery and CO<sub>2</sub> Sequestration in Shale Gas Reservoirs: A Feasibility Study, in *SPE International Conference on CO<sub>2</sub> Capture, Storage, and Utilization. 2010*, Society of Petroleum Engineers: New Orleans, Louisiana, USA. p. 18.
35. Liu, B., et al., New perspectives on utilization of CO<sub>2</sub> sequestration technologies in cement-based materials. *Construction and Building Materials*, 2021. **272**: p. 121660.
36. Friedmann, S.J., Geological Carbon Dioxide Sequestration. *Elements*, 2007. **3**(3): p. 179-184.
37. Kanaboshi, H., et al., Cost-efficient measures in the oil refinery and petrochemical sectors for the reduction of CO<sub>2</sub> emissions under the Paris Agreement and air pollution under the MARPOL Convention. *Energy and Climate Change*, 2021. **2**: p. 100027.

38. Ma, Z. and P.G. Ranjith, Review of application of molecular dynamics simulations in geological sequestration of carbon dioxide. *Fuel*, 2019. **255**: p. 115644.
39. Anderson, O.L., Geologic CO<sub>2</sub> sequestration: who owns the pore space. *Wyo. L. Rev.*, 2009. **9**: p. 97.
40. Chen, B., et al., Geologic CO<sub>2</sub> sequestration monitoring design: A machine learning and uncertainty quantification based approach. *Applied Energy*, 2018. **225**: p. 332-345.
41. IEA, Global energy-related CO<sub>2</sub> emissions. 2021.
42. Liu, H., X. Rao, and H. Xiong, Evaluation of CO<sub>2</sub> sequestration capacity in complex-boundary-shape shale gas reservoirs using projection-based embedded discrete fracture model (pEDFM). *Fuel*, 2020. **277**: p. 118201.
43. Mohd Amin, S., D.J. Weiss, and M.J. Blunt, Reactive transport modelling of geologic CO<sub>2</sub> sequestration in saline aquifers: The influence of pure CO<sub>2</sub> and of mixtures of CO<sub>2</sub> with CH<sub>4</sub> on the sealing capacity of cap rock at 37°C and 100bar. *Chemical Geology*, 2014. **367**: p. 39-50.
44. Fathi, E. and I.Y. Akkutlu, Multi-component gas transport and adsorption effects during CO<sub>2</sub> injection and enhanced shale gas recovery. *International Journal of Coal Geology*, 2014. **123**: p. 52-61.
45. Berawala, D.S. and P. Østebø Andersen. Evaluation of multicomponent adsorption kinetics for CO<sub>2</sub> enhanced gas recovery from tight shales. in SPE Europec featured at 81st EAGE Conference and Exhibition. 2019. OnePetro.
46. Zhou, L., et al., Modeling and Upscaling of Binary Gas Coal Interactions in CO<sub>2</sub> Enhanced Coalbed Methane Recovery. *Procedia Environmental Sciences*, 2012. **12**: p. 926-939.
47. Lyu, Q., et al., The role of supercritical carbon dioxide for recovery of shale gas and sequestration in gas shale reservoirs. *Energy & Environmental Science*, 2021. **14**(8): p. 4203-4227.
48. Liu, D., et al., CO<sub>2</sub> sequestration with enhanced shale gas recovery. *Energy Sources, Part A: Recovery, Utilization, and Environmental Effects*, 2021. **43**(24): p. 3227-3237.
49. Huang, J., et al., Evaluation of CO<sub>2</sub> injection into shale gas reservoirs considering dispersed distribution of kerogen. *Applied Energy*, 2020. **260**: p. 114285.
50. Bemani, A., et al., Estimation of adsorption capacity of CO<sub>2</sub>, CH<sub>4</sub>, and their binary mixtures in Quidam shale using LSSVM: Application in CO<sub>2</sub> enhanced shale gas recovery and CO<sub>2</sub> storage. *Journal of Natural Gas Science and Engineering*, 2020. **76**: p. 103204.
51. Meng, X., et al., Performance Evaluation of CO<sub>2</sub> Huff-n-Puff Gas Injection in Shale Gas Condensate Reservoirs. *Energies*, 2019. **12**(1): p. 42.
52. Pu, H., Y. Wang, and Y. Li, How CO<sub>2</sub>-Storage Mechanisms Are Different in Organic Shale: Characterization and Simulation Studies. *SPE Journal*, 2018. **23**(03): p. 661-671.
53. Zhu, G., et al., Forming mechanisms and heterogeneity of source rock: A case study in Dongying Depression. *J Mineral Petrol*, 2003. **23**(4): p. 95-100.
54. Kim, T.H., J. Cho, and K.S. Lee, Evaluation of CO<sub>2</sub> injection in shale gas reservoirs with multi-component transport and geomechanical effects. *Applied Energy*, 2017. **190**: p. 1195-1206.
55. Eshkalak, M.O., et al., Enhanced Gas Recovery by CO<sub>2</sub> Sequestration versus Re-fracturing Treatment in Unconventional Shale Gas Reservoirs, in Abu Dhabi International Petroleum Exhibition and Conference. 2014, Society of Petroleum Engineers: Abu Dhabi, UAE. p. 18.
56. Li, Z. and D. Elsworth, Controls of CO<sub>2</sub>-N<sub>2</sub> gas flood ratios on enhanced shale gas recovery and ultimate CO<sub>2</sub> sequestration. *Journal of Petroleum Science and Engineering*, 2019. **179**: p. 1037-1045.
57. Sun, H., et al., Numerical study of CO<sub>2</sub> enhanced natural gas recovery and sequestration in shale gas reservoirs. *International Journal of Greenhouse Gas Control*, 2013. **19**: p. 406-419.
58. Bybee, K., Proper Evaluation of Shale-Gas Reservoirs Leads to More-Effective Hydraulic-Fracture Stimulation. *Journal of Petroleum Technology*, 2009. **61**(07): p. 59-61.

59. Godec, M., et al., Enhanced Gas Recovery and CO<sub>2</sub> Storage in Gas Shales: A Summary Review of its Status and Potential. *Energy Procedia*, 2014. **63**: p. 5849-5857.
60. Hardy, J., Characterization of Organic Pores within High-Maturation Shale Gas Reservoirs, in SPE Annual Technical Conference and Exhibition. 2019, Society of Petroleum Engineers: Calgary, Alberta, Canada. p. 6.
61. Gasparik, M., et al. 2013.
62. Ji, L., et al., Experimental investigation of main controls to methane adsorption in clay-rich rocks. *Applied Geochemistry*, 2012. **27**(12): p. 2533-2545.
63. Muther, T., et al., Contribution of gas adsorption–desorption in Marcellus shale for different fractured well configurations. *Journal of Petroleum Exploration and Production Technology*, 2022: p. 1-16.
64. Cipolla, C.L., et al. Reservoir Modeling in Shale-Gas Reservoirs. in SPE Eastern Regional Meeting. 2009.
65. Yu, W. and K. Sepehrnoori, Sensitivity Study and History Matching and Economic Optimization for Marcellus Shale, in SPE/AAPG/SEG Unconventional Resources Technology Conference. 2014, Unconventional Resources Technology Conference: Denver, Colorado, USA. p. 15.
66. Dahaghi, A.K. and S.D. Mohaghegh, Numerical Simulation and Multiple Realizations for Sensitivity Study of Shale Gas Reservoirs, in SPE Production and Operations Symposium. 2011, Society of Petroleum Engineers: Oklahoma City, Oklahoma, USA. p. 11.
67. Abolghasemi, E. and P.Ø. Andersen, The influence of adsorption layer thickness and pore geometry on gas production from tight compressible shales. *Advances in Geo-Energy Research*, 2022. **6**(1): p. 4-22.
68. Muther, T., et al., Contribution of gas adsorption–desorption in Marcellus shale for different fractured well configurations. *Journal of Petroleum Exploration and Production Technology*, 2022. **12**(8): p. 2213-2228.
69. Yang, S., et al., Effect of fracture on gas migration, leakage and CO<sub>2</sub> enhanced shale gas recovery in Ordos Basin. *Energy Procedia*, 2018. **154**: p. 139-144.
70. Zhan, J., et al., A Systematic Reservoir Simulation Study on Assessing the Feasibility of CO<sub>2</sub> Sequestration in Liquid-Rich Shale Gas Reservoirs with Potential Enhanced Gas Recovery, in Offshore Technology Conference Asia. 2018, Offshore Technology Conference: Kuala Lumpur, Malaysia. p. 14.
71. Du, X.-D., et al., Investigation of CO<sub>2</sub>–CH<sub>4</sub> Displacement and Transport in Shale for Enhanced Shale Gas Recovery and CO<sub>2</sub> Sequestration. *Journal of Energy Resources Technology*, 2017. **139**(1): p. 012909.
72. Liu, D., R. Agarwal, and Y. Li, Numerical simulation and optimization of CO<sub>2</sub> enhanced shale gas recovery using a genetic algorithm. *Journal of Cleaner Production*, 2017. **164**: p. 1093-1104.
73. Jiang, J., Y. Shao, and R.M. Younis, Development of a Multi-Continuum Multi-Component Model for Enhanced Gas Recovery and CO<sub>2</sub> Storage in Fractured Shale Gas Reservoirs, in SPE Improved Oil Recovery Symposium. 2014, Society of Petroleum Engineers: Tulsa, Oklahoma, USA. p. 17.
74. Ray, S. A Quick Review of Machine Learning Algorithms. in 2019 International Conference on Machine Learning, Big Data, Cloud and Parallel Computing (COMITCon). 2019.
75. Ali, J. Neural networks: a new tool for the petroleum industry? in European petroleum computer conference. 1994. OnePetro.
76. Sircar, A., et al., Application of machine learning and artificial intelligence in oil and gas industry. *Petroleum Research*, 2021. **6**(4): p. 379-391.
77. Rezaee, R. and J. Ekundayo, Permeability Prediction Using Machine Learning Methods for the CO<sub>2</sub> Injectivity of the Precipice Sandstone in Surat Basin, Australia. *Energies*, 2022. **15**(6): p. 2053.

78. Anifowose, Ensemble machine learning: An untapped modeling paradigm for petroleum reservoir characterization. *Journal of Petroleum Science and Engineering*, 2017. **151**: p. 480-487.
79. Vikara, D., D. Remson, and V. Khanna, Machine learning-informed ensemble framework for evaluating shale gas production potential: Case study in the Marcellus Shale. *Journal of Natural Gas Science and Engineering*, 2020. **84**: p. 103679.
80. Bhattacharya, S., et al., Application of predictive data analytics to model daily hydrocarbon production using petrophysical, geomechanical, fiber-optic, completions, and surface data: A case study from the Marcellus Shale, North America. *Journal of Petroleum Science and Engineering*, 2019. **176**: p. 702-715.
81. Orrù, P.F., et al., Machine Learning Approach Using MLP and SVM Algorithms for the Fault Prediction of a Centrifugal Pump in the Oil and Gas Industry. *Sustainability*, 2020. **12**(11): p. 4776.
82. Syed, F.I., et al., Smart shale gas production performance analysis using machine learning applications. *Petroleum Research*, 2022. **7**(1): p. 21-31.
83. Han, D., et al. Production forecasting for shale gas well in transient flow using machine learning and decline curve analysis. in *Asia Pacific Unconventional Resources Technology Conference*, Brisbane, Australia, 18-19 November 2019. 2020. Unconventional Resources Technology Conference.
84. Niu, W., J. Lu, and Y. Sun, Development of shale gas production prediction models based on machine learning using early data. *Energy Reports*, 2022. **8**: p. 1229-1237.
85. Tahmasebi, P., F. Javadpour, and M. Sahimi, Data mining and machine learning for identifying sweet spots in shale reservoirs. *Expert Systems with Applications*, 2017. **88**: p. 435-447.
86. Asala, H.I., et al. A Machine Learning Approach to Optimize Shale Gas Supply Chain Networks. in *SPE Annual Technical Conference and Exhibition*. 2017.
87. Kalantari-Dahaghi, A., S. Mohaghegh, and S. Esmaili, Coupling numerical simulation and machine learning to model shale gas production at different time resolutions. *Journal of Natural Gas Science and Engineering*, 2015. **25**: p. 380-392.
88. Nait Amar, M., et al., Modeling of methane adsorption capacity in shale gas formations using white-box supervised machine learning techniques. *Journal of Petroleum Science and Engineering*, 2022. **208**: p. 109226.
89. Meng, M., R. Zhong, and Z. Wei, Prediction of methane adsorption in shale: Classical models and machine learning based models. *Fuel*, 2020. **278**: p. 118358.
90. Rabbani, A. and M. Babaei, Image-based modeling of carbon storage in fractured organic-rich shale with deep learning acceleration. *Fuel*, 2021. **299**: p. 120795.
91. Hassan Baabbad, H.K., E. Artun, and B. Kulga, Understanding the Controlling Factors for CO<sub>2</sub> Sequestration in Depleted Shale Reservoirs Using Data Analytics and Machine Learning. *ACS Omega*, 2022. **7**(24): p. 20845-20859.
92. Dai, J., et al., Major progress in the natural gas exploration and development in the past seven decades in China. *Petroleum Exploration and Development*, 2019. **46**(6): p. 1100-1110.
93. Wua, K., et al., Adsorbed Gas Surface Diffusion and Bulk Gas Transport in Nanopores of Shale Reservoirs with Real Gas Effect-Adsorption-Mechanical Coupling, in *SPE Reservoir Simulation Symposium*. 2015, Society of Petroleum Engineers: Houston, Texas, USA. p. 31.
94. Ma, Y., et al., Simplified Local Density Theory for Modeling Adsorbed Gas and Estimation of Gas-In-Place of Unconventional Gas Condensate Reservoirs, in *International Petroleum Technology Conference*. 2016, International Petroleum Technology Conference: Bangkok, Thailand. p. 23.
95. Ambrose, R.J., et al., Shale Gas-in-Place Calculations Part I: New Pore-Scale Considerations. *SPE Journal*, 2012. **17**(01): p. 219-229.

96. Ansari, R., et al., More Accurate Quantification of Free and Adsorbed Gas in Shale Reservoirs, in SPWLA 60th Annual Logging Symposium. 2019, Society of Petrophysicists and Well-Log Analysts: The Woodlands, Texas, USA. p. 23.
97. Weniger, P., et al., High-pressure methane and carbon dioxide sorption on coal and shale samples from the Paraná Basin, Brazil. *International Journal of Coal Geology*, 2010. **84**(3): p. 190-205.
98. Lu, X.-C., F.-C. Li, and A.T. Watson, Adsorption Studies of Natural Gas Storage in Devonian Shales. *SPE Formation Evaluation*, 1995. **10**(02): p. 109-113.
99. Adesida, A.G., et al., Characterization of Barnett Shale Kerogen Pore Size Distribution using DFT Analysis and Grand Canonical Monte Carlo Simulations, in SPE Annual Technical Conference and Exhibition. 2011, Society of Petroleum Engineers: Denver, Colorado, USA. p. 14.
100. Verba, C., D. Crandall, and J. Moore, Multiscale Shale Pore Characterization, in SPE/AAPG/SEG Unconventional Resources Technology Conference. 2016, Unconventional Resources Technology Conference: San Antonio, Texas, USA. p. 11.
101. Passey, Q.R., et al., From Oil-Prone Source Rock to Gas-Producing Shale Reservoir - Geologic and Petrophysical Characterization of Unconventional Shale Gas Reservoirs, in International Oil and Gas Conference and Exhibition in China. 2010, Society of Petroleum Engineers: Beijing, China. p. 29.
102. Schettler, P.D., Jr. and C.R. Parmely, Contributions to Total Storage Capacity in Devonian Shales, in SPE Eastern Regional Meeting. 1991, Society of Petroleum Engineers: Lexington, Kentucky. p. 12.
103. Bustin, A.M.M., R.M. Bustin, and X. Cui, Importance of Fabric on the Production of Gas Shales, in SPE Unconventional Reservoirs Conference. 2008, Society of Petroleum Engineers: Keystone, Colorado, USA. p. 29.
104. Merey, S. and C. Sinayuc, Analysis of carbon dioxide sequestration in shale gas reservoirs by using experimental adsorption data and adsorption models. *Journal of Natural Gas Science and Engineering*, 2016. **36**: p. 1087-1105.
105. Li, B., et al. The Condition of Capillary Condensation and Its Effects on Adsorption Isotherms of Unconventional Gas Condensate Reservoirs. in SPE Annual Technical Conference and Exhibition. 2013.
106. Clarkson, C., R. Bustin, and J. Levy, Application of the mono/multilayer and adsorption potential theories to coal methane adsorption isotherms at elevated temperature and pressure. *Carbon*, 1997. **35**(12): p. 1689-1705.
107. Chai, D., et al., Gas transport in shale matrix coupling multilayer adsorption and pore confinement effect. *Chemical Engineering Journal*, 2019. **370**: p. 1534-1549.
108. Brunauer, S. and P.H. Emmett, The use of low temperature van der Waals adsorption isotherms in determining the surface areas of various adsorbents. *Journal of the American Chemical Society*, 1937. **59**(12): p. 2682-2689.
109. Schepers, K.C., et al., Reservoir Modeling in Support of Shale Gas Exploration, in Latin American and Caribbean Petroleum Engineering Conference. 2009, Society of Petroleum Engineers: Cartagena de Indias, Colombia. p. 17.
110. Wu, P. and R. Aguilera, Uncertainty Analysis of Shale Gas Simulation: Consideration of Basic Petrophysical Properties, in SPE Unconventional Resources Conference Canada. 2013, Society of Petroleum Engineers: Calgary, Alberta, Canada. p. 19.
111. Du, C., et al., A Workflow for Integrated Barnett Shale Gas Reservoir Modeling and Simulation, in Latin American and Caribbean Petroleum Engineering Conference. 2009, Society of Petroleum Engineers: Cartagena de Indias, Colombia. p. 12.
112. Gale, J.F., R.M. Reed, and J. Holder, Natural fractures in the Barnett Shale and their importance for hydraulic fracture treatments. *AAPG bulletin*, 2007. **91**(4): p. 603-622.



113. Grieser, W.V., et al., Data Analysis of Barnett Shale Completions, in SPE Annual Technical Conference and Exhibition. 2006, Society of Petroleum Engineers: San Antonio, Texas, USA. p. 12.
114. Frantz, J.H., et al. Evaluating barnett shale production performance-using an integrated approach. in SPE annual technical conference and exhibition. 2005. Society of Petroleum Engineers.
115. Daigle, H., S. Ezidiegwu, and R. Turner, Determining Relative Permeability In Shales By Including The Effects Of Pore Structure On Unsaturated Diffusion And Advection, in SPE Annual Technical Conference and Exhibition. 2015, Society of Petroleum Engineers: Houston, Texas, USA. p. 22.
116. Kenomore, M., et al., Economic Appraisal of Shale Gas Reservoirs, in SPE Europec featured at 80th EAGE Conference and Exhibition. 2018, Society of Petroleum Engineers: Copenhagen, Denmark. p. 19.
117. Lancaster, D.E., et al., Reservoir Evaluation, Completion Techniques, and Recent Results From Barnett Shale Development in the Fort Worth Basin. 1992.
118. Iddphonc, R., J. Wang, and L. Zhao, Review of CO<sub>2</sub> injection techniques for enhanced shale gas recovery: Prospect and challenges. *Journal of Natural Gas Science and Engineering*, 2020. **77**: p. 103240.
119. Zee Ma, Y., Chapter 1 - Unconventional Resources from Exploration to Production, in *Unconventional Oil and Gas Resources Handbook*, Y.Z. Ma and S.A. Holditch, Editors. 2016, Gulf Professional Publishing: Boston. p. 3-52.
120. Grieser, B. and J. Bray. Identification of Production Potential in Unconventional Reservoirs. in *Production and Operations Symposium*. 2007.
121. Rogner, H.-H., An assessment of world hydrocarbon resources. *Annual review of energy and the environment*, 1997. **22**(1): p. 217-262.
122. Bocora, J., Global Prospects for the Development of Unconventional Gas. *Procedia - Social and Behavioral Sciences*, 2012. **65**: p. 436-442.
123. Meakin, P., et al., Shale gas: Opportunities and challenges. *Environmental Geosciences*, 2013. **20**(4): p. 151-164.
124. Ghanizadeh, A., et al. Petrophysical and Geomechanical Characteristics of Canadian Tight Oil and Liquid-Rich Gas Reservoirs. in *SPE/CSUR Unconventional Resources Conference – Canada*. 2014.
125. Sondergeld, C.H., et al., Petrophysical Considerations in Evaluating and Producing Shale Gas Resources, in *SPE Unconventional Gas Conference*. 2010, Society of Petroleum Engineers: Pittsburgh, Pennsylvania, USA. p. 34.
126. Biswas, D. Shale Gas Predictive Model SGPM – An Alternate Approach to Predict Shale Gas Production. in *SPE Eastern Regional Meeting*. 2011.
127. Arogundade, O. and M. Sohrabi, A Review of Recent Developments and Challenges in Shale Gas Recovery, in *SPE Saudi Arabia Section Technical Symposium and Exhibition*. 2012, Society of Petroleum Engineers: Al-Khobar, Saudi Arabia. p. 31.
128. Hu, G., et al., Engineering Microorganisms for Enhanced CO<sub>2</sub> Sequestration. *Trends in Biotechnology*, 2019. **37**(5): p. 532-547.
129. IEA. *Annual Energy Outlook 2017*. 2018; Available from: [https://www.eia.gov/outlooks/aeo/pdf/0383\(2017\).pdf](https://www.eia.gov/outlooks/aeo/pdf/0383(2017).pdf).
130. Metz, B., et al., *IPCC special report on carbon dioxide capture and storage*. 2005: Cambridge: Cambridge University Press.
131. Lai, X., et al., Feasibility Analyses and Prospects of CO<sub>2</sub> Geological Storage by Using Abandoned Shale Gas Wells in the Sichuan Basin, China. *Atmosphere*, 2022. **13**(10): p. 1698.
132. Mamora, D.D. and J.G. Seo, Enhanced Gas Recovery by Carbon Dioxide Sequestration in Depleted Gas Reservoirs, in *SPE Annual Technical Conference and Exhibition*. 2002, Society of Petroleum Engineers: San Antonio, Texas. p. 9.

133. Denney, D., Carbon Dioxide Storage Capacity of Organic-Rich Shales. *Journal of Petroleum Technology*, 2011. **63**(07): p. 114-117.
134. Zamirian, M., K. Aminian, and S. Ameri, Measurement of Key Shale Petrophysical Properties, in *SPE Annual Technical Conference and Exhibition*. 2015, Society of Petroleum Engineers: Houston, Texas, USA. p. 11.
135. Huo, P., et al., CO<sub>2</sub> geological sequestration: Displacement behavior of shale gas methane by carbon dioxide injection. *International Journal of Greenhouse Gas Control*, 2017. **66**: p. 48-59.
136. Liu, J., et al., Experimental evaluation of CO<sub>2</sub> enhanced recovery of adsorbed-gas from shale. *International Journal of Coal Geology*, 2017. **179**: p. 211-218.
137. Settari, A., V. Swami, and F. Javadpour. A Numerical Model for Multi-mechanism Flow in Shale Gas Reservoirs with Application to Laboratory Scale Testing-(SPE-164840). in *75th EAGE Conference & Exhibition incorporating SPE EUROPEC 2013*. 2013. European Association of Geoscientists & Engineers.
138. Josse, J. and F. Husson, Handling missing values in exploratory multivariate data analysis methods. *Journal de la Société Française de Statistique*, 2012. **153**(2): p. 79-99.
139. Afrianti, Y., S. Indratno, and U. Pasaribu. Imputation algorithm based on copula for missing value in timeseries data. in *2014 2nd International Conference on Technology, Informatics, Management, Engineering & Environment*. 2014. IEEE.
140. Saar-Tsechansky, M. and F. Provost, Handling missing values when applying classification models. 2007.
141. Godfrey, K.R., Correlation methods. *Automatica*, 1980. **16**(5): p. 527-534.
142. Makowski, D., et al., Methods and algorithms for correlation analysis in R. *Journal of Open Source Software*, 2020. **5**(51): p. 2306.
143. St»hle, L. and S. Wold, Analysis of variance (ANOVA). *Chemometrics and Intelligent Laboratory Systems*, 1989. **6**(4): p. 259-272.
144. Hauke, J. and T. Kossowski, Comparison of values of Pearson's and Spearman's correlation coefficients on the same sets of data. *Quaestiones geographicae*, 2011. **30**(2): p. 87.
145. Schober, P., C. Boer, and L.A. Schwarte, Correlation Coefficients: Appropriate Use and Interpretation. *Anesthesia & Analgesia*, 2018. **126**(5).
146. Armstrong, R.A., Should Pearson's correlation coefficient be avoided? *Ophthalmic and Physiological Optics*, 2019. **39**(5): p. 316-327.
147. Sawyer, S.F., *Analysis of Variance: The Fundamental Concepts*. *Journal of Manual & Manipulative Therapy*, 2009. **17**(2): p. 27E-38E.
148. De Winter, J.C., S.D. Gosling, and J. Potter, Comparing the Pearson and Spearman correlation coefficients across distributions and sample sizes: A tutorial using simulations and empirical data. *Psychological methods*, 2016. **21**(3): p. 273.
149. Puth, M.-T., M. Neuhäuser, and G.D. Ruxton, Effective use of Spearman's and Kendall's correlation coefficients for association between two measured traits. *Animal Behaviour*, 2015. **102**: p. 77-84.
150. Cui, X., R.M. Bustin, and L. Chikatamarla, Adsorption-induced coal swelling and stress: Implications for methane production and acid gas sequestration into coal seams. *Journal of Geophysical Research: Solid Earth*, 2007. **112**(10).
151. Zou, J., R. Rezaee, and K. Liu, Effect of Temperature on Methane Adsorption in Shale Gas Reservoirs. *Energy & Fuels*, 2017. **31**(11): p. 12081-12092.
152. Fatah, A., et al., A Review on the influence of CO<sub>2</sub>/shale interaction on shale properties: implications of CCS in shales. *Energies*, 2020. **13**(12): p. 3200.
153. EIA, Shale gas production drives world natural gas production growth. 2016.
154. Rahm, D., Regulating hydraulic fracturing in shale gas plays: The case of Texas. *Energy Policy*, 2011. **39**(5): p. 2974-2981.


155. Vermuyen, J.P., Geomechanical studies of the Barnett shale, Texas, USA. 2011: Stanford University.
156. Nuttal, B.C., Reassessment of CO<sub>2</sub> sequestration capacity and enhanced gas recovery potential of middle and upper Devonian black shales in the Appalachian Basin. MRCSP Phase II Topical Report October 2005–October 2010. Midwest Regional Carbon Sequestration Partnership. 2010.
157. Klewiah, I., et al., Review of experimental sorption studies of CO<sub>2</sub> and CH<sub>4</sub> in shales. *Journal of Natural Gas Science and Engineering*, 2020. **73**: p. 103045.
158. Mahesh, B., Machine learning algorithms-a review. *International Journal of Science and Research (IJSR)*. [Internet], 2020. **9**: p. 381-386.
159. Alpaydin, E., Introduction to machine learning. 2020: MIT press.
160. Hastie, T., R. Tibshirani, and J. Friedman, Overview of supervised learning, in *The elements of statistical learning*. 2009, Springer. p. 9-41.
161. Wang, H., C. Ma, and L. Zhou. A Brief Review of Machine Learning and Its Application. in *2009 International Conference on Information Engineering and Computer Science*. 2009.
162. Cunningham, P., M. Cord, and S.J. Delany, Supervised learning, in *Machine learning techniques for multimedia*. 2008, Springer. p. 21-49.
163. Haifeng, W. and H. Dejin. Comparison of SVM and LS-SVM for Regression. in *2005 International Conference on Neural Networks and Brain*. 2005.
164. Bhatia, N.K., A.H. El-Hag, and K.B. Shaban. Machine learning-based regression and classification models for oil assessment of power transformers. in *2020 IEEE international conference on informatics, IoT, and enabling technologies (ICIOT)*. 2020. IEEE.
165. Zhao, C.Y., et al., Application of support vector machine (SVM) for prediction toxic activity of different data sets. *Toxicology*, 2006. **217**(2): p. 105-119.
166. Zou, J., Y. Han, and S.-S. So, Overview of artificial neural networks. *Artificial Neural Networks*, 2008: p. 14-22.
167. Schmidhuber, J., Deep learning in neural networks: An overview. *Neural Networks*, 2015. **61**: p. 85-117.
168. Bala, R. and D. Kumar, Classification using ANN: A review. *Int. J. Comput. Intell. Res*, 2017. **13**(7): p. 1811-1820.
169. Kotsiantis, S.B., Decision trees: a recent overview. *Artificial Intelligence Review*, 2013. **39**(4): p. 261-283.
170. Myles, A.J., et al., An introduction to decision tree modeling. *Journal of Chemometrics: A Journal of the Chemometrics Society*, 2004. **18**(6): p. 275-285.
171. Song, Y.-Y. and Y. Lu, Decision tree methods: applications for classification and prediction. *Shanghai archives of psychiatry*, 2015. **27**(2): p. 130-135.
172. Allah Bukhsh, Z., et al., Predictive maintenance using tree-based classification techniques: A case of railway switches. *Transportation Research Part C: Emerging Technologies*, 2019. **101**: p. 35-54.
173. Fawagreh, K., M.M. Gaber, and E. Elyan, Random forests: from early developments to recent advancements. *Systems Science & Control Engineering: An Open Access Journal*, 2014. **2**(1): p. 602-609.
174. Choudhary, R. and H.K. Gianey. Comprehensive review on supervised machine learning algorithms. in *2017 International Conference on Machine Learning and Data Science (MLDS)*. 2017. IEEE.
175. Liaw, A. and M. Wiener, Classification and regression by randomForest. *R news*, 2002. **2**(3): p. 18-22.
176. Mahesh, B., Machine Learning Algorithms -A Review. 2019.
177. Ghahramani, Z. Unsupervised learning. in *Summer school on machine learning*. 2003. Springer.
178. Celebi, M.E. and K. Aydin, Unsupervised learning algorithms. 2016: Springer.

179. Badgwell, T.A., J.H. Lee, and K.-H. Liu, Reinforcement learning—overview of recent progress and implications for process control. *Computer Aided Chemical Engineering*, 2018. **44**: p. 71-85.
180. Arulkumaran, K., et al., Deep reinforcement learning: A brief survey. *IEEE Signal Processing Magazine*, 2017. **34**(6): p. 26-38.
181. Rubin, D.B., Inference and missing data. *Biometrika*, 1976. **63**(3): p. 581-592.
182. Ezekiel, M., *Methods of correlation analysis*. 1941.
183. Jović, A., K. Brkić, and N. Bogunović. A review of feature selection methods with applications. in 2015 38th international convention on information and communication technology, electronics and microelectronics (MIPRO). 2015. Ieee.
184. Akossou, A. and R. Palm, Impact of data structure on the estimators R-square and adjusted R-square in linear regression. *Int. J. Math. Comput*, 2013. **20**(3): p. 84-93.
185. Lee, K.-Y., et al., Comparison and analysis of linear regression & artificial neural network. *International Journal of Applied Engineering Research*, 2017. **12**(20): p. 9820-9825.

# Appendix

## A. Copyright Agreement

The copyright agreements between the journals and author to reuse the author's own publication in this thesis are listed as following:

 Help Live Chat


**Effect of reservoir pressure and total organic content on adsorbed gas production in shale reservoirs: a numerical modelling study**

**SPRINGER NATURE** Author: Moataz Mansi et al  
Publication: Arabian Journal of Geosciences  
Publisher: Springer Nature  
Date: Jan 10, 2022  
Copyright © 2022, The Author(s)

**Creative Commons**  
This is an open access article distributed under the terms of the [Creative Commons CC BY](#) license, which permits unrestricted use, distribution, and reproduction in any medium, provided the original work is properly cited.  
You are not required to obtain permission to reuse this article.  
To request permission for a type of use not listed, please contact [Springer Nature](#)

---

**Statistical Analysis of Controlling Factors on Enhanced Gas Recovery by CO<sub>2</sub> Injection in Shale Gas Reservoirs**

 Author: Moataz Mansi, Mohamed Almobarak, Christopher Lagat, et al  
Publication: Energy & Fuels  
Publisher: American Chemical Society  
Date: Jan 1, 2023  
Copyright © 2023, American Chemical Society

**PERMISSION/LICENSE IS GRANTED FOR YOUR ORDER AT NO CHARGE**


This type of permission/license, instead of the standard Terms and Conditions, is sent to you because no fee is being charged for your order. Please note the following:


- Permission is granted for your request in both print and electronic formats, and translations.
- If figures and/or tables were requested, they may be adapted or used in part.
- Please print this page for your records and send a copy of it to your publisher/graduate school.
- Appropriate credit for the requested material should be given as follows: "Reprinted (adapted) with permission from (COMPLETE REFERENCE CITATION). Copyright (YEAR) American Chemical Society." Insert appropriate information in place of the capitalized words.
- One-time permission is granted only for the use specified in your RightsLink request. No additional uses are granted (such as derivative works or other editions). For any uses, please submit a new request.

If credit is given to another source for the material you requested from RightsLink, permission must be obtained from that source.

[BACK](#) [CLOSE WINDOW](#)

---

 Help Live Chat

 **Application of supervised machine learning to predict the enhanced gas recovery by CO<sub>2</sub> injection in shale gas reservoirs**

Author: Moataz Mansi, Mohamed Almobarak, Jamiu Ekundayo, Christopher Lagat, Quan Xie  
Publication: Petroleum  
Publisher: Elsevier  
Date: Available online 23 February 2023  
© 2023 Southwest Petroleum University. Publishing services by Elsevier B.V. on behalf of KeAi Communications Co. Ltd.

**Content Excluded**  
This content has been excluded from the RightsLink's service. Please contact Elsevier directly with your request.  
The article selected has been excluded for permissions processing by Elsevier. It cannot be processed through RightsLink at this time.  
Please submit your request by completing Elsevier's permission request form.  
You may also contact an [Elsevier representative](#) directly with any questions.  
Please include the content information (article title, author, date, issn, volume, issue), a link to the content on the Web if appropriate and any details regarding your specific request.